UNIVERSITY OF CALIFORNIA SAN DIEGO

Adaptation of innate immune cells to persistent viral infection

A dissertation submitted in partial satisfaction of the
requirements for the degree Doctor of Philosophy

in

Biology

by

Yeara Jo

Committee in charge:

Professor Elina Zuniga, Chair
Professor Jack Bui
Professor Ananda Goldrath
Professor Li-Fan Lu
Professor Wei Wang

2019

The Dissertation of Yeara Jo is approved, and it is acceptable in quality and form for publication on microfilm and electronically:

_____

_____

_____

_____

_____
Chair

University of California San Diego

2019

DEDICATION

To my Family!

To all the friends who supported me!

TABLE OF CONTENTS

LIST OF FIGURES

LIST OF TABLES

ACKNOWLEDGEMENTS

I would like to acknowledge Professor Elina Zuniga for her support as the chair of my committee. I would like to thank my committee members for their contribution to my academic development. I would also like to acknowledge the Zuniga lab members, without whom I would not have finished this work. Their support and intellectual input have been invaluable. I would also like to thank immunology group at UCSD with who provided me with great feedback on my projects and willingly shared many resources with me.

Chapter 2, in part, is a reprint of the material as it appears in Immunity Macal, M and Jo, Y et al 2018. Yeara Jo was one of the two primary investigators and authors of this paper. I would like to thank co-authors Dr. Monica Macal, Dr. Simone Dallari, Dr. Aaron Chang, Dr. Jihong Dai, Dr. Shobha Swaminathan, Dr. Ellen Wehrens and Dr. Patricia Fitzgerald-Bocarsly for their contributions.

Chapter 3, in part, is currently being prepared for submission for publication of the material by Jo, Y. Yeara Jo was the primary investigator and author of this material. I would like to thank Dr. Kai Zhang and Dr. Wei Wang for their bioinformatics expertise and Dr. Simone Dallari and Nuha Marooki for their assistance with preparing for samples. I would also like to acknowledge UCSD IGM genomics center for making my RNA-seq libraries and performing sequencing on my samples.

VITA

2012 Bachelor of Science, California Institute of Technology

2019 Doctor of Philosophy, University of California San Diego

PUBLICATIONS

M Macal*, **Y Jo***, S Dallari, AY Chang, J Dai, S Swaminathan, EJ Wehrens, P Fitzgerald-Bocarsly, and EI Zúñiga "Self-renewal and toll-like receptor signaling sustain exhausted plasmacytoid dendritic cells during chronic viral infection" Immunity 48, 730-744 e735, doi:10.1016/j.immuni.2018.03.020 (2018). * indicates co-first authors.

JA Harker, KA Wong, S Dallari, P Bao, A Dolgoter, **Y Jo**, EJ Wehrens, M Macal, and EI Zuniga "Interleukin-27R signaling mediates early viral containment and impacts innate and adaptive immunity after chronic lymphocytic choriomeningitis virus infection" J Virol 92, doi:10.1128/JVI.02196-17 (2018).

S Dallari, M Macal, ME Loureiro, **Y Jo**, L Swanson, C Hesser, P Ghosh, EI Zuniga "Src family kinases Fyn and Lyn are constitutively activated and mediate plasmacytoid dendritic cell responses" Nat Commun 8, 14830, doi:10.1038/ncomms14830 (2017)

AB Artyukhin*, JJ Yim, J Srinivasan, Y Izrayelit, N Bose, SH von Reuss, **Y Jo**, JM Jordan, LR Baugh, M Cheong, PW Sternberg, L Avery, and FC Schroeder "Succinylated octopamine ascarosides and a new pathway of biogenic amine metabolism in Caenorhabditis elegans." Journal of Biological Chemistry. 288(26):18778-83. doi: 10.1074/jbc.C113.477000 (2013)

Y Izrayelit*, J Srinivasan, SL Campbell, **Y Jo**, SH von Reuss, MC Genoff, PW Sternberg, and FC Schroeder "Targeted Metabolomics Reveals a Male Pheromone and Sex-Specific Ascaroside Biosynthesis in Caenorhabditis elegans." ACS Chemical Biology 7(8):1321-5. doi: 10.1021/cb300169c (2012)

FIELDS OF STUDY

Genetics and chemical Biology
Professor Paul Sternberg, PhD

Studies in Immune response to pathogens
Professor Elina Zuniga, PhD

ABSTRACT OF THE DISSERTATION

Adaptation of innate immune cells to persistent viral infection

by

Yeara Jo

Doctor of Philosophy in Biology

University of California San Diego, 2019

Professor Elina Zuniga, Chair

During chronic infections, sustained cell adaptation has been mostly studied in the adaptive immune compartment but much less is known on how innate immune cells adjust to a persistently infectious milieu. Particularly, dendritic cells (DCs), which are central players in immune responses, adapt during chronic infections. However, the underlying mechanisms remain largely unknown. Thus, to understand how short-lived innate cells adapt to lifelong persistent infections, we first studied plasmacytoid DCs (pDCs), which specialize in Type I Interferon (IFN-I) production and often become functionally exhausted in chronic settings. Using a murine chronic viral infection model of lymphocytic choriomeningitis virus (LCMV), we found that bone marrow pDC progenitors exhibited quantitative and qualitative defects and failed to generate functional pDCs *ex vivo* in an IFN-I-dependent manner. Exhausted pDC numbers were, however, maintained by peripheral self-renewal via sustained proliferation of CD4- pDC subsets that was induced by

IFN-I receptor and Toll-like receptor 7 (TLR7) signaling in a cell-intrinsic manner. In contrast, functional impairment of exhausted pDCs was independent of IFN-I receptor signaling. We further studied mechanisms underlying adaptation of progenitors, that can give rise to conventional DCs (cDCs) as well as pDCs, by determining the transcriptional and chromatin landscapes of bone marrow DC progenitors from LCMV-infected mice and applying these datasets to Taiji algorithm to predict the activity of transcription factors (TFs). We found that, Glucocorticoid Modulatory Element Binding Protein 1 (Gmeb1), which was predicted to exhibit increased activity in progenitors during LCMV infection, suppressed pDC development in a glucocorticoid-dependent manner. Further studies revealed that glucocorticoid suppressed pDC development during LCMV infection. Gmeb1 also promoted development but suppressed maturation of cDC1s in a glucocorticoid-independent manner. Overall, our work provides a framework to understand how innate immune adaptation can be triggered and sustained during chronic viral infection. Moreover, by highlighting novel TF regulators of DC progenitors and their progeny, our work enhances our understanding of DC biology and unveils potential therapeutic targets to harness DCs.

Chapter 1. Introduction

1.1 Immune adaptations during chronic infection

Chronic infections, including Human Immunodeficiency Virus (HIV) infection, Hepatitis B Virus (HBV) infection, Hepatitis C Virus (HCV) infection, mycobacterium tuberculosis and malaria, represent a major health burden. Immunosuppression is a hallmark of chronic infections, limiting the immune response to both the ongoing pathogen as well as unrelated microbes, cancer and vaccination[1-3].

Adaptation to changes in environment is an evolutionarily conserved process observed at all levels of organization comprising an organism from cells to whole organism. Sustained presence of viral loads during persistent viral infection also poses a wide variety of changes in the environment faced by the immune system, including continuous stimulation of the receptors on immune cells that recognize these pathogens, a distinct cytokine milieu generated by immune responses, and altered levels of oxygen and nutrients, among others. Therefore, it is conceivable from an evolutionary point of view that persistent viral infection will lead diverse components of the immune system to adapt their functions and re-calibrate their responses in accordance with these changes in order to constantly establish an equilibrium with dynamically changing environment, keep the infectious virus in check, and prevent death caused by excessive immune responses. In this sense, while detrimental for host defense, such immunosuppression can be seen as a host adaptation to enable long-term survival and co-existence with the pathogen. Indeed, hosts with genetic ablation of core immunosuppressors often die after infection (despite enhanced microbial control)[2,3]. Nevertheless, short-term therapeutic relief of some immunosuppressors during infection can be tolerated and beneficial in clearing the persistent pathogen and/or secondary insults[3,4]. On the other hand, identifying the mechanisms underlying cellular adaptations

leading to immunosuppression during chronic infections could highlight ways to mimic such immunosuppression in instances where excessive immune responses cause illness, such as autoimmune and inflammatory diseases.

Such adaptations have been extensively studied in adaptive immune cells such as T cells and B cells, which undergo functional exhaustion during chronic infections and cancer[4,5]. During chronic infection in which infection persists after the effector phase where priming of naïve T cells by antigen, co-stimulation, and inflammation differentiates them into effector T cells, T cells undergo functional exhaustion[6]. T cell exhaustion involves a hierarchical loss of capacity to co-produce cytokines (such as IFN-γ, tumor necrosis factor (TNF) and IL-2), a progressive increase in the amount and diversity of inhibitory receptors expressed (such as PD-1, LAG-3, CD160, and CD244), and loss of proliferative capacity and *ex vivo* killing ability, eventually followed by physical deletion[6]. B cell exhaustion occurs in a very similar manner to that described for CD4+ and CD8+ T cells in several models of persistent viral infections and are characterized by reduced capacity to proliferate in response to *de novo* stimuli and an increased expression of multiple inhibitory receptors[5]. Multiple pathways including not only persistent antigen stimulation but also absence of CD4+ T cell help, negative costimulatory signals delivered by inhibitory receptors, pro- or anti-inflammatory cytokines as well as immunoregulatory cells all contribute to development of T cell exhaustion[7].

1.2 Lymphocytic Choriomeningitis Virus (LCMV) as a model system to understand immune adaptation to chronic infection

LCMV is one of the most representative examples of viruses that significantly enhanced our understanding of immune systems, including seminal work detailing concepts such as immune

tolerance, immunodominance, MHC restriction and the basis for viral persistence[8]. First discovered in 1930s as a causative agent of meningeal inflammation in mice and humans[9,10], LCMV is the prototypic member of the Old World Arenaviridae family, which also includes Lassa virus, a causative agent of severe hemorrhagic fever[11]. LCMV is a negative-sense RNA virus with two single-stranded genome segments named S (3.4 kb), which encodes viral nucleoprotein (NP) and glycoprotein (GP), and L (7.2 kb), which encodes polymerase (L) and small RING finger protein (Z)[12-14].

The unique strength of the LCMV model to study viral pathogenesis comes from the relatively non-cytopathic nature of LCMV such that injury and cell destruction during LCMV infection in its natural murine host result from the host immune responses rather than direct virus-mediated effects[15]. Also, comparison and contrast among different variants of LCMV that induce a broad range of immune responses have proven invaluable in elucidating components of functional and effective immune responses as well as immunosuppression. While LCMV Armstrong (ARM) and LCMV Clone 13 (Cl13) differ by only two amino acids[16,17], these differences can cause initial differences in infection and replication in dendritic cells (DCs)[18,19], followed by difference in persistence. While LCMV ARM is cleared by day 8 post-infection (p.i.), LCMV Cl13 infection causes viremia that can last up to 3 months and virus can persist in some tissues indefinitely[20]. With these features, LCMV was a model where the most well-established immune adaptation to chronic infection, T cell exhaustion, was first discovered[21,22]. Last, but not the least, strength of LCMV model in immunology research is that the results in experimental models could be extended to human diseases including chronic infections such as HIV and HBV infections as well as non-infectious diseases like cancer[15].

1.3 Subsets and functions of DCs

DCs form a bridge between innate and adaptive immune responses by linking innate immune sensing of the environment to the initiation of adaptive immune responses[23]. These cells can be broadly classified into two classes: plasmacytoid DCs (pDCs) and conventional or myeloid DCs (cDCs / mDCs).

pDCs have unique secretory "plasmacytoid" morphology similar to that of plasma cells and specialize in rapid and massive production of type I interferon (IFN-I) in response to self or foreign nucleic acids recognized by a set of pattern recognition receptors expressed in these cells such as Toll-like receptor (TLR) 7 and TLR9[24,25]. IFN-I is a pleiotropic cytokine with roles in inducing antimicrobial states in infected and neighboring cells to limit the spread of infectious agents, promoting natural killer cell functions, and enhancing the development of high-affinity antigen-specific T and B cell responses and immunological memory by activating the adaptive immune system[26]. Potent ability of pDCs to produce IFN-I as well as pro-inflammatory cytokines such as IL-12 and IL-6 supports their roles in these diverse biological processes[27]. In addition, pDCs express MHC class I (MHCI) and MHC class II (MHCII) molecules together with co-stimulatory markers including CD80, CD86 and CD40, which enable them to cross-prime CD8+ T cells and present antigen to CD4+ T cells, albeit not as efficiently as cDCs[27-32]. Finally, upon activation, pDCs also secrete chemokines such as CXC-chemokine ligand 8 (CXCL8), CXCL9, CXCL10, CXCL13, CC-chemokine ligand 3 (CCL3), CCL4, CCL5, and CCL22 to attract immune cells to sites of infection or inflammation[33-35]. On the other hand, pDCs can also promote tolerogenic immune responses depending on their activation states via expression of express indoleamine 2,3-dioxygenase (IDO), ICOSL, OX40L, programmed cell death protein 1 ligand 1 (PDL1) and/or granzyme B[36-41].

cDCs are specialized in antigen presentation with an enhanced ability to sense tissue injuries, capture and process antigens, migrate loaded with antigens to the T cell zone, and present antigens to T lymphocytes to prime them[24]. cDCs in lymphoid tissues can be divided into at least two main subpopulations, conventional type 1 DCs (cDC1s) characterized by CD8α and CD103 and conventional type 2 DCs (cDC2s) characterized by CD11b expression[42]. cDC1s are functionally specialized in cross-presenting exogenous antigens on MHCI molecules to activate T helper (Th) 1 and cytotoxic CD8+ T cells[43,44] and exhibit superior capacity to secrete IL-12[45], supporting their roles in defenses against intracellular pathogens and tumors[42,46,47]. Compared to cDC1s, cDC2s are superior in the induction of CD4+ T cell immunity because of their prominent expression of MHCII presentation machinery[42]. They have capacity to cross-present antigen under certain circumstances[48,49].Intestinal CD103+CD11b+ cDCs, which are dependent on Notch2 signaling for their development in an analogous manner to a subset of splenic cDC2s[50], have been shown to locally generate IL-23 to mediate antimicrobial responses against *Citrobacter rodentium* essential for host survival[51] and to produce IL-6 to support Th17 differentiation and defenses against extracellular pathogens[52]. cDC2s also produce proinflammatory chemokines such as CCL3, CCL4, and CCL5[53] in response to TLR stimuli. On the other hand, some circumstantial evidences suggest that a different subset of cDC2s, which are dependent on Klf4, modulate optimal Th2 responses, thereby supporting defenses against parasites and allergens[47].

1.4 Roles of DCs during antiviral defenses and their alteration during chronic viral infection

Multiple functions of different DC subsets endow DCs with crucial roles in mounting effective antiviral defenses. In murine models, pDCs have been shown to be important for innate protection against acute cytopathic viruses such as MHV[54]. pDCs have also been demonstrated to

facilitate the survival and accrual of virus-specific CD8+ cytotoxic T cells and CD4+ helper T cells during VSV and LCMV infection[54,55]. Multiple studies have also established the importance of DC subsets other than pDCs in antiviral defenses in murine models and human patients. For example, a depletion study showed that CD11c+ DCs are essential in innate resistance and optimal activation of NK and T cell responses to herpes simplex virus type 1 (HSV-1) infection in mice[56]. During influenza virus infection in mice, DCs are required for secondary antigen-dependent interactions with influenza-specific CD8+ T cells in addition to initial interaction for priming to incur effective protective CD8+ T cell responses[57]. Furthermore, in humans, HIV-1 controllers have been found to have improved abilities to recognize HIV-1 through cytoplasmic immune sensors and secrete IFN-I more potently in response to viral infection, possibly facilitating DC-mediated induction of highly potent antiviral HIV-1-specific T cells[58].

Despite the importance of DCs in immune responses during viral infections, they are adapted and their functions are altered during chronic viral infections[59-62]. It is well established that chronic LCMV infection as well as human chronic infections such as HBV, HCV, and HIV infection compromises DC maturation[63-65] and antigen presenting capacity[66,67]. During chronic LCMV infection, DCs express lower levels of MHC and co-stimulatory molecules at day 22 p.i. (when DCs fail to prime T cells) vs. day 1 p.i. (when DCs successfully prime T cells)[68]. Multiple studies have previously reported hypo-functionality of pDCs during chronic viral infections. pDCs are initially fully capable of releasing copious amounts of IFN-I[3,69], but during later phases of infection, they fail to produce IFN-I in response to the ongoing viral infection, synthetic TLR ligands, or unrelated viruses, and this is accompanied by compromised innate responses and control of secondary opportunistic viral infections[3,70-72]. Consistently, in contrast to its massive up-regulation hours after infection, systemic IFN-I is profoundly attenuated at later stages during

chronic viral infections in mice and humans, with low levels of IFN-I and/or an "interferon signature" persisting in tissues[3,69,70,73-75]. Prophylactic pDC stimulation, delayed IFN-I down-regulation, or IFN-I inoculation before or after infection with a chronic virus enhances T cell responses and host resistance, indicating that the rapid and profound IFN-I attenuation during chronic viral infection promotes T cell exhaustion and viral persistence[71,76-79]. While pDCs loses their cytokine production capacity, pDCs acquire the ability to stimulate naïve CD4+ T cells, albeit less efficiently than cDCs in response to activation by HIV-1[80]. Several studies have reported altered cytokine production by mDCs as well. Chronic HBV and HCV infection have been shown to reduce mDC production of proinflammatory cytokines such as IL-12[81,82] and TNFα[67]. Some virulent respiratory syncytial virus (RSV) strains have also been shown to impair IFN-α and IL-12 secretion by mDCs[83]. Importantly, in addition to downregulation of proinflammatory cytokine production, chronic viral infection has been associated with upregulation of anti-inflammatory cytokine production such as IL-10[62]. Expansion of IL-10-producing immunoregulatory antigen presenting cells (iAPCs), which include CD8α−CD4+ DCs[84], has been shown to induced by both acute and chronic LCMV infection, while this population only further amplifies and persists in parallel with the viral replication kinetics during persistent LCMV infection[85]. HCV and HIV-1 infection also induce IL-10 production by DCs[86,87].

Persistent viral infection incurs quantitative changes in DCs in addition to functional changes. Several studies have demonstrated that both pDCs and mDCs are depleted in peripheral blood[70,88] but accumulate in lymph nodes of HIV-infected patients[89,90]. Accumulation of pDCs was also reported in spleens from HIV+ patients with high proviral loads[91]. Depletion of circulating pDCs has similarly been observed in Simian Immunodeficiency Virus (SIV)-infected macaques, whereas number of circulating CD1c+ mDC, equivalent to cDC2s, was increased in these

animals[92]. Quantitative impairment of pDCs in peripheral blood was also found in HBV- and HCV-infected patients[93,94]. While the aforementioned reports have observed depletion of circulating pDCs in contrast to their accumulation in lymphoid organs, other studies have reported consistent decline in number of pDCs in both peripheral blood and lymphoid organs at later stages after LCMV, HIV and SIV infections[72,95,96]. Changes in number of pDCs in lymphoid organs upon viral infection could vary depending on the timepoint of study due to their rapid dynamics of mobilization and recruitment into lymphoid organs followed by apoptosis[96], possibly mediated by IFN-I as shown in multiple murine models of systemic viral infection[97]. In addition, during chronic LCMV infection, splenic DCs demonstrate compromised expansion in response to FMS-like tyrosine kinase ligand (Flt3L)[65], a growth factor that can expand DCs *in vivo*[98], suggesting that compromised expansion may also contribute to reduction in number of DCs in lymphoid organs. Homeostasis among different DC subsets during viral infection can be further affected by some DC subsets that acquire capacity to transform into different type of DCs, such as pDCs that become able to convert into cDC2s during LCMV infection[99], or inflammatory monocytes that traffic to draining lymph nodes and become able to present viral antigens to naïve T cells by acquiring DC phenotypes[100].

1.5 Cellular and transcriptional basis of DC development

While multiple studies have suggested gradual restriction of non-DC lineage potential from multipotency of lymphoid-primed multipotent progenitors (LMPPs) as origin of DCs[47], a recent study that used 'cellular barcoding' to trace the *in vivo* fate of LMPPs and hematopoietic stem cells (HSCs) at the single-cell level suggested an early fate imprinting giving rise to a population with clonal bias to develop into DCs[101]. While paradigm of developmental pathway for different DC

subsets is still changing with emergence of new studies, it is well established that Flt3L-Flt3 axis is required for both pDC and cDC development[98,102], with PU.1 playing a critical role in this axis by regulating Flt3 expression[103] and PI3K-mTOR signaling and Stat3 pathway acting downstream of Flt3L[104,105].

While Flt3L-driven developmental program is shared between cDCs and pDCs, specification of pDCs requires the E protein transcription factor (TF) TCF4 (E2-2)[106,107]. STAT3 stimulates expression of TCF4 in response to Flt3L[108]. Not only TCF4 but also its targets SPIB and BCL11A have been shown to be important for pDC development[109-112]. In addition, MTG16 and ZEB2 can also promote pDC development by repressing E protein inhibitor ID2 and prevent ID2 from intervening with the TCF4-driven transcriptional program[113,114]. In terms of cellular origin of pDCs, one unique property of pDC development is the presence of separate myeloid and lymphoid pathways, both of which generate cells that would be commonly classified as pDCs based on their surface phenotype and IFN-I production capacity but would be distinguished from each other based on RAG1 gene expression and IgH gene rearrangement[115]. The myeloid pathway to pDCs includes common DC progenitors (CDPs), which can give rise to both pDCs and cDCs[116,117]. A more recent report has identified a CD115-CD127- CDP-like population derived from either CDPs or LMPPs as a more pDC-biased DC progenitor, which expresses high level of TCF4 and can still give rise to cDCs but has more prominent potential to generate pDCs[118]. Potential to generate cDCs is still maintained further along this developmental pathway up to CCR9- pDC-like precursors, which express surface markers for mature pDCs other than CCR9 and spontaneously differentiate into CCR9+ pDCs but are still flexible enough to generate cDC-like cells upon exposure to tissue-specific or context-dependent factors such as intestinal epithelial cell–derived factors or recombinant GM-CSF *in vitro*[119]. On the other hand, the lymphoid pathway

to pDCs includes common lymphoid progenitors (CLPs), which can also give rise to B cells[120], and expression of SiglecH, Ly6D, IL-7Rα, CD81 and CD2 defines development into further pDC-committed pre-pDCs[121,122].

While some precursor population with larger pDC potential along myeloid developmental pathway of pDC still retains some cDC potential, major cDC developmental pathway bifurcates from pDC developmental pathway at the level of CDPs and gives rise to more committed precursors of cDCs (pre-cDCs), which exit the bone marrow (BM) and seed peripheral tissues before differentiating locally into mature cDC subsets[123,124]. Pre-cDCs can be distinguished from other immune lineages by Zbtb46 expression[125]. Transcriptional signatures of the cDC1 and cDC2 lineages emerge at the single-cell level from the CDP stage and distinct subpopulations of pre-cDCs committed to cDC1 or cDC2 lineages are already identifiable before they migrate to periphery[126].

TFs that play important roles as regulators of development of the cDC1 lineage include IRF8, BATF3, NFIL3 and ID2[127-130]. While epistatic relationships among these TFs and requirement for each factor at different stages of cDC1 development have been unclear, a recent study reported that cDC1 fate specification requires transient activation of E-protein-dependent enhancer located 41 kilobases downstream of the transcription start site of Irf8 (+41-kb Irf8 enhancer) in CDPs and pre-cDC1s[131]. However, this enhancer becomes inactive in mature cDC1s[131] and instead, completion of cDC1 development requires +32-kb Irf8 enhancer, to which Batf3 binds and maintains autoactivation of Irf8[132]. Consistent with switching in Irf8 enhancer usage, Nfil3 expression is required for the transition from $Zeb2^{hi}Id2^{lo}$ CDPs to $Zeb2^{lo}Id2^{hi}$ CDPs, which represent the earliest committed cDC1 progenitors, and exclusion of pDC potential by blocking activity of TCF4[133]. Additionally, Etv6 has been suggested as another important TF for

cDC1 development that optimizes the resolution of cDC1 and pDC expression programs and the functional fitness of cDC1[134]. STAT5 can also promote cDC1 production and inhibit pDC generation by stimulating Id2 expression in response to GM-CSF[108].

While it is well established that Irf4 is critical for development of cDC2s[135], there are multiple transcriptional programs and signaling pathways that possibly emerge after cDC1/cDC2 bifurcation and dictate development of different subsets of cDC2s, consistent with extensive heterogeneity of this population[47]. Esam^{high} splenic cDC2 subset requires Notch-RBPJ signaling and lymphotoxin beta receptor signaling for functional differentiation[50,136]. In addition, Klf4 is necessary for the emergence of cDC2 subset that is essential for Th2 response to several stimuli[137].

1.6 Alteration in DC development from progenitors during chronic viral infection

Multiple viral infections including parvovirus B19, cytomegalovirus, hepatitis B virus, dengue virus, measles virus, and LCMV can cause quantitative and qualitative defects in BM progenitor cells directly by infecting them and/or indirectly by altering the capacity of BM stromal cells to support progenitor development[138]. Depletion of early BM hematopoietic progenitor cells and impairment in their capacity to differentiate into DCs were also observed during HIV-1 infection[139,140]. In contrast, other papers have shown that TLR-Myd88 signaling stimulates differentiation of myeloid progenitors and even some lymphoid progenitors into DCs[141]. In line with this, vaccinia virus infection results in the expansion of hematopoietic stem cells and increased development of CLPs and pDCs[142]. On the other hand, one study showed that, when upon local injection of TLR agonists, CDPs were not altered in their lineage differentiation and proliferative capacity[143]. Instead, CDPs could sense TLR agonists migrate to reactive lymph nodes to preferentially give rise to DCs in inflamed lymph nodes[143]. Conflicting results from different

studies suggest that TLR challenge with synthetic agonists or pathogen can have differential effects on progenitors depending on its duration or specific localization.

Viral infection could also alter number and differentiation capacity of BM progenitor cells by affecting systemic cytokine milieu of the host. For example, DC progenitors generated under the influence of IL-10 can give rise to DC subset that induces antigen-specific expansion of functional regulatory T cells that could be activated to create an immunosuppressive environment[144]. On the other hand, activation of gp130, which can be utilized by IL-6, IL-11, IL-27, leukemia inhibitory factor (LIF), Oncostatin M (OSM), Ciliary NeuroTropic Factor (CNTF), cardiotrophin 1, and cardiotrophin-like cytokine[145], can promote expansion of multipotent progenitor (MPP) while inhibiting Flt3L-driven DC differentiation, whereas GM-CSF can drive differentiation of MPP into inflammatory DC[146]. Additionally, infection of BM cells with LCMV Cl13 or measles virus inhibits their differentiation into DCs in an IFN-I, STAT2-dependent manner[65,147]. Inflammatory cytokines can also affect DC development from progenitors by differentially regulating TF expression, as in the case of infection with intracellular pathogens where IL-12 and IFN-γ induce Batf and Batf2 that can compensate for the role of Batf3 in cDC1 development[148], and this could be also relevant in viral infection which induces similar inflammatory milieu.

1.7 Transcriptional and epigenetic regulation of immune cells during chronic viral infection

Adaptation of immune cells to chronic viral infection has been extensively studied in T cells at the genomic level. Gene expression profiles of exhausted CD8+ T cells in comparison to their functional counterparts from acute infection have been well characterized in the context of LCMV infection[149]. This study elucidated changes in expression of genes involved in multiple

pathways encompassing T cell receptor signaling, cytokine signaling, chemotaxis, adhesion, migration, and metabolism in an unbiased manner and defined distinct molecular signature of exhausted CD8+ T cells[149]. A growing body of evidence supports distinct chromatin features of different subsets of genes play active roles in differential biological responses in addition to gene expression differences[150]. Indeed, one study demonstrated that demethylation of the Pdcd1 locus (which encodes PD-1) commonly occurs in CD8+ T cells upon acute and chronic LCMV infection but is sustained only during chronic infection, leaving the locus poised for rapid PD-1 expression[151]. Recent studies have also characterized chromatin landscapes of exhausted CD8+ T cells from chronic LCMV infection and compared them to functional CD8+ T cells from acute LCMV infection[152,153]. These studies showed that CD8+ T cell exhaustion entailed a broad remodeling of enhancer landscape[152,153]. ~50% of chromatin-accessible regions were already differentially accessible between acute and chronic infection at d8 p.i. and large proportion of them persisted until d27 p.i.[153]. Moreover, an exhaustion-specific enhancer identified in this study regulated PD-1 expression[153]. These studies indicate that epigenetic regulation, in addition to regulation of gene expression, can play an important role in immune cell fate during viral infection.

TFs regulate multiple biological processes by differentially binding to accessible chromatin regions and regulating differential expression of their target genes. Differentiation into exhausted CD8+ T cells upon chronic viral infection also involved change in expression and binding of multiple TFs[149,152,153]. However, the expression level of a TF does not always correlate with its activity and a TF that does not vary in its own expression level can possibly exhibit differential activities and influential roles in different contexts[154]. Recently, a group developed a software package called Taiji, which integrates Assay for Transposase-Accessible Chromatin using sequencing (ATAC-seq) and RNA-sequencing (RNA-seq) data and implements personalized

PageRank analysis to assess the global biological importance of TFs in each condition based on chromatin features of their target genes and prediction of their activities[155]. This computational strategy has already successfully predicted TFs with previously unappreciated roles to have crucial regulatory functions in the differentiation of circulating and resident memory CD8+ T cells[156,157]. Collectively, these studies suggest that integration of gene expression, chromatin accessibility, TF expression and activity can provide a comprehensive view of regulatory network that can serve as a powerful tool to identify regulators of immune adaptation during viral infection in multiple cell types.

1.8 Bidirectional communication between immune and neuroendocrine pathways during viral infection

Viral infection can have further effects on host immune responses through modification of host endocrine system. Viruses can destroy endocrine organs and/or induce systemic production of soluble stress mediators. For example, hypothalamic-pituitary-adrenal (HPA) axis can be activated during persistent viral infection and restrain immune responses by releasing of glucocorticoids[158,159]. Persistent levels of glucocorticoids induced by overactivation of HPA axis can induce immunosuppressive effects by impairing Th1 immunity and zinc bioavailability[160]. Persistent levels of proinflammatory cytokines during viral infection can have further impacts on neuroendocrine pathway by inducing muscle and liver growth hormone resistance, inhibiting Insulin Growth Factor-1 (IGF-1) activity. They can also trigger release of leptin to reduce food intake, thereby inhibiting host growth and altering environmental signals[160], which in turn can reprogram immune cell metabolism and affect immune responses[161]. There are multiple mechanisms by which hormones can affect host immune responses and these have been well

characterized for glucocorticoids. For example, glucocorticoids bind the glucocorticoid receptors (GRs) and translocate to the nucleus to exert genomic effects or stay in the cytoplasm and mitochondria to exert non-genomic effects[162]. Importantly, the effect of neuroendocrine signals on immune cells is not only determined by the concentration of hormones, but also by sensitivity of the receptors for these mediators on immune cells[163]. For example, LCMV Cl13 infection induces peak corticosterone responses detectable at the serum level around day 7 p.i. while LCMV clone E350 fails to induce a glucocorticoid response[159]. However, LCMV E350-infected animals exhibited a significantly greater GR activation in response to an acute injection of corticosterone on day 7 p.i. compared to uninfected control mice, suggesting an increased sensitivity to corticosterone regardless of corticosterone concentration[164]. Collectively, these studies highlight that bidirectional communication between immune and neuroendocrine pathways that can significantly contribute to shaping immune responses during viral infection depending on hormone levels and sensitivity.

Chapter 2: Self-renewal and TLR signaling sustain exhausted pDCs during chronic viral infection

2.1 Summary

While characterization of T cell exhaustion has unlocked powerful immunotherapies, the mechanisms sustaining adaptations of short-lived innate cells to chronic inflammatory settings remain unknown. During murine chronic viral infection, we found that concerted events in BM and spleen mediated by IFN-I and TLR7 maintained a pool of functionally exhausted pDCs. In the BM, IFN-I compromised the number and the developmental capacity of pDC progenitors, which generated dysfunctional pDCs. Concurrently, exhausted pDCs in the periphery were maintained by self-renewal via IFN-I- and TLR7-induced proliferation of CD4- subsets. These findings unveil the mechanisms sustaining a self-perpetuating pool of functionally exhausted pDCs and provide a framework to decipher long-term exhaustion of other short-lived innate cells during chronic inflammation.

2.2 Introduction

While host adaptations have been extensively studied in adaptive immune compartments such as T cells and B cells, much less is known about the mechanisms mediating long-term adaptations in the innate immune system. It is unclear how innate immune adaptation can be sustained long-term given that (in contrast to T cells and B cells) innate cells are generally short-lived. pDCs are innate immune cells with potent IFN-I production capacity with important roles in antiviral defenses[25], but multiple murine and human chronic viral infections induce functional loss of pDCs accompanied by dynamic changes in their numbers[70-72,91,93,94,96]. However, the

mechanisms maintaining the numbers of exhausted pDCs and their functional loss during chronic settings remain unknown.

In the present study, we used persistent LCMV Cl13 infection in its natural murine host to unravel the mechanisms underlying the long-term maintenance of exhausted pDCs and their impaired IFN-I-production-capacity. We revealed that pDC exhaustion coincided with reduction of multiple BM progenitors with potential to generate pDCs and their failure to generate functional pDCs, which correlated with down-regulation of the pDC master regulator E2-2 and its downstream target TFs, SpiB and Bcl11a. Strikingly, such BM suppression was accompanied by sustained proliferation of $CD4^-$ pDC subsets in BM and periphery, which renewed the exhausted pDC pool. Importantly, we found that IFN-I receptor (IFNAR) signaling was responsible for suppression of progenitors accompanied by their E2-2 down-regulation in the BM while, together with TLR7, induced pDC proliferation. On the other hand, IFNAR was dispensable for pDC functional loss. Together, these findings provide the first anatomical, cellular and molecular explanation for the long-term exhaustion of a typically short-lived IFN-I producing cell during chronic viral infections.

2.3 Results

2.3.1 Both spleen and BM pDCs exhibited sustained functional exhaustion during chronic LCMV infection

We have previously reported that spleen pDCs, identified by co-expression of B220 and CD11c, exhibited long-lasting functional exhaustion during chronic LCMV infection (i.e. days 5-30 p.i.[72]). To further validate these findings and investigate if pDC exhaustion also occurs in the BM, we adopted a more rigorous pDC gating strategy that included the pDC marker BST2[165,166]

(Fig. 2-1A). Consistent with our previous report[72], splenic pDCs from both LCMV ARM- and Cl13-infected mice showed a dramatic reduction in IFN-I production in response to CpG when compared to uninfected controls at days 5 and 10 p.i., which was sustained only in pDCs from Cl13-infected mice at day 30 p.i. (Fig. 2-1B). Importantly, sustained suppression of IFN-I production was also observed in BM pDCs from Cl13 (but not ARM)-infected mice (Fig. 2-1C). Furthermore, the more rigorous pDC gate revealed reduced TNF-α production by splenic and BM pDCs isolated at day 5 or 10 after either ARM or Cl13 infection (Fig. 2-2A). This defect was, however, fully or partially recovered 30 days after both infections. Finally, expression of CD86 after CpG stimulation was comparable or enhanced in splenic and BM pDCs from ARM or Cl13 infected versus uninfected mice (Fig. 2-2B), indicating that exhausted pDCs were still responsive to TLR stimulation. These data indicated that both splenic and BM pDCs acquired functional defects upon infection with either acute or persistent LCMV. Importantly, while pDCs from acutely infected mice recovered few weeks after infection, functional pDC exhaustion was sustained in the chronic setting.

2.3.2 BM pDC progenitors exhibited sustained reduction and inability to generate functional pDCs after chronic LCMV infection

Given that pDCs are short-lived[167,168], we reasoned that sustained pDC exhaustion during chronic LCMV infection (i.e. day 5-30 p.i.[72]) might involve long-term adaptations occurring at the level of pDC progenitors in the BM. To evaluate this possibility, we first assessed the effect of acute and chronic LCMV infection on the numbers of BM progenitors that have been reported to generate pDCs: CLP, CDP, and CD115- CDP-like pDC progenitors (reviewed in [27]). As shown in Fig. 2-1D, the percentage and number of CLPs were reduced by day 10 p.i. and numbers remained

significantly decreased only in Cl13-infected mice by day 30 p.i.. The numbers of CDPs and CD115- progenitors tend to initially increase at day 5 p.i. but were also reduced by day 10 p.i. in both ARM- and Cl13-infected mice compared to uninfected controls. Importantly, at day 30 p.i., CD115- progenitor numbers were restored while CDP numbers remained reduced in Cl13 (but not ARM)-infected mice. Similarly, the numbers of common myeloid progenitors (CMP), which can give rise to pDCs via CDP[115], were also reduced in both ARM- and Cl13- infected mice at day 10 p.i. while such reduction was sustained only in the latter group at day 30 p.i. (Fig. 2-3A&B). In contrast, the numbers of granulocyte-monocyte progenitors (GMP) were not significantly reduced in neither acute nor chronic LCMV infections at any of the time points studied (Fig. 2-3A&C). Remarkably, when BM was cultured in the presence of Flt3L to induce DC development *in vitro*, pDC generation was significantly compromised in cultures derived from LCMV Cl13 or ARM-infected mice at day 5, 10 and 30 p.i. (Fig. 2-1E). To validate these findings *in vivo*, we transferred Lin-c-kit$^{int/lo}$Flt3+ cells from uninfected or LCMV Cl13-infected mice at day 30 p.i. into uninfected or infection-matched recipient mice, respectively, and quantified donor-derived pDCs after 10 days. In line with the BM-Flt3L culture results (Fig. 2-1E), we observed a profound decrease in the number of donor-derived pDCs when recipient mice had received BM progenitors from Cl13-infected versus uninfected donors (Fig. 2-3D&E).

To further understand BM progenitor adaptations after infection, we next evaluated the function of pDCs derived from BM progenitors. pDCs from Flt3L-cultures of BM obtained from LCMV ARM- or Cl13-infected mice at days 5 and/or 10 p.i. showed signs of functional loss as indicated by their ablated IFN-I production in response to TLR stimulation (Fig. 2-1F). Importantly, however, this compromised BM capacity to generate functional pDCs was sustained in LCMV Cl13-infected mice by day 30 p.i., whereas BM-derived pDCs from LCMV ARM-infected mice

exhibited restored IFN-I production upon CpG-A stimulation (Fig. 2-1F), although we continued observing reduced response to CpG-B at day 30 after ARM infection (not shown).

Together, these results indicated that both acute and chronic infections compromised for long-term the ability of the BM to generate pDCs. In addition, our results showed sustained ablation of BM progenitors with potential to generate pDCs (e.g. CLP and CDP) and lasting functional exhaustion of BM-derived pDCs in chronically infected hosts, suggesting that multiple mechanisms curtailed BM generation of functional pDCs during chronic infection.

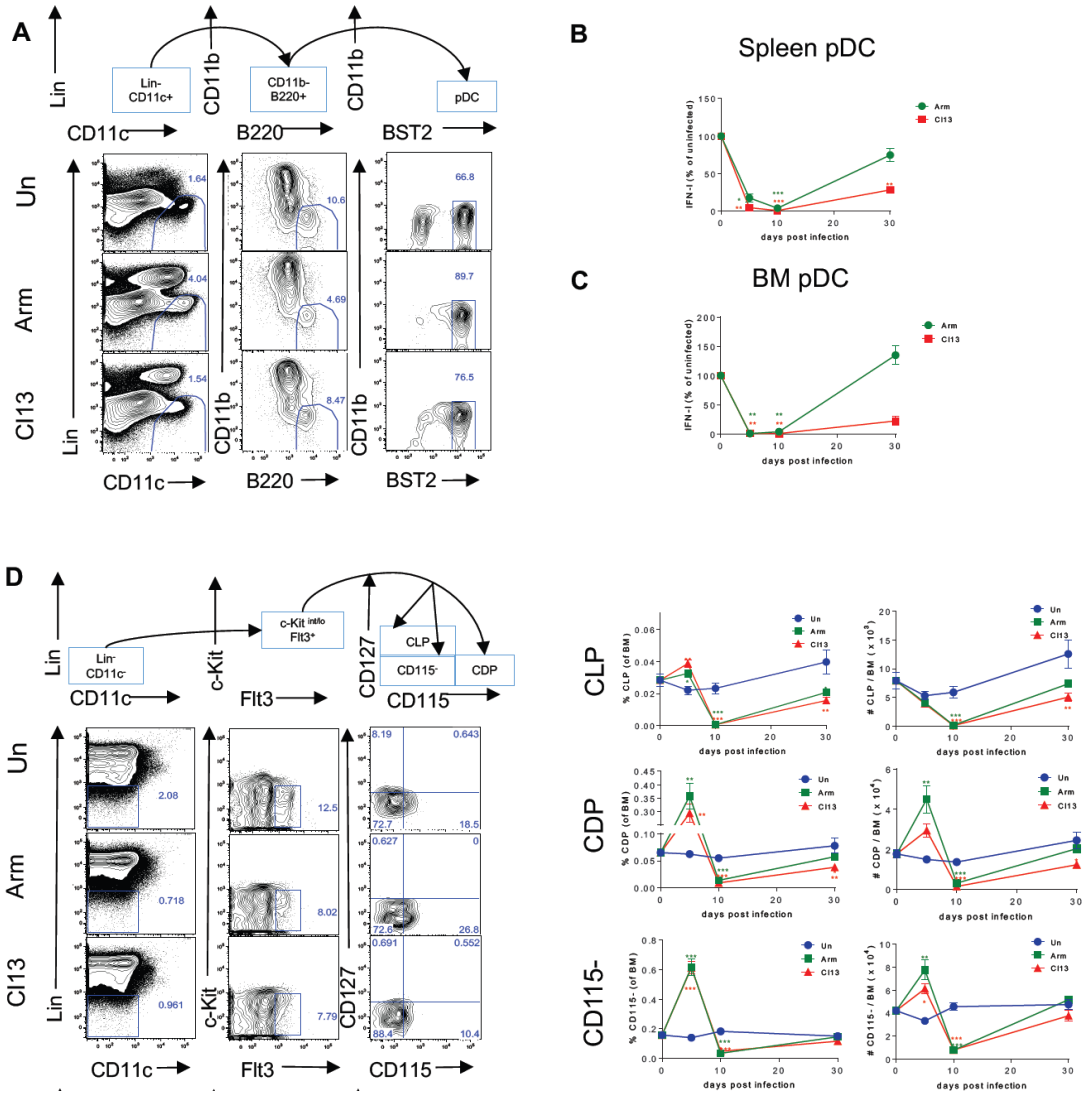

Figure 2-1. BM pDC progenitors are reduced in number and have compromised capacity to generate functional pDCs long-term after chronic LCMV infection. Wild-type (WT) mice were infected with LCMV ARM (green) or Cl13 (red) or left uninfected (blue) and sacrificed at days 5, 10, and 30 p.i. (A) Representative flow cytometric analysis of pDCs as Lin$^-$ CD11c$^+$CD11b$^-$B220$^+$BST2$^+$ in spleen at day 10 p.i. Lineage-negative gating (Lin) includes markers for Thy1.2, CD19, and NK1.1. (B-C) FACS-purified splenic pDCs (B) or BM pDCs (C) were stimulated with CpG-B for 15 hours and IFN-I activity in the supernatant was quantified. Graphs depict the percentage change in IFN-I activity normalized to the uninfected mice processed in parallel at each time point. (D) Representative flow cytometric analysis of BM pDC progenitors at day 10 p.i. where CLPs were identified as Lin$^-$c-kit$^{int/lo}$Flt3$^+$CD115$^-$CD127$^+$, CDPs as Lin$^-$c-kit$^{int/lo}$Flt3$^+$CD115$^+$CD127$^-$, and CD115$^-$ as Lin$^-$c-kit$^{int/lo}$Flt3$^+$CD115$^-$CD127$^-$. Lin includes markers for Thy1.2, CD19, NK1.1, CD3, CD4, CD8, B220, CD11b, Gr-1, and Ter119. Graphs depict the percentage (left) and the absolute number (right) of indicated progenitors in BM at each time point.

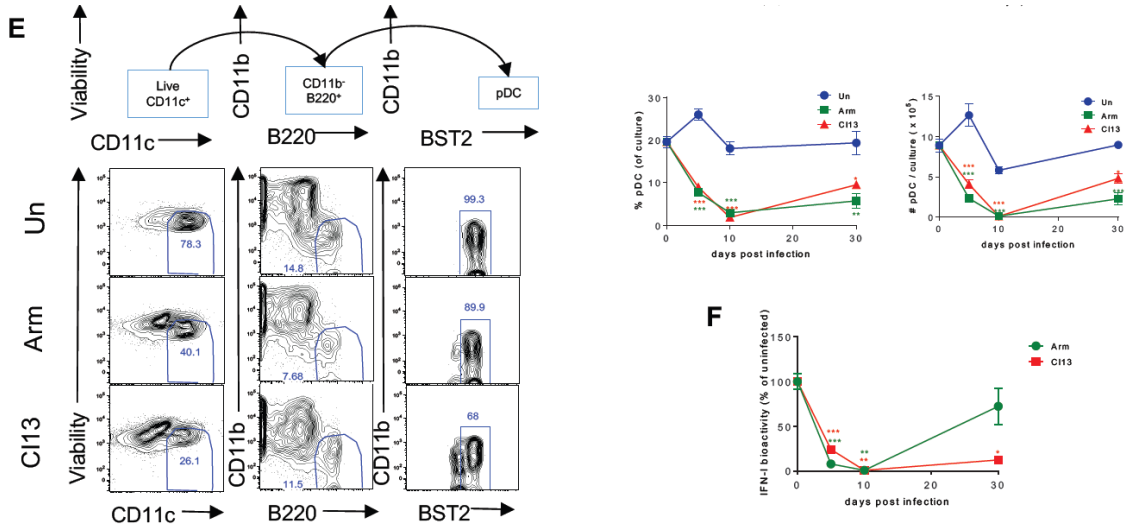

Figure 2-1. BM pDC progenitors are reduced in number and have compromised capacity to generate functional pDCs long-term after chronic LCMV infection, **Continued** (E) BM cells were cultured with Flt3L and pDCs were identified as $CD11c^{+}CD11b^{-}B220^{+}BST2^{high}$ at day 8 post-culture. Representative FACS plots for BM-Flt3L-derived pDCs and graphs depicting their percentage (left) and absolute number (right) in the culture are shown. (F) FACS-purified BM-Flt3L-derived pDCs were stimulated with CpG-A for 15 hours and IFN-I activity in the supernatant was quantified. Graph depicts the percentage change in IFN-I activity normalized to the culture from uninfected mice processed in parallel at each time point. Graphs depict mean ± SEM. Data are representative of 2-3 independent experiments with 3-10 mice/group. *p<0.05, **p<0.01, ***p<0.001 (one-way Anova to compare ARM-infected (green asterisks) and Cl13-infected (red asterisks) groups to uninfected group processed in parallel at each time point).

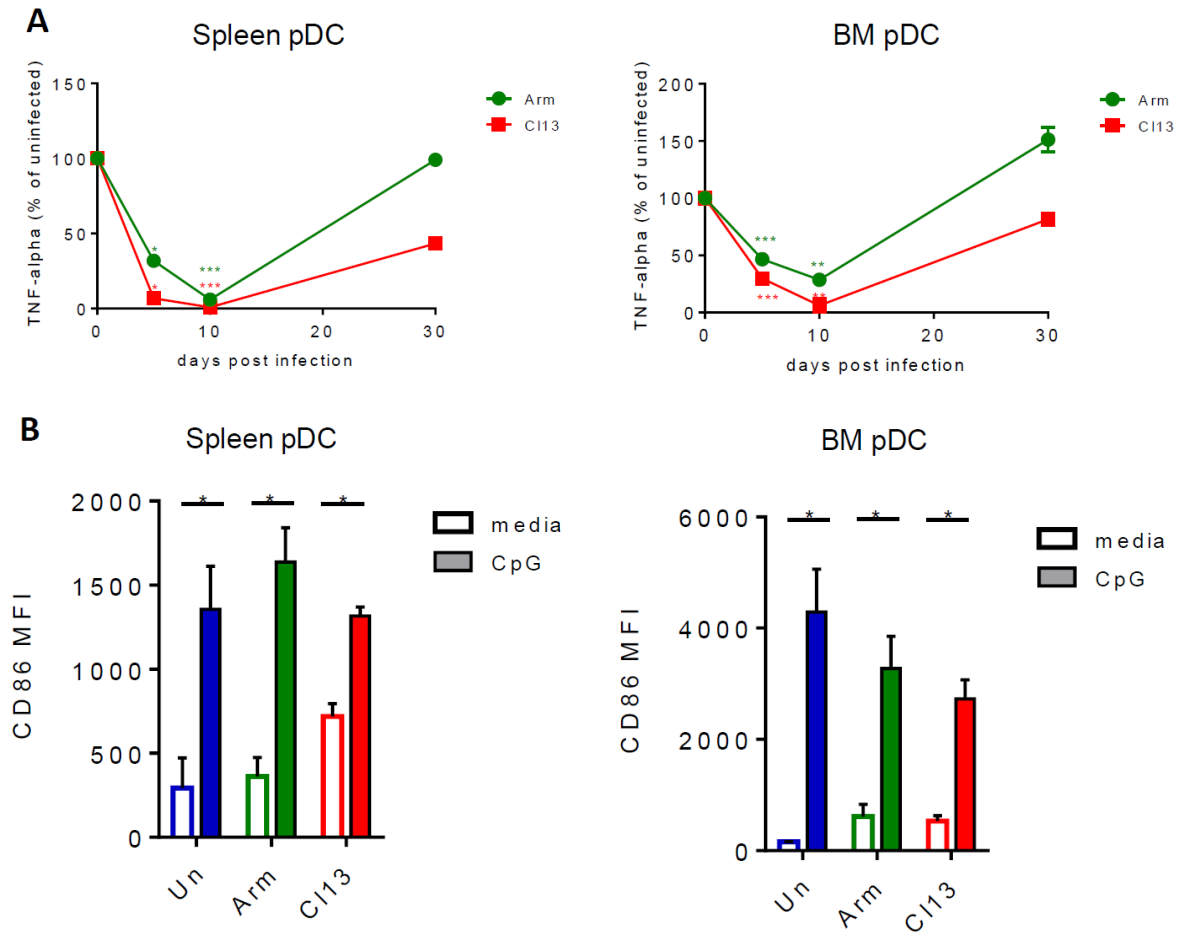

Figure 2-2. pDCs respond to TLR stimulation, but produce reduced amount of TNF-alpha early during acute and chronic LCMV infection. Wild-type (WT) mice were infected with LCMV ARM (green) or Cl13 (red) or left uninfected (blue) and sacrificed at day 5, 10, and 30 p.i. FACS-purified splenic pDCs (left) or BM pDCs (right) were stimulated with CpG-B 1668 for 15 hours. (A) ELISA was used to quantify TNF-α in the supernatant. Graphs depict the percentage change in TNF-α normalized to uninfected mice processed in parallel at each time point. (B) Flow cytometry was used to evaluate CD86 expression on pDCs. Graphs depict CD86 MFI in spleen pDCs at day 10 p.i. (left) and BM pDCs at day 5 p.i. (right) that were untreated (open bar) or stimulated with CpG-B (filled bar). Graphs depict mean ± SEM. Data are representative of 2-3 independent experiments with 3-10 mice/group. *p<0.05, **p<0.01, ***p<0.001 (one-way Anova to compare ARM-infected (green asterisks) and Cl13-infected group (red asterisks) to uninfected group processed in parallel at each time point (A) or unpaired, two-tailed t-test to compare CpG-B stimulated samples to unstimulated controls (B)).

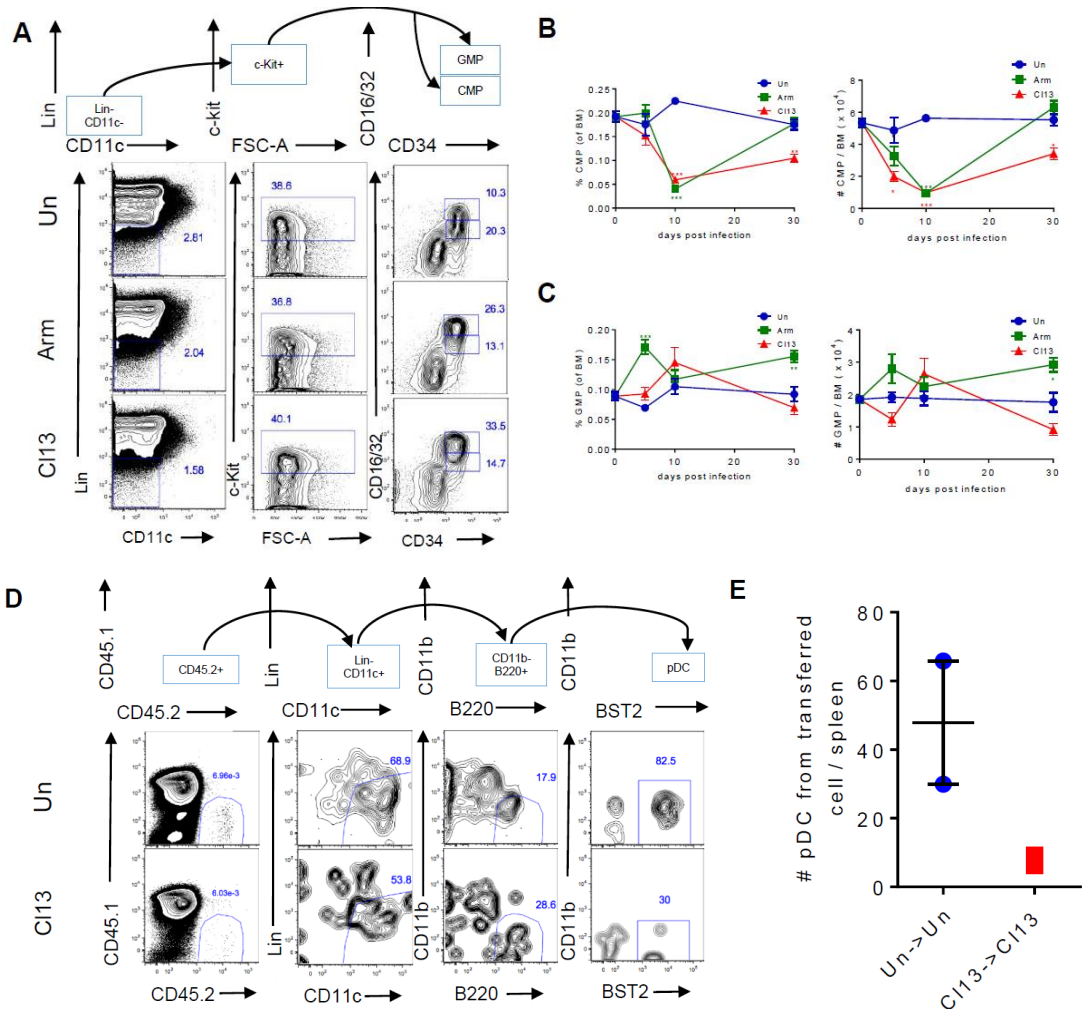

Figure 2-3. CMPs, but not GMPs, are reduced throughout Cl13 infection and BM progenitors show impaired capacity to generate pDCs *in vivo*. WT mice were infected with LCMV ARM (green) or Cl13 (red) or left uninfected (blue) and sacrificed at days 5, 10, and 30 p.i. (A) Gating strategy and representative FACS plots for CMPs and GMPs in BM at day 10 p.i. where CMPs were identified as Lin$^-$c-kit$^+$CD34$^+$CD16/32^{int} and GMPs as Lin$^-$c-kit$^+$CD34$^+$CD16/32^{hi}. Lin includes markers for Thy1.2, CD19, NK1.1, CD3, CD4, CD8, B220, CD11b, Gr-1, and Ter119. (B-C) Proportions (left) and absolute numbers (right) of CMPs (B) and GMPs (C) in BM. (D-E) FACS-purified Lin$^-$c-Kit$^{int/lo}$Flt3$^+$ progenitors (1.5 x 10^4 cells) from CD45.2$^+$ uninfected or Cl13-infected donor mice at day 30 p.i. were injected intravenously into CD45.1$^+$ non-irradiated uninfected or infection-matched recipients, respectively. Mice were sacrificed at day 10 after transplantation (day 40 p.i.), and spleen cells were analyzed by flow cytometry after T and B cell depletion. (D) Gating strategy and representative FACS plots for donor-derived spleen pDCs within live cells. (E) Absolute numbers of CD45.2$^+$ donor-derived spleen pDCs at day 10 after transplantation. Graphs depict mean + SEM. Data are representative of 2-3 independent experiments with 3-5 mice/group (A-C) or pooled from 2 independent experiments where 3-4 mice / group were pooled for analysis in each experiment. *p<0.05, **p<0.01, ***p<0.001 (one-way Anova to compare ARM-infected (green asterisks) and Cl13-infected (red asterisks) groups to uninfected group processed in parallel at each time point (B-C)).

2.3.3 Splenic and BM pDCs proliferated and expanded CD4- subsets throughout chronic LCMV infection

We next investigated whether the aforementioned loss in BM pDC progenitors and diminished BM pDC generation affected overall pDC numbers. In agreement with apoptosis of pDCs early during infection[97] and the long-term reduction in the capacity of BM to generate pDCs that we observed after LCMV ARM and Cl13 infections (Fig 2-1E), spleen pDC numbers were significantly reduced at days 5 and 30 after both infections (Fig. 2-4A, [72]). Strikingly, however, the numbers of BM pDCs were mostly unchanged at all the time points studied (Fig. 2-5A) and spleen pDC numbers were restored or even enhanced at day 10 (Fig. 2-4A) after LCMV ARM and Cl13 infections. To determine how pDC numbers were maintained or restored despite the reduced generation of pDCs from the BM, we investigated the presence of proliferating cells within the spleen and BM pDC population over the course of LCMV ARM and Cl13 infection. Consistent with previous studies[167,168], we detected <2% proliferating pDCs in the spleen from uninfected mice, as indicated by expression of the nuclear antigen Ki67 and in vivo BrdU incorporation (Fig. 2-4B&C). In sharp contrast, we observed a substantial number of proliferating pDCs in spleen (Fig. 2-4B&C) and BM (Fig. 2-5B&C) from both LCMV ARM and Cl13 infected mice at day 5 p.i., a phenotype that was sustained (albeit to lesser extent) at day 10 and 30 after chronic (but not acute) LCMV infection. Importantly, BrdU was also incorporated by pDCs from LCMV Cl13-infected, but not uninfected, mice when splenocytes were cultured *ex vivo*, further supporting the proliferative capacity of splenic pDCs during LCMV Cl13 infection (Fig. 2-5D).

Proliferating CD4-CCR9- and CD4-CCR9+ pDC subsets, which exhibit pDC phenotypic markers and potent IFN-I production capacity, have been reported in the BM of uninfected mice as immature pDCs or immediate precursors of CD4+CCR9+ pDCs[119,168,169]. On the other hand,

almost all splenic pDCs express CCR9 and do not proliferate under steady-state conditions[119,168,169]. Strikingly, in contrast to almost undetectable CD4-CCR9- pDCs in uninfected mice, we detected an increased number of CD4-CCR9- cells within splenic pDCs from both LCMV ARM- and Cl13-infected mice at day 5 p.i., a phenotype that was sustained at day 10 and 30 after chronic (but not acute) LCMV infection (Fig. 2-4D). Moreover, while none of the spleen pDC subsets exhibited significant proliferation in uninfected mice, both CD4-CCR9+ and CD4-CCR9- pDC subpopulations contained a significant proportion of proliferating cells at day 5 after either ARM or Cl13 infections, and this was only sustained in the latter infection setting at days 10 and 30 p.i. (Fig. 2-4E). A similar pattern was observed in the BM at day 5, 10 and 30 after ARM and Cl13 infection (Fig. 2-5E&F) and in both compartments the CD4-CCR9- pDC subpopulation showed the highest proliferation in ARM-infected mice at day 5 p.i. and throughout Cl13 infection (Fig. 2-4E and 2-5F). Altogether, these data indicated that while BM pDC generation was compromised, CD4- subsets within differentiated BM and spleen pDCs significantly expanded to replenish functionally compromised pDCs early after acute and chronic LCMV infections and this phenotype was sustained for long-term in the chronic infection setting.

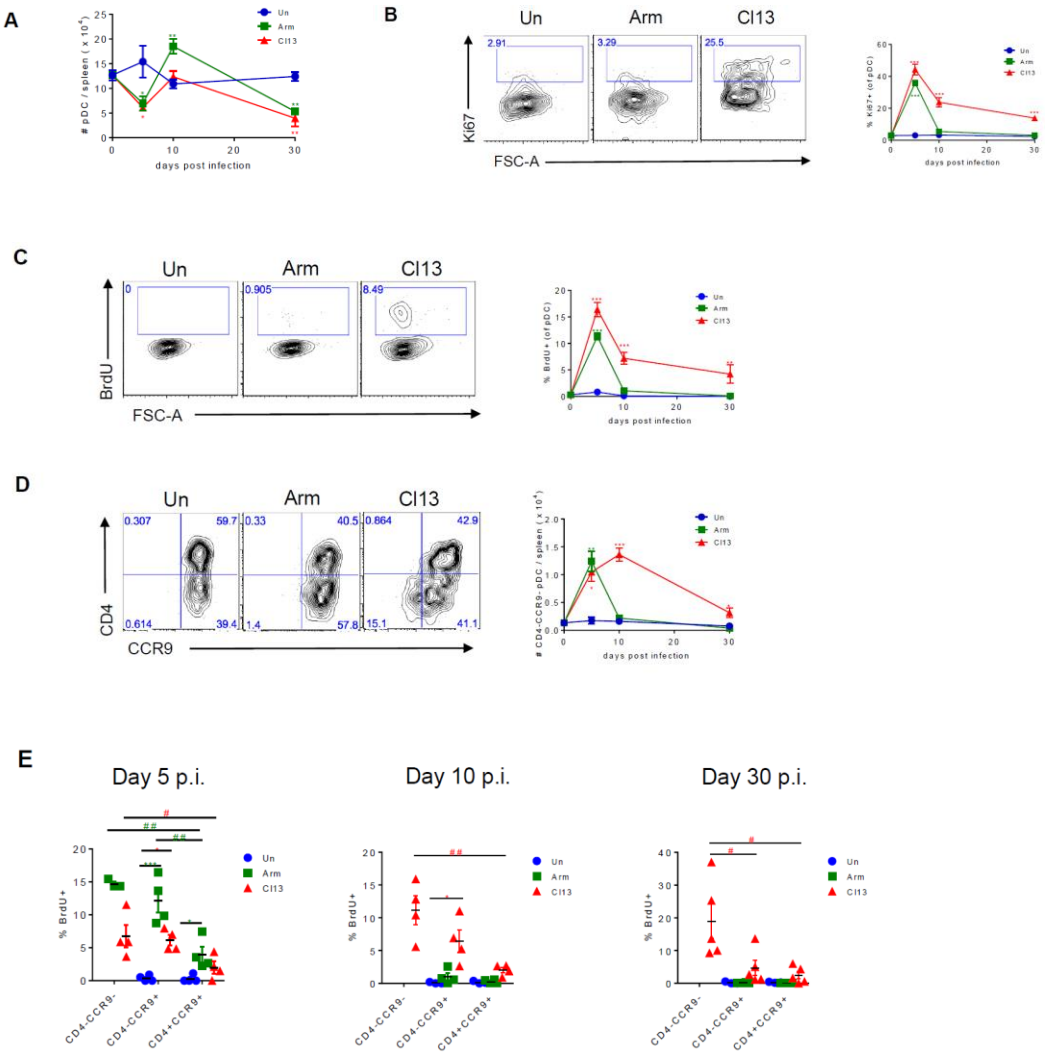

Figure 2-4. Splenic pDCs proliferate and CD4- subsets expand throughout chronic LCMV infection. WT mice were infected with LCMV ARM (green) or Cl13 (red) or left uninfected (blue) and sacrificed at day 5, 10, and 30 p.i. Splenic pDCs were analyzed to determine their absolute number (A), Ki67 expression (B), BrdU incorporation *in vivo* (C), absolute number of $CD4^{-}CCR9^{-}$ pDC subset (D) and BrdU incorporation by $CD4^{+}CCR9^{+}$, $CD4^{-}CCR9^{+}$, and $CD4^{-}CCR9$- subsets (E). (B-D) Representative FACS plots indicate spleen pDCs from day 10 p.i. (A-E) Graphs depict mean ± SEM. Data are representative of 2-3 independent experiments with 3-5 mice/group. (A) Data obtained at day 10 after Cl13 infection are representative of 11 independent repeats with 7 and 4 experiments showing enhanced or unchanged pDC numbers vs. uninfected controls, respectively. (E) Symbols represent individual mice. *, # $p<0.05$, **, ## $p<0.01$, *** $p<0.001$ (one-way Anova to compare ARM-infected (green asterisks) and Cl13-infected group (red asterisks) to uninfected group processed in parallel at each time point (A-E) or to compare $CD4^{+}CCR9^{+}$, $CD4^{-}CCR9^{+}$, and $CD4^{-}CCR9^{-}$ subsets in ARM-infected (green pounds) or Cl13-infected group (red pounds) (E)).

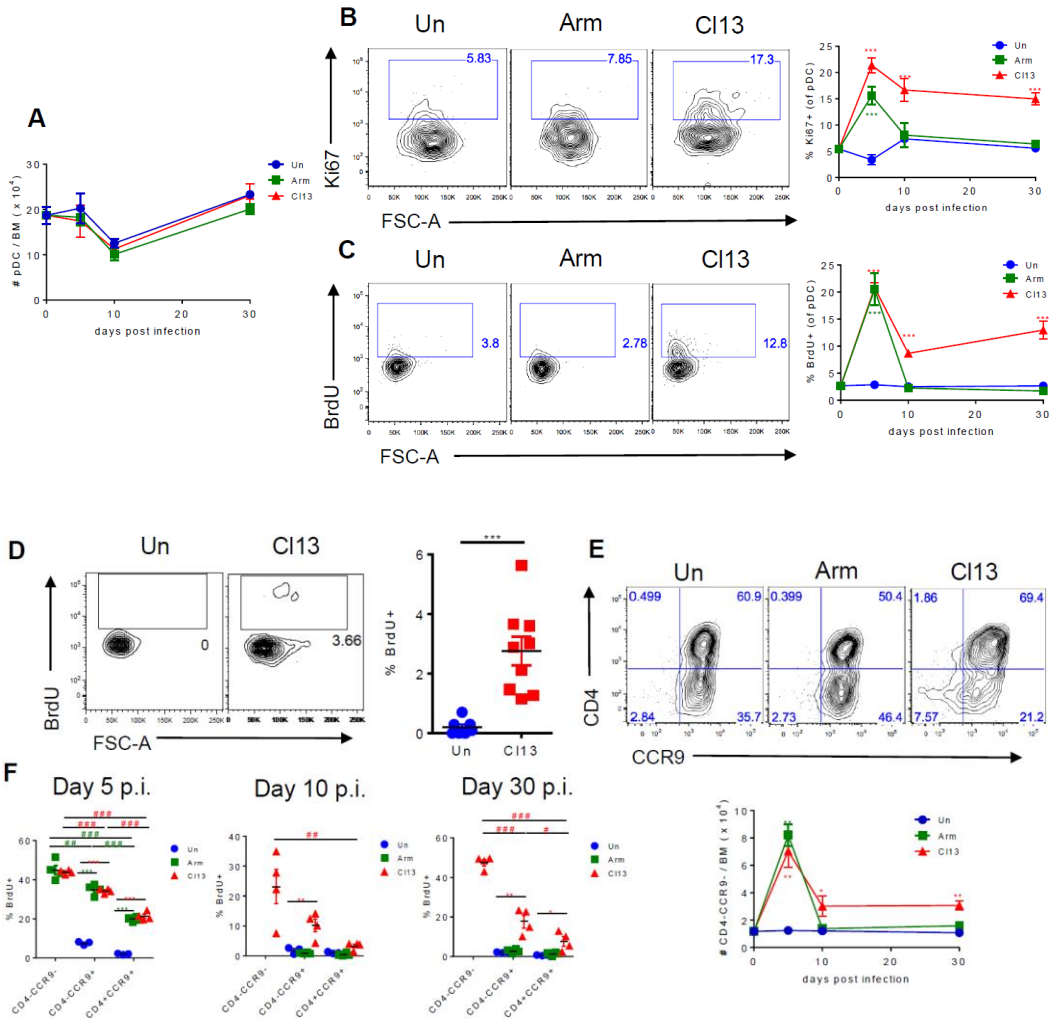

Figure 2-5. Local proliferation of pDCs with expansion of CD4- pDC subsets is sustained in BM of Cl13 infected mice and splenic pDCs incorporate BrdU *ex vivo*. (A-C, E-F) WT mice were infected with LCMV ARM (green) or Cl13 (red) or left uninfected (blue) and sacrificed at day 5, 10, and 30 p.i. BM pDCs were analyzed to determine their absolute number (A), Ki67 expression (B), BrdU incorporation *in vivo* (C), absolute number of $CD4^{-}CCR9^{-}$ subsets (E) and BrdU incorporation by $CD4^{+}CCR9^{+}$, $CD4^{-}CCR9^{+}$, and $CD4^{-}CCR9^{-}$ subsets at each time point. (F). Representative FACS plots for BM pDCs from day 10 p.i. are shown (B, C, and E). (D) WT mice were infected with LCMV Cl13 (red) or left uninfected (blue) and sacrificed at day 9 p.i. Representative FACS plots for BrdU incorporation by splenic pDCs after 7 hour *ex vivo* culture in the presence of BrdU. Graphs depict mean ± S.E.M . and symbols represent individual mice. Data are representative of 2-3 independent experiments with 3-5 mice/group (A-C, E-F). Data are pooled from 2 independent experiments with 3-5 mice/group (D). *, # $p<0.05$, **, ## $p<0.01$, ***, ### $p<0.001$ (one-way Anova to compare ARM-infected (green asterisks) and Cl13-infected (red asterisks) group to uninfected group processed in parallel at each time point (A-C, E-F) or to compare $CD4^{+}CCR9^{+}$, $CD4^{-}CCR9^{+}$, and $CD4^{-}CCR9^{-}$ subpopulations in ARM-infected (green pounds) or Cl13-infected group (red pounds) (F) or unpaired, two-tailed t-test (D)).

2.3.4 E2-2, SPIB and BCL11A are down-regulated in pDCs and their progenitors from LCMV Cl13-infected mice

Given that the aforementioned phenotypes in BM progenitors and differentiated pDCs were all present at day 9 after Cl13 infection (Fig. 2-1. 2-4 and 2-5), we focused on this time-point and infection model to characterize their adaptations at the transcriptional level and the mechanisms involved. Because the class I helix-loop-helix TF E2-2 is a master regulator of pDC development, lineage commitment and function[106], we first compared E2-2 expression in BM progenitors and pDCs from uninfected and Cl13-infected mice. We observed a significant down-regulation in the transcript levels of E2-2 (encoded by *Tcf4*) in FACS-purified BM progenitors and splenic pDCs isolated at day 9 p.i. from Cl13-infected vs. uninfected mice (Fig. 2-6A&B). The down-regulation of *Tcf4* transcripts in Cl13-infected mice appeared of functional significance as transcripts of downstream target TFs, SPIB and BCL11A, also important in pDC development and/or function[106,109,111,112], were similarly reduced in both BM progenitors and splenic pDCs from Cl13-infected vs. uninfected mice (Fig. 2-6A&B), although *Bcl11a* reduction in splenic pDCs only reached significance in 2 out of 4 independent experiments (not shown). Furthermore, pDCs derived from BM of Cl13-infected mice also exhibited a significant decrease in transcripts of *Tcf4*, *Spib* and *Bcl11a* (Fig. 2-6C).

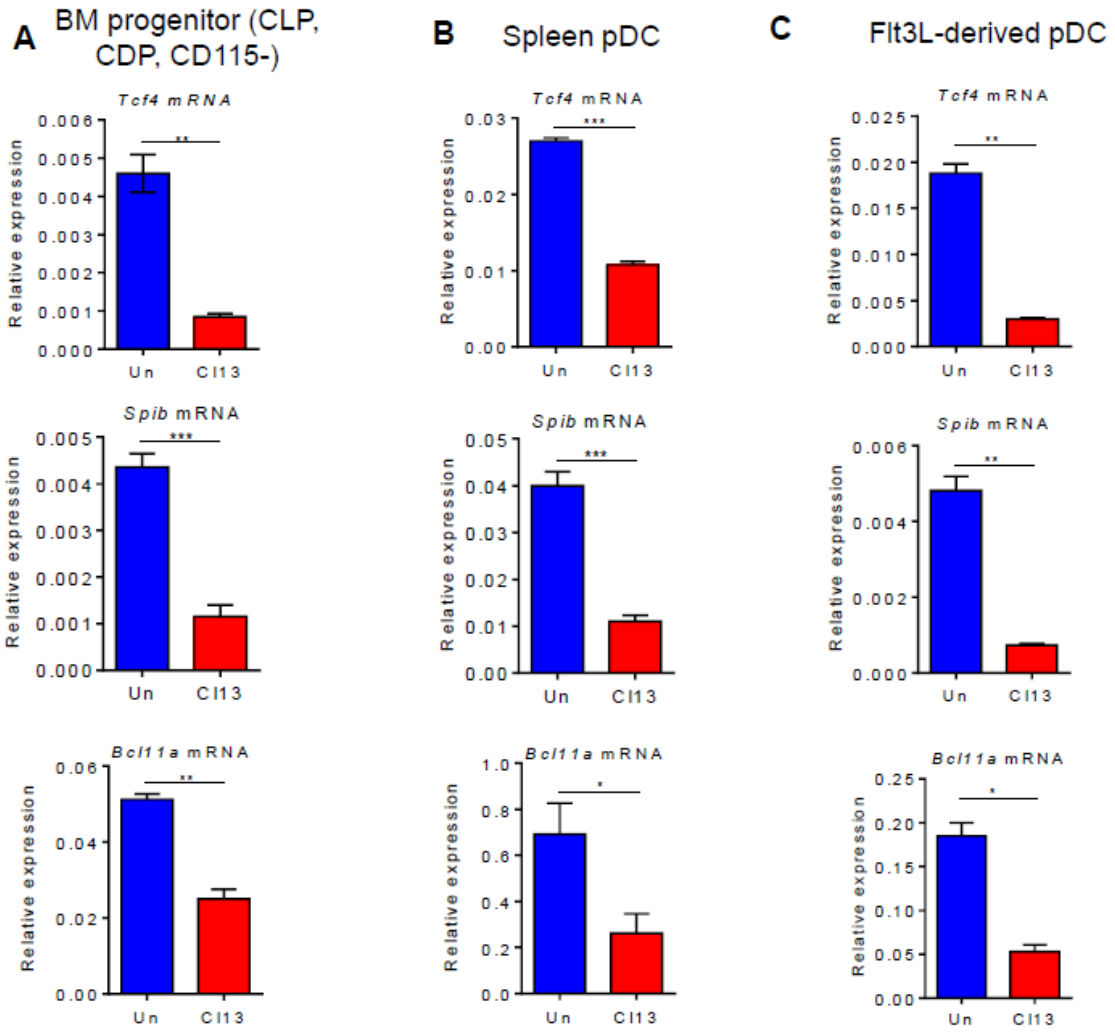

Figure 2-6. E2-2, Spib and Bcl11a are down-regulated in pDCs and their progenitors from LCMV Cl13-infected mice. WT mice were infected with LCMV Cl13 (red) or left uninfected (blue) and sacrificed at day 9 p.i. FACS-purified BM progenitors ($Lin^{-}c\text{-}kit^{int/lo}Flt3^{+}$) (A) and splenic pDCs (B) were evaluated for *Tcf4* (top), *Spib* (middle), and *Bcl11a* (bottom) transcripts relative to *Gapdh*. Lin includes markers for Thy1.2, CD19, NK1.1, CD3, CD4, CD8, B220, CD11b, Gr-1, and Ter119. (C) BM cells were cultured with Flt3L for 8 days and FACS-purified BM-Flt3L-derived pDCs were evaluated for *Tcf4* (top), *Spib* (middle), and *Bcl11a* (bottom) transcripts relative to *Gapdh*. Data are representative of 2-3 independent experiments with 3-4 mice / group. Bars depict mean ± SEM. *p<0.05, **p<0.01, ***p<0.001 (unpaired, two-tailed t-test).

2.3.5 IFNAR-signaling reduces pDC progenitor numbers, their E2-2 expression, and BM pDC generation during chronic LCMV infection

Next, we investigated the mechanisms underlying the numerical and developmental adaptations in BM pDC progenitors. Previous studies demonstrated that IFN-I inhibited development of conventional dendritic cells during chronic LCMV infection[65,147], whereas recombinant IFN-α treatment enhanced BM pDC generation *in vitro* and *in vivo*[170]. To test whether IFN-I induced in the context of Cl13 infection modulated BM pDC progenitors, we treated mice with anti-IFNAR neutralizing (n) Ab before and throughout the infection and monitored the number of BM progenitors and their potential to generate pDCs at day 9 p.i. We observed a restored or enhanced number of BM pDC progenitors in Cl13-infected mice treated with anti-IFNAR nAb in comparison to the isotype-treated group (Fig. 2-7A). Furthermore, significantly increased numbers of pDCs were generated in BM-Flt3L cultures from Cl13-infected mice that received anti-IFNAR nAb (Fig. 2-7B). Consistently, *Tcf4* expression was restored in pooled BM progenitors from anti-IFNAR nAb-treated Cl13-infected mice (Fig. 2-7C). To investigate if IFNAR signaling regulated BM pDC progenitors in a cell-intrinsic manner, we next analyzed WT:*Ifnar*$^{-/-}$ mixed BM chimeras after Cl13 infection. In these chimeras, we observed a slight increase in the *Ifnar*$^{-/-}$ (CD45.2^{+}) vs. WT (CD45.1^{+}) BM pDC progenitors (Fig. 2-7D), suggesting that IFN-I regulation of BM progenitors was partly cell-intrinsic. In contrast, no difference was detected in *Tcf4* expression in BM progenitors from WT vs. *Ifnar*$^{-/-}$ compartments (Fig. 2-7E), indicating that IFN-I also regulated BM progenitors in a cell-extrinsic manner.

Altogether, these results demonstrated that IFN-I regulated BM pDC progenitors via cell-intrinsic and -extrinsic pathways, contributing to the numerical reduction of BM progenitors, their diminished E2-2 expression, and their limited capacity to generate pDCs.

2.3.6 IFNAR signaling promotes splenic pDC proliferation and expansion of CD4$^-$ pDC subsets during chronic LCMV infection, but is dispensable for pDC functional exhaustion

IFN-I signaling has been shown to induce pDC apoptosis after viral infections[97]. Thus, we reasoned that by preventing pDC apoptosis and restoring BM pDC generation, IFNAR blockade should increase the number of pDCs in periphery. However, LCMV Cl13-infected mice that received anti-IFNAR nAb exhibited reduced numbers of splenic pDCs compared with their isotype-treated counterparts at day 9 p.i. (Fig. 2-8A). Because the number of splenic pDCs during Cl13 infection would be impacted by pDC proliferation, we next investigated whether anti-IFNAR nAb treatment modulated proliferating pDCs. We observed that IFNAR blockade during Cl13 infection diminished pDC proliferation, as indicated by reduced Ki67$^+$ and BrdU$^+$ pDCs compared with isotype treatment in infected mice (Fig. 2-8B&C). Consistently, the numbers of CD4$^-$CCR9$^-$ and CD4$^-$CCR9$^+$ splenic pDC subsets were reduced in infected mice that received anti-IFNAR nAb, while the number of CD4$^+$CCR9$^+$ pDCs was not significantly changed (Fig. 2-8D). To investigate if the IFN-I induction of pDC proliferation was cell-intrinsic, we again analyzed WT:*Ifnar*$^{-/-}$ mixed BM chimeras. We observed that Ki67 expression and *in vivo* BrdU incorporation were significantly reduced in *Ifnar*$^{-/-}$ vs. WT pDCs from Cl13-infected chimeras (Fig 2-8E&F), indicating that IFN-I promoted pDC proliferation in a cell-intrinsic manner. These data demonstrated that IFN-I induced the expansion of highly proliferative pDC subsets and promoted self-renewal of the exhausted pDC pool.

We next investigated the effect of IFN-I on the pDC functional-loss during chronic LCMV infection. We observed that both BM-derived and splenic pDCs from Cl13-infected mice treated with anti-IFNAR nAb or isotype control showed similarly impaired IFN-I production after *ex vivo* TLR stimulation (Fig. 2-9A&B). These data suggested that the loss of pDC IFN-I-production

capacity occurred via an IFNAR-independent pathway. Given that arenavirus nucleoprotein (NP) can suppress IFN-I induction[171] and that pDCs are productively infected by LCMV Cl13[172], we explored the possibility that the suppression of pDC IFN-I production could be explained by overwhelming viral dissemination and NP expression in pDCs. Flow cytometric analysis of LCMV NP, however, demonstrated that the majority of pDCs did not express detectable NP at day 9 after Cl13 infection (Fig. 2-9C), suggesting that loss of pDC IFN-I production capacity may be, at least in part, a consequence of cellular adaptations to chronic viral infection and could not be fully explained by an anti-IFN-I effects of viral products in infected pDCs.

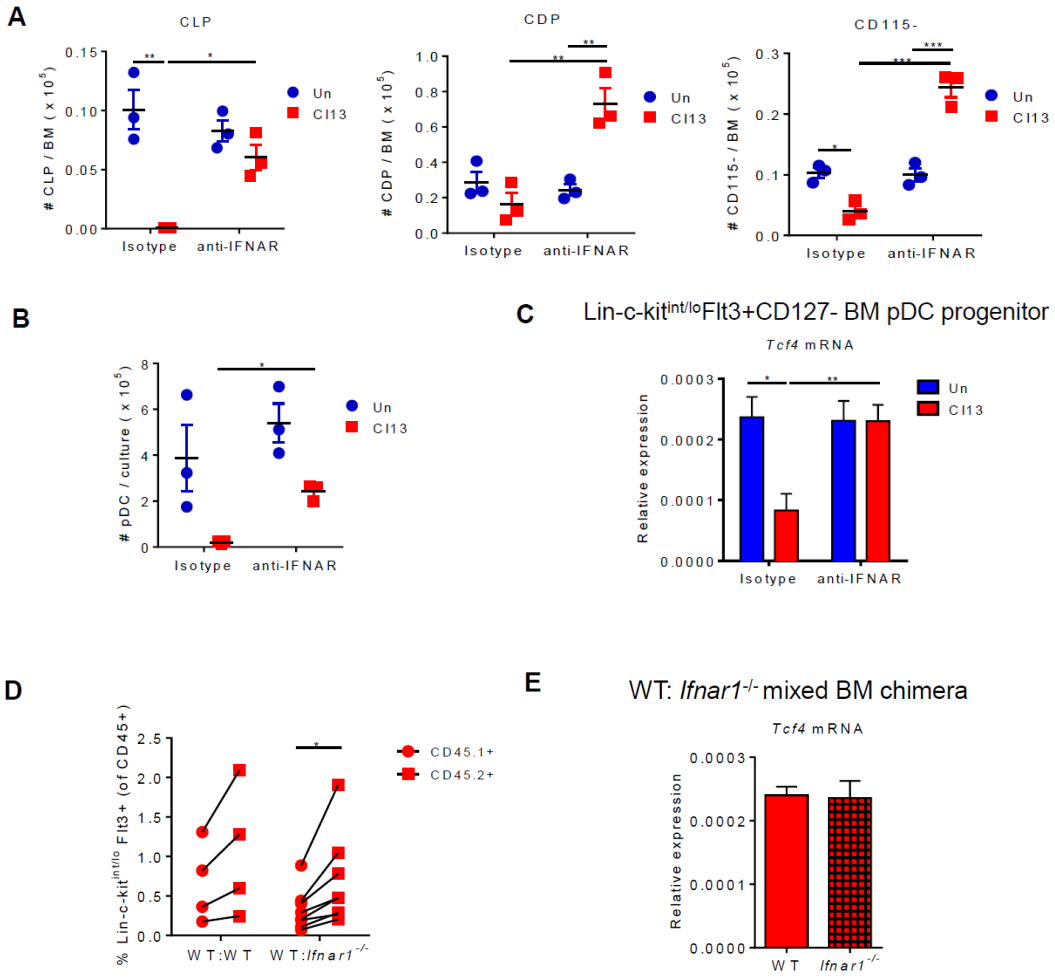

Figure 2-7. IFN-I signaling suppresses BM pDC progenitors during chronic LCMV infection. (A-C) WT mice were treated with isotype or anti-IFNAR nAb beginning 1 day before and throughout LCMV Cl13 infection and sacrificed at day 9 p.i. Absolute number of CLPs, CDPs, and CD115$^-$ (A) and pDCs derived from BM-Flt3L-cultures (continuing treatment with isotype or anti-IFNAR nAb *in vitro*) at day 8 post-culture (B) were quantified. (C) FACS-purified BM pDC progenitors (Lin-c-kit$^{int/lo}$Flt3$^+$CD127$^-$) were evaluated for *Tcf4* expression relative to *Gapdh*. Lin includes markers for Thy1.2, CD19, NK1.1, CD3, CD4, CD8, B220, CD11b, Gr-1, and Ter119. (D-E) Mixed BM chimeras were generated using BM from WT (CD45.1$^+$) and WT or *Ifnar*$^{-/-}$ (CD45.2$^+$) mice and infected with LCMV Cl13 for 9 days. (D) Percentages of Lin$^-$c-kit$^{int/lo}$Flt3$^+$ pDC progenitors within CD45.1$^+$ or CD45.2$^+$ cells in BM of mixed chimeras. Connected symbols indicate values from the same mouse. (E) FACS-purified Lin$^-$c-kit$^{int/lo}$Flt3$^+$ BM pDC progenitors from WT and *Ifnar*$^{-/-}$ compartment were evaluated for *Tcf4* transcripts relative to *Gapdh*. Bars depict mean ± SEM and symbols represent individual mice. Data are representative of 2-3 independent experiments with 3-4 mice / group (A-C and E) or pooled from 2 independent experiments with 2-4 mice/group (D). *p<0.05, **p<0.01 (two-way Anova (A-C), paired t-test (D), or unpaired, two-tailed t-test (E)).

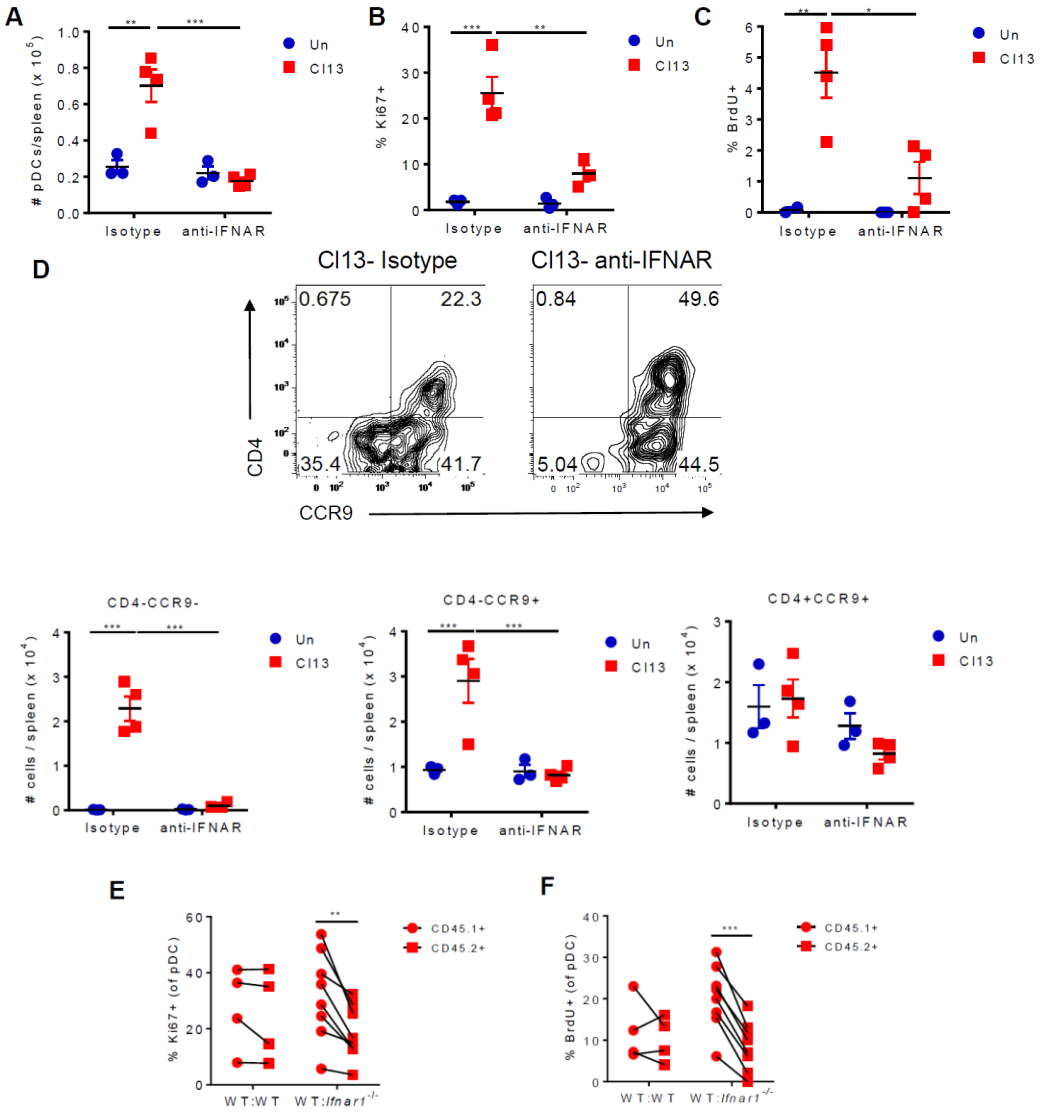

Figure 2-8. IFN-I signaling promotes splenic pDC proliferation and increase in CD4- pDC subsets during chronic LCMV infection. (A-D) WT mice were treated with isotype or anti-IFNAR nAb beginning 1 day before and throughout LCMV Cl13 infection and sacrificed at day 9 p.i. Splenic pDCs were evaluated for their absolute numbers (A), Ki67 expression (B), BrdU incorporation (C), and numbers of $CD4^+CCR9^+$, $CD4^-CCR9^+$, and $CD4^-CCR9^-$ subsets (D). (D) Representative FACS plots indicate frequency of $CD4^+CCR9^+$, $CD4^-CCR9^+$, and $CD4^-CCR9^-$ subsets in spleen pDCs. (E-F) Mixed BM chimeras were generated using BM from WT ($CD45.1^+$) and WT or *Ifnar*$^{-/-}$ ($CD45.2^+$) mice and infected with LCMV Cl13 for 9 days. Splenic pDCs from the $CD45.1^+$ or $CD45.2^+$ compartment were analyzed to determine their Ki67 expression (E) and BrdU incorporation *in vivo* (F). Data are representative of 1 (C) or 2 (A, B, and D) independent experiments with 3-4 mice/group or pooled from 2 independent experiments with 2-4 mice/group (E-F). Bars depict mean ± SEM. Symbols represent individual mice. *p<0.05, **p<0.01, ***p<0.001 (two-way Anova (A-D) or paired t-test (E-F)).

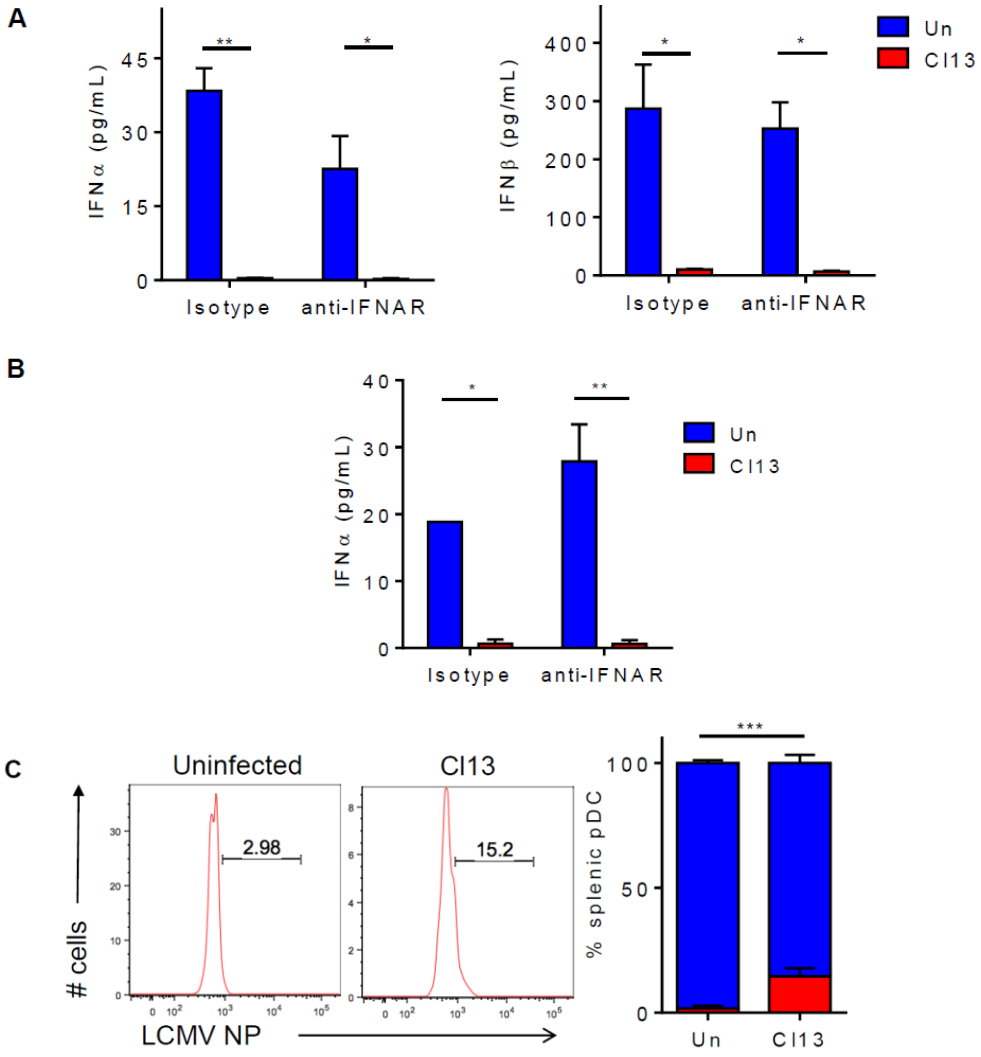

Figure 2-9. Functional exhaustion of pDCs is not caused by IFN-I signaling or overwhelming NP expression in pDCs. (A-B) WT mice were treated with isotype or anti-IFNAR nAb beginning 1 day before and throughout LCMV Cl13 infection and sacrificed at day 9 p.i. (A) BM was cultured with Flt3L (continuing treatment with isotype or anti-IFNAR nAb in vitro) and at day 8 post-culture, FACS-purified pDCs were stimulated with CpG-B for 15 hours. Levels of IFNα (left) and IFNβ (right) were determined in culture supernatants by ELISA. (B) FACS-purified splenic pDCs were stimulated with CpG-B for 6 hours and supernatants were evaluated for IFNα by ELISA. (C) WT mice were infected with LCMV Cl13 or left uninfected. LCMV NP expression was quantified by flow cytometry at day 9 p.i. Representative histograms are shown and graphs depict percentage of splenic pDCs that are NP negative (blue) or positive (red). Data are representative of 2 independent experiments where 4-7 mice/group were pooled (A-B) or with 3 mice/group (C). Bars depict mean ± SEM. *p<0.05, **p<0.01, ***p<0.001 (two-way Anova (A-B) or unpaired, two-tailed t-test (C)).

2.3.7 TLR7 signaling induces pDC proliferation after chronic LCMV infection

Since uninfected pDCs can sense LCMV via TLR7[172], we hypothesized that persistent TLR7 stimulation may contribute to pDC proliferation. To discern whether TLR7 signaling induced pDC proliferation in a cell-intrinsic manner, we generated WT:*Tlr7*$^{-/-}$ mixed BM chimeras and infected them with LCMV Cl13. We observed that both Ki67 expression and *in vivo* BrdU incorporation were significantly reduced in pDCs from the *Tlr7*$^{-/-}$ vs. WT compartments (Fig. 2-10A&B) indicating that direct TLR7 signaling also contributed to pDC proliferation after chronic LCMV infection. Overall, our results indicated that the same TLR7 signaling that induces pDC maturation and IFN-I production at day 1 after LCMV Cl13 infection[172] promoted self-renewal of exhausted pDCs at later stages of infection.

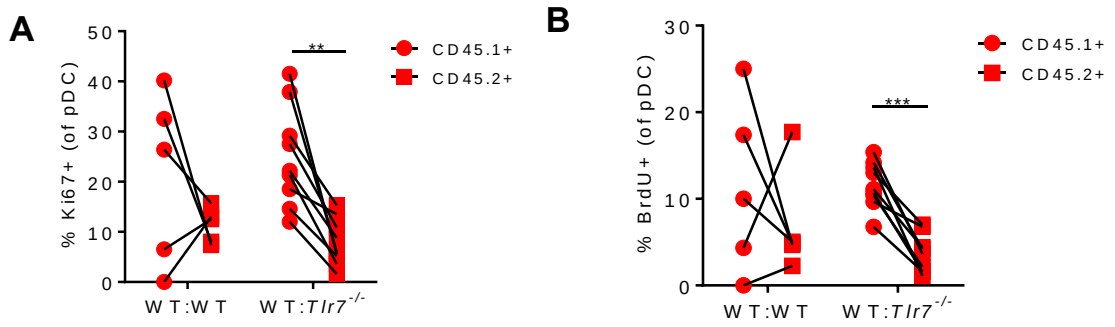

Figure 2-10. TLR7 promotes their proliferation during chronic LCMV infection. Mixed BM chimeras were generated using BM from WT (CD45.1^{+}) and *Tlr7*$^{-/-}$ (CD45.2^{+}) mice and infected with LCMV Cl13 for 9 days. Splenic pDCs were evaluated for Ki67 expression (A) and BrdU incorporation *in vivo* (B). Symbols represent individual mice. Data are pooled from 2 independent experiments with 2-5 mice/group. **p<0.01, ***p<0.001 (paired t-test).

2.4 Discussion

Production of soluble mediators, including IFN-I, after recognition of conserved pathogen-associated molecular patterns (PAMPs) represents a cornerstone of innate immune responses[173]. Therefore, the sustained silencing of systemic IFN-I (in the face of copious levels of PAMPs)

during chronic viral infections[3,69,72,75,174] is highly intriguing and suggests long-term innate adaptations to the chronic infectious environment through distinctive regulatory mechanisms. In sharp contrast to T and B cells, very little is known about this adaptation in typically short-lived innate immune cells. Here we used LCMV chronic infection in its natural rodent host to study the adaptation of a prominent innate immune cell, pDC, that switches from being the most powerful IFN-I-producing cell hours after infection[172] to a functionally exhausted cell unable to secrete IFN-I, not only in response to the ongoing infection, but also upon secondary unrelated stimuli[72]. Unexpectedly, our study suggested that the maintenance of an exhausted pDC pool during chronic infection was achieved via two mechanisms that independently regulated pDC numbers and loss of function. On one hand, IFN-I signaling exerted a previously unrecognized negative-feedback-loop, limiting *de novo* pDC generation from BM progenitors while promoting (together with TLR7) self-renewal of exhausted pDCs in the periphery. On the other hand, an IFNAR-independent pathway curtailed the IFN-I-production capacity in pDCs.

Remarkably, all progenitor and pDC adaptations that we observed during chronic LCMV infection were also detected early after acute LCMV infection, supporting the view that they represent general responses to microbial exposure. It is important to note, however, that most of these adaptations were only sustained long-term during chronic (but not acute) LCMV infection, suggesting that a persisting infectious environment is necessary to perpetuate them. Remarkably E2-2 was reduced in both BM progenitors and differentiated pDCs. Given that E2-2 and its down-stream targets SPIB and BCL11A are all critical for pDC development, pDC lineage commitment and/or function[106,109,111,112], it is conceivable that their down-regulation contributed, at least partially, to the limited generation of functional pDCs from BM and/or the functional loss of exhausted pDCs. Although the relative contribution of different mechanisms underlying pDC and

progenitor adaptations may vary in different type of infections, the data from Fitzgerald-Bocarsly lab showed that pDCs from a small cohort of viremic HIV-infected patients also exhibited reduced expression of E2-2 and its downstream target TFs SPIB and BCL11A, suggesting that conserved transcriptional adaptations may accompany regulation of pDCs in murine and human chronic viral infections.

Our data also revealed that IFN-I mediated the suppression of BM progenitors and their down-regulation of E2-2 after chronic LCMV infection. Notably, an initial IFN-I peak and/or a persistently low IFN-I signature have been described not only after chronic LCMV infection but also during infections with SIV, HIV, HCV and HBV[3,69,70,74,75]. Therefore, it is likely that the IFN-I-ablation of BM progenitors and suppression of pDC generation from BM extends to chronic viral infections in humans, where decreased numbers of circulating pDCs have been reported[70,93,94]. It must be noted that our mechanistic studies of progenitor adaptations during chronic LCMV infection focused on day 9 p.i. when these phenotypes were profound after acute LCMV infection as well. An initial elevation of IFN-I also occurs during acute infection and therefore likely plays a role in both the transient and sustained BM adaptations that we observed also after acute (LCMV ARM) infection. While the effect of IFN-I signaling on sustained adaptation of BM progenitors during chronic LCMV infection awaits investigation, it is plausible that ablation of CLP and CDP, which were only sustained after chronic (but not acute) infection, depends on prolonged IFN-I signaling during chronic LCMV infection[175]. Notably, a previous report demonstrated that (under non-infectious conditions) rIFN-α enhances pDC generation from BM progenitors *ex vivo* and *in vivo*[170]. This apparent discrepancy between Li et al. and our findings may be explained by factors in the infectious environment that may modulate the outcome of IFN-I signaling in BM progenitors and/or cell-extrinsic IFN-I effects that may indirectly impact BM progenitors during infection.

Indeed, our studies in mixed chimeras indicated that both cell-intrinsic and -extrinsic pathways mediated IFN-I regulation of BM progenitors during chronic LCMV infection.

In sharp contrast to non-infectious conditions, our data demonstrate outstanding Ki67 expression and BrdU incorporation in splenic and BM pDCs early after acute and chronic LCMV infection. We found that the highest pDC proliferation at ~day 5 p.i., the earliest time point studied, was followed by significant contraction, with sustained proliferation to a lower degree at later stages after chronic (but not acute) LCMV infection. This is in agreement with increased BrdU incorporation and Ki67 expression in pDCs from SIV-infected macaques[96,174,176]. *Ex vivo* BrdU incorporation was, however, not detected in the original SIV infection study[96], likely because a relatively early time point and a single macaque were investigated, thereby leading to the interpretation that Ki67+ or BrdU+ pDCs represent cells recently egressed from BM rather than local proliferating cells[96,174]. Importantly, our study provides compelling evidence for *ex vivo* BrdU incorporation by splenic pDCs from chronically infected mice, demonstrating significant pDC proliferation in the periphery. Furthermore, we show that pDC proliferation was associated with the expansion of splenic CD4- pDC subsets and, even more remarkably, that such proliferation was mediated by pDC-intrinsic IFNAR and TLR7 signaling. We propose that initial TLR7 signaling and IFN-I elevation may induce expansion of splenic and BM CD4- pDC subsets and pDC proliferation after both acute and chronic LCMV infection while continuous TLR-stimulation and low IFN-I levels sustained during chronic viral infection perpetuates self-renewal of exhausted pDCs. We also propose that the initial, more robust, pDC proliferation that occurred early after acute and chronic infections allows restoration of pDC numbers after their initial ablation[97], resulting in the accumulation of pDCs in lymphoid organs that we observed at day 10 after LCMV infection and that others have reported in HIV-infected patients[89-91]. Such pDC

accumulation suggests that pDC proliferation can outweigh pDC apoptosis[97] and the limited BM pDC generation we described here. It should be noted, however, that (in line with decreased IFN-I levels[69,70,72,75]) pDC proliferation was attenuated by days 10-30 p.i., providing an explanation for the decline in pDC numbers observed at later stages after LCMV, HIV and SIV infections[72,95,96]. Furthermore, the rate of BM pDC egress and recruitment to non-lymphoid tissues may also fluctuate throughout chronic infection and is expected to influence pDC numbers in lymphoid organs.

It is tempting to speculate that the evolutionary driver of the rapidly triggered pDC exhaustion in both acute and chronic infections may have been the need for limiting IFN-I-induced immunopathology, which can be lethal after bacterial infections[73,177]. Furthermore, maintenance of an exhausted pDC pool via local-self-renewal may provide an infected host with greater plasticity to tailor pDC functions according to pathogen load or other cues in the nearby environment. Sustained IFN-I exhaustion comes, however, with a cost for the infected host, who becomes compromised to mount optimal innate responses and control certain secondary infections and tumors[70,72,178,179]. Remarkably, Dr. Monica Macal's data from Zuniga lab showed that prevention of pDC functional exhaustion after chronic viral infection did not enhance morbidity or mortality (at least in the context of ubiquitous TLR7 deficiency) and instead associated with increased systemic IFN-I levels and enhanced resistance to a secondary pathogen. This finding opens the exciting possibility that transient recovery from innate exhaustion could be combined with existing treatments targeting adaptive immune cells in order to enable more effective control of chronic infections and their associated opportunistic pathogens and/or tumors. Furthermore, relieving pDC exhaustion could represent a powerful strategy to increase endogenous IFN-I production in the tumor microenvironment, converting "cold" tumors that are not attacked by the

immune system into "hot" tumors that exhibit better prognosis and response to immunotherapies[180]. Given the opposing effects of IFN-I on the immune response[3,73,74,177], however, it should be noted that the ultimate consequences of recovering pDC IFN-I exhaustion will be determined by multiple factors such as the pathogen or tumor susceptibility to interferon stimulated genes, the degree of adaptive immune-exhaustion and the timing as well as the isoforms and extent of IFN-I recovery. Nonetheless, as basic knowledge of the mechanisms controlling T cell exhaustion resulted in novel immunotherapies for chronic infections and tumors[4,181], further understanding of innate immune exhaustion will likely illuminate new strategies to treat chronic diseases. Our study provides an anatomical, cellular and molecular explanation for the sustained exhaustion of pDCs during persistent viral infection and brings forth a framework to understand long-term exhaustion of other short-lived innate cells in chronic settings

2.5 Materials and Methods

2.5.1 Experimental Model and Subject Details

Mice

Female C57BL/6 mice (6-8 weeks old) were purchased from The Jackson Laboratory. *Tlr7*$^{-/-}$ mice were obtained from Dr. Maripat Corr (University of California, San Diego)[182]. *Ifnar*$^{-/-}$ mice were obtained from Dr. Charles Surh (La Jolla Institute for Allergy and Immunology). All mice were housed under specific-pathogen-free conditions at the University of California, San Diego. Mice were bred and maintained in a closed breeding facility and mouse handling and experiments conformed to the requirements of the National Institute of Health and the Institutional Animal Care and Use Guidelines of UC San Diego. Unless stated otherwise, experiments were initiated in mice (female and male) at 7-12 weeks of age.

Virus strains

Mice were infected with 2×10^6 plaque-forming units (pfu) of LCMV Arm (ARM) or LCMV clone 13 (Cl13) intravenously (i.v.) via tail vein. Viruses were propagated on BHK cells and quantified by plaque assay performed on Vero cells[183]. Briefly, Vero cell monolayers were infected with 500 μL of serially diluted viral stock and incubated for 60 minutes at 37°C in 5% CO_2 with gentle shaking every 15 minutes. Agarose overlay was added to infected cells and placed in incubator for 6 days at 37°C in 5% CO_2. Cells were fixed with formaldehyde and stained with crystal violet for 5 minutes at room temperature and plaques were counted.

Cell lines

ISRE-L929 reporter cells (male origin, provided by Dr, Bruce Beutler, University of Texas South Western Medical Center) were cultured in DMEM containing 10% FBS, penicillin-streptomycin, and supplements of L-glutamine. $1x10^6$ cells were passaged every 3-4 days. Cells were washed in PBS pH 7.4 then lifted from culture flasks with 0.05% Trypsin-EDTA. Trypsin was deactivated by addition of serum containing media.

Primary cell culture

BMDCs were differentiated at the concentration of $2x10^6$ cells/ml for 8 days in 5ml of RPMI-1640 supplemented with 10% (vol/vol) fetal bovine serum, L-glutamine, penicillin-streptomycin, and HEPES pH 7.2) supplemented with 100ng/mL Flt3L and 50μM β-mercaptoethanol. Half of the medium was replaced after 5 days with fresh cytokines added.

2.5.2 Method details

Mouse Cell Purification

Spleens were incubated with 1mg/mL collagenase D for 20 min at 37˚C and passed through a 100µm strainer to achieve a single cell suspension. For purification of spleen or BM pDCs, splenocytes or BM cells were enriched with PanDC microbeads using an Automacs system (Miltenyi) or by using EasySep™ Mouse Streptavidin RapidSpheres™ Isolation Kit (Stemcell Technologies), biotin-conjugated anti-Thy1.2 (53-2.1), and anti-CD19 (6D5). PanDC+ fractions or fractions unbound to streptavidin beads were stained with propidium iodide (PI) and FACS-purified using a BD ARIA II (BD Biosciences) for pDCs ($PI^-CD11c^{intermediate/dim}CD11b^-B220^+BST2^+$) after B (CD19), T (Thy1.2) and NK (Nk1.1) cell exclusion. Plasma cells (CD138) were also excluded for purification of BM pDCs. BM pDC progenitors were enriched by using EasySep™ Mouse Streptavidin RapidSpheres™ Isolation Kit (Stemcell Technologies,), biotin-conjugated anti-Thy1.2 (53-2.1), anti-B220 (RA3-6B2), anti-CD11b (M1/70), anti-CD4 (RM4-5), anti-CD19 (6D5) and anti-CD8 (536.7). Fractions unbound to streptavidin beads were stained with PI and FACS-purified using a BD ARIA II (BD) for progenitors ($PI^-CD11c^-c\text{-}Kit^{intermediate/dim}Flt3^+$) after B (CD19, B220), T (Thy1.2, CD3, CD4, and CD8), NK (Nk1.1), red blood cell (Ter119), granulocyte (Gr-1), and monocyte (CD11b) exclusion. pDCs derived from culture of BM cells with Flt3L were stained and sorted as $PI^-CD11c^+CD11b^-B220^+BST2^{high}$. Purity of the cells was > 95% (data not shown).

Flow Cytometry

The following antibodies were used to stain single cell suspensions prepared from murine BM or spleens: Thy 1.2 (53-2.1), CD19 (eBio1D3), NK 1.1 (PK136), Gr-1 (RB6-8C5), CD11c (N418), CD11b (M1/70), B220 (RA36B2), BST2 (eBio927), CD45.2 (104), CD4 (RM4-5), CD8 (53-6.7), Ter119 (TER-119), CD3 (145-2C11), CD45.1 (A20), MHC class II (I-A/I-E) (M5/114.15.2), CCR9 (eBioCW-1.2), Ki67 (SolA15), c-kit (2B8), CD115 (AFS98), Flt3 (A2F10),

Streptavidin, CD127 (eBioRDR5), CD86 (GL1), CD34 (RAM34), CD16/32 (93), and CD138 (281-2). PI or Ghost dye (Tonbo Biosciences, San Diego, CA) was used to exclude dead cells. Cells were pre-incubated with CD16/CD32 Fc block (BD Pharmingen) prior to surface staining. Staining for Ki67 (SolA15) was performed as directed using the Foxp3 / Transcription Factor Staining kit. To measure *in vivo* BrdU incorporation in pDCs, mice were injected with 2mg BrdU (Sigma Aldrich). 16 hours later, spleens were harvested and splenocytes were stained using the BrdU Flow kit (BD Biosciences) following manufacturer instructions. To measure BrdU incorporation *ex vivo*, splenocytes were cultured at a concentration of 2×10^6 cells/ml with 10mM BrdU. 7 hours later, cells were harvested and stained using the BrdU Flow kit (BD Biosciences) following manufacturer instructions. Cells were acquired with a LSRII flow cytometer (BD Biosciences) and data were analyzed using FlowJo software 9.9.6 (Treestar, Inc.).

Cytokine Measurements

For cytokine measurement in culture supernatants, spleen or BM cells from individual mice in the same group were pooled prior to FACS purification. FACS-purified pDCs (3×10^4 cells/well) were incubated in 120ul RPMI-1640 supplemented with 10% (vol/vol) fetal bovine serum, L-glutamine, penicillin-streptomycin, and HEPES pH 7.2) supplemented with 50μM β-mercaptoethanol in the presence or absence of CpG-B 1668 (Integrated DNA Technologies) at 0.1μM (Flt3L culture-derived pDC) or 1μM (splenic and BM pDC) or CpG-A 1585 (InvivoGen) at 0.5uM for 6 or 15 hours at 37˚C. Supernatants were collected and stored at −80°C until further analysis. IFN-I bioactivity was measured with reference to a recombinant mouse IFNβ standard (Sigma-Aldrich) using ISRE-L929 reporter cells (L-929 cell line transfected with an interferon-sensitive luciferase)[184]. IFNα and IFNβ were measured by Lumikine mIFNα and Lumikine Xpress mIFNβ ELISA (InvivoGen), respectively, following manufacturer instructions. TNFα was

measured by Mouse TNF alpha ELISA Ready-SET-Go!® (eBioscience) following manufacturer instructions. Graphs depicting cytokine measurements in this paper represent individual wells of stimulation.

Quantitative Real-time RT-PCR (qRT-PCR) Analysis

For qRT-PCR analysis, spleen or BM cells from individual mice in the same group were pooled prior to FACS purification. Total RNA was extracted using RNeasy kits (Qiagen), digested with DNase I (RNase-free DNase set; Qiagen) and reverse-transcribed into cDNA using Superscript III RT (Invitrogen). The expression of various genes was quantified using Fast SYBR Green Master Mix (Thermo Fisher Scientific) or TaqMan™ Fast Universal PCR Master Mix with probe sets from the Universal Probe Library (Roche) and a Real-Time PCR Detection System (Applied Biosystems) or CFX384 Touch Real-Time PCR Detection System (Bio-Rad). The following primers for the test genes and probe sets were used: *Gapdh* Taqman (probe #9) – Forward (5'- AGCTTGTCATCAACGGGAAG-3'), Reverse (5'- TTTGATGTTAGTGGGGTCTCG-3'), *Gapdh* Sybr – Forward (5'- CATGGCCTTCCGTGTTCCTA-3'), Reverse (5'- CCTGCTTCACCACCTTCTTGAT -3'), *Tcf4* Taqman (probe #9) – Forward (5'- ATTTGTGGCCATTGAAGGTT -3'), Reverse (5'- GTCCCTAAGGCAGCCATTC -3'), *Spib* Sybr – Forward (5'- AAATCCGCAAGGTCAAACGC -3'), Reverse (5'- TTCAGGGGGAGTACAGAGGG -3'), *Bcl11a* Sybr – Forward (5'- TGGTATCCCTTCAGGACTAGGT -3'), Reverse (5'-TCCAAGTGATGTCTCGGTGGT-3'). The relative transcript levels were normalized against murine *Gapdh* or human *GAPDH* as described previously (Macal et al., 2016). Graphs depicting qRT-PCR analysis of murine genes in this paper represent technical triplicates from one representative experiment.

In vivo IFNAR Blockade

WT mice were treated with 500µg/mouse intraperitoneally (i.p.) with neutralizing antibody (nAb) to IFNAR (clone MAR1-5A3; BioXCell) or Anti-Mouse IgG1 Isotype Control (clone MOPC-21; BioXCell) on days -1 and 0 post-LCMV Cl13-infection. Mice were then treated with 250µg/mouse anti-IFNAR nAb or isotype control i.p. on days 2, 4, and 6 post-LCMV Cl13 infection as previously described[175]. Uninfected control mice were similarly treated in parallel.

Generation of Mixed BM Chimeras

WT CD45.1$^+$ C57BL/6 recipient mice were sub-lethally irradiated with 1000 rads and reconstituted with a 1:1 mix of BM cells from CD45.1$^+$ WT mice and CD45.2$^+$ Tlr7$^{-/-}$ or *Ifnar* $^{-/-}$ mice (or CD45.2$^+$ WT mice for WT:WT controls). 5-10x10^6 total mixed BM cells were transferred i.v. into the irradiated recipient mice, which were treated with antibiotics (Trimethoprim 8 mg/ml and Sulfamethoxazole 40 mg/ml supplied in drinking water; Akorn) for 3 weeks to prevent infection and allow immune reconstitution. Reconstitution was analyzed 8 weeks after BM transfer by determining the ratio of CD45.1$^+$ to CD45.2$^+$ immune subsets in blood by flow cytometry.

In vivo Progenitor Transfer Assay

FACS-purified Lin$^-$c-kit$^{int/lo}$Flt3$^+$ progenitors (1.5 x 10^4 cells) from CD45.2$^+$ uninfected or Cl13-infected donor mice at day 30 p.i. were injected i.v. into CD45.1$^+$ non-irradiated uninfected or infection-matched recipient mice, respectively. Mice were sacrificed at day 10, and spleen cells were analyzed by flow cytometry after splenocytes were enriched by using EasySep™ Mouse Streptavidin RapidSpheres™ Isolation Kit (Stemcell Technologies), biotin-conjugated anti-Thy1.2 (53-2.1), and anti-CD19 (6D5).

Quantification and statistical analysis

All statistical parameters are described in figure legends. Student's t tests (two-tailed, unpaired, or where indicated paired), one-way Anova, two-way Anova, and multiple comparisons were performed by using GraphPad Prism 6.0 (GraphPad). Significance was defined as $p \leq 0.05$. In all figures, error bars indicate S.E.M.

2.6 Acknowledgements

Chapter 2, in part, is a reprint of the material as it appears in Immunity Macal, M and Jo, Y et al 2018. Yeara Jo was one of the two primary investigators and authors of this paper. I would like to thank co-authors Dr. Monica Macal, Dr. Simone Dallari, Dr. Aaron Chang, Dr. Jihong Dai, Dr. Shobha Swaminathan, Dr. Ellen Wehrens and Dr. Patricia Fitzgerald-Bocarsly for their contributions.

Chapter 3. Genomic analysis of bone marrow progenitors during viral infection reveals novel dendritic cell regulators

3.1 Summary

DCs play a central role in immune responses, but they adapt during acute and chronic infections, showing altered development from BM progenitors and suboptimal maturation. However, the underlying mechanisms remain largely unknown. We determined the transcriptional and chromatin landscapes of bone marrow DC progenitors from lymphocytic choriomeningitis virus (LCMV)-infected mice and applied these datasets to Taiji algorithm to predict the activity of transcription factors (TFs). Glucocorticoid Modulatory Element Binding Protein 1 (Gmeb1), which was predicted to exhibit increased activity in progenitors during LCMV infection, suppressed plasmacytoid(p) DC development in a glucocorticoid-dependent manner. Further studies revealed that glucocorticoid suppressed pDC development during LCMV infection. On the other hand, Gmeb1 promoted development but suppressed maturation of classical(c) DC1s in a glucocorticoid-independent manner. Zinc Finger Protein 524 (Zfp524), which was predicted to exhibit decreased activity in progenitors during LCMV infection, promoted proinflammatory cytokine production in pDCs while inhibiting cytokine production in cDCs. These results highlight novel TF regulators of DCs, deepening our understanding of DC biology, and unveils potential therapeutic targets to harness DCs in diseases.

3.2 Introduction

We and others have described several adaptations of DC progenitors during acute and chronic infections that affect DC progeny, including impaired DC development, maturation and

altered cytokine production[65,185]. Many immune adaptations sustained in progenitors during chronic infections are also observed, albeit mostly transiently, after acute infection, indicating that these are part of general responses to microbial exposure[185]. However, the mechanisms underlying initiation of such adaptations remain largely unknown.

To understand the mechanisms involved and potentially extend the significance of our study to acute infections, we determined the transcriptional and chromatin landscapes of BM DC progenitors from lymphocytic LCMV-infected mice, via RNA-Seq and ATAC-Seq[186], respectively, at day 8 p.i.. when ARM- and Cl13-infected mice show the same progenitor phenotypes[185]. Consistently, transcriptome and chromatin landscapes of progenitors from ARM- and Cl13-infected mice were more closely related to each other than their counterparts from uninfected mice and involved alterations in gene signatures, including apoptosis and metabolic pathways. In addition to changes in expression of multiple TFs revealed by RNA-seq, Taiji algorithm, which integrates ATAC-seq and RNA-seq datasets to assess the global importance of TFs, identified 11 known DC regulators and 24 TFs with no previous connection to DC biology to have altered activity in progenitors upon infection. Among these candidate TF regulators, Gmeb1, which was predicted to exhibit increased activity in progenitors from LCMV-infected mice, suppressed pDC development in a glucocorticoid-dependent manner. We further found that glucocorticoid suppressed pDC development during *in vivo* LCMV infection. Furthermore, Gmeb1 promoted development but suppressed maturation of cDC1s in a glucocorticoid-independent manner. On the other hand, Zfp524, which was predicted to exhibit decreased activity in LCMV-infected mice, promoted proinflammatory cytokine production in pDCs while inhibiting cytokine production in cDCs. Together, these results define gene expression and chromatin signatures of infection-induced adaptations of DC progenitors and highlight novel TF regulators

of DC progenitors including Gmeb1 and Zfp524, which modulate DC development, maturation, and/or function, significantly deepening our understanding of DC biology and unveiling potential new targets for DC-based immunotherapies for both chronic and acute illnesses.

3.3 Results

3.3.1 Acute and chronic LCMV infection introduce large-scale alterations in transcriptome in DC progenitors

We previously reported that, after chronic LCMV infection, pDC progenitors were reduced in numbers and compromised in their capacity to develop into pDCs and that pDCs that developed from these progenitors had reduced cytokine production capacity[185]. Importantly, we observed that all progenitor adaptations sustained during chronic infection were also detectable early after acute infection[185], suggesting that mechanisms common to acute and chronic infection initiate progenitor adaptations. In order to investigate mechanisms that drive alterations in progenitors after LCMV infection in an unbiased manner, we performed RNA-seq to compare the transcriptomes of FACS-purified progenitors from naïve, LCMV ARM- or Cl13-infected mice (Fig. 3-1A). In parallel, we also globally assessed chromatin landscapes by ATAC-seq[186]. DC progenitors used in this study included CLPs, CDPs, and CD115- CDP-like cells, all of which have been previously demonstrated to contribute to generation of pDCs as well as cDCs[47]. Analyses were performed at day 8 p.i., where the progenitors from ARM- and Cl13-infected mice demonstrated common phenotypes but deviated to the largest extent from their counterparts from naïve mice. Hierarchical clustering between samples and principal component analysis (PCA) revealed that progenitors from naïve mice had distinct gene signatures, whereas their counterparts from ARM- and Cl13-infected mice were more closely related to each other (Fig. 3-1B and C).

More genes were downregulated than those that were upregulated in progenitors upon both ARM and Cl13 infection (>2-fold change, False Discovery Rate (FDR) < 0.05), with larger number upon Cl13 infection (Fig. 3-1D). Approximately 70% of differentially expressed genes (DEGs) upon ARM infection were also differentially expressed upon Cl13 infection, supporting the similarities in transcriptomic changes in response to two infections at day 8 p.i. (Fig. 3-1D). There were DEGs in ARM vs. Cl13 infection, but the differences in expression levels were attenuated compared to those in ARM or Cl13 vs. naïve (Fig. 3-1E). Together with numerous pathways related to immune responses as expected with infections, several pathways related to metabolic processes were over-represented by genes that were upregulated upon both ARM and Cl13 infection, suggesting that progenitors become more metabolically active upon infection (Fig. 3-1F). Genes that were upregulated in progenitors upon Cl13 compared to ARM infection were particularly involved in immune responses to foreign pathogen, reflecting the continued viremia in contrast to viral clearance after acute infection at the time point studied (Fig. 3-1G). On the other hand, pathways related to cell cycle progression were over-represented by genes that were downregulated upon both ARM and Cl13 infection, suggesting the presence of blocks at certain stages of progenitor cell cycles (Fig. 3-1H). In addition, consistent with compromised pDC development that we have previously reported at day 8-10 post both ARM and Cl13 infection[185], 161 out of 357 genes defined as pre-pDC signature in a recent study[121] were differentially regulated in progenitor upon both ARM and Cl13 infection (Fig. 3-1I) and gene set enrichment analysis (GSEA) showed that genes that were significantly downregulated in progenitors during both ARM and Cl13 infection were enriched for pre-pDC signature (Fig. 3-1J). Pre-pDC signature genes that were significantly reduced during infections included markers that were recently reported to define priming/commitment towards pDC lineage, Ly6d and Siglech[121,122] (Fig. 3-1K). Consistently,

frequency of Ly6d+Siglech+ precursors within DC progenitors was decreased upon infection (Fig. 3-1L). On the other hand, 123 out of 458 genes defined as pre-cDC signature were differentially regulated in progenitor upon both ARM and Cl13 infection (Fig. 3-1M). Interestingly, GSEA showed that genes that were significantly upregulated in progenitors during both ARM and Cl13 infection were enriched for pre-cDC signature (Fig. 3-1N), suggesting that DC progenitors are biased to commit to cDCs upon infection. Taken together, both LCMV ARM and Cl13 infection drive large-scale changes in transcriptome of DC progenitors in a similar manner, which alter the number and developmental capacity of these cells, particularly compromising further differentiation into pDCs while promoting differentiation into cDCs.

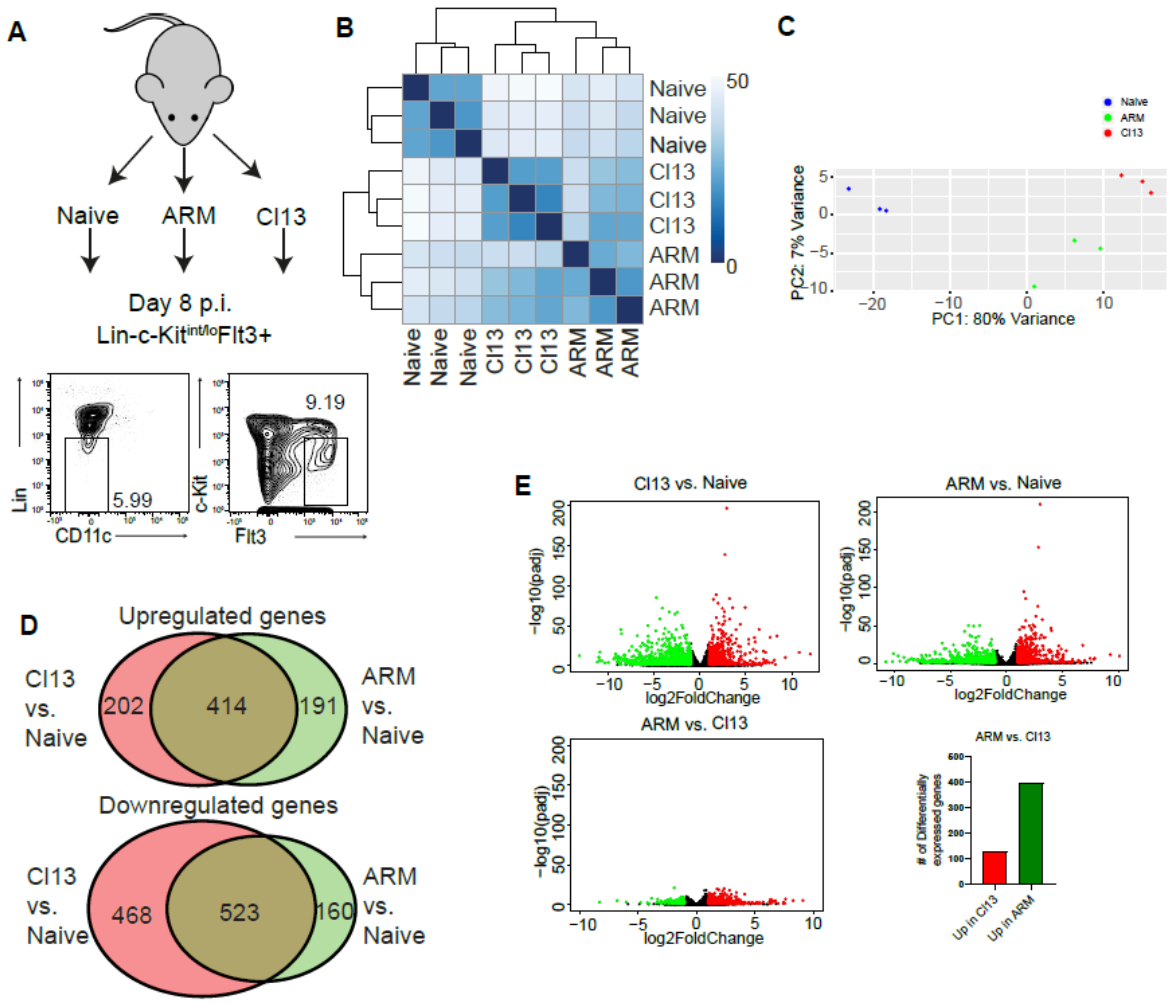

Figure 3-1. Acute and chronic LCMV infection induce large-scale changes in transcriptomes in DC progenitors. WT mice were infected with LCMV ARM or LCMV Cl13 or left uninfected and sacrificed at day 8 p.i. BM DC progenitors (Lin−c-kit$^{int/lo}$Flt3+) were isolated by flow cytometry for 3 independent RNA-seq analyses. Lin includes markers for Thy1.2, CD19, NK1.1, CD3, CD4, CD8, B220, CD11b, Gr-1, CD11c and Ter119. (A) Schematic and representative FACS plot for purification of DC progenitors. (B) Hierarchical clustering of RNA-seq profiles by using Euclidean distance. (C) Principal component analysis of RNA-seq profiles. Replicates are represented as separate data points and color-coded by presence/type of infection. (D) Overlap between differentially upregulated or downregulated genes from Cl13 vs. naïve and Arm vs. naïve comparisons. RSEM counts were used to compute differentially regulated genes with FDR < 0.05 and >2-fold change by DESeq2. (E) Volcano plot of differentially expressed genes (DEGs) with FDR < 0.05. Red dots indicate significantly upregulated genes and green dots indicate significantly downregulated genes (>2-fold change). Bar graph shows number of DEGs in progenitors from ARM vs. Cl13 comparison.

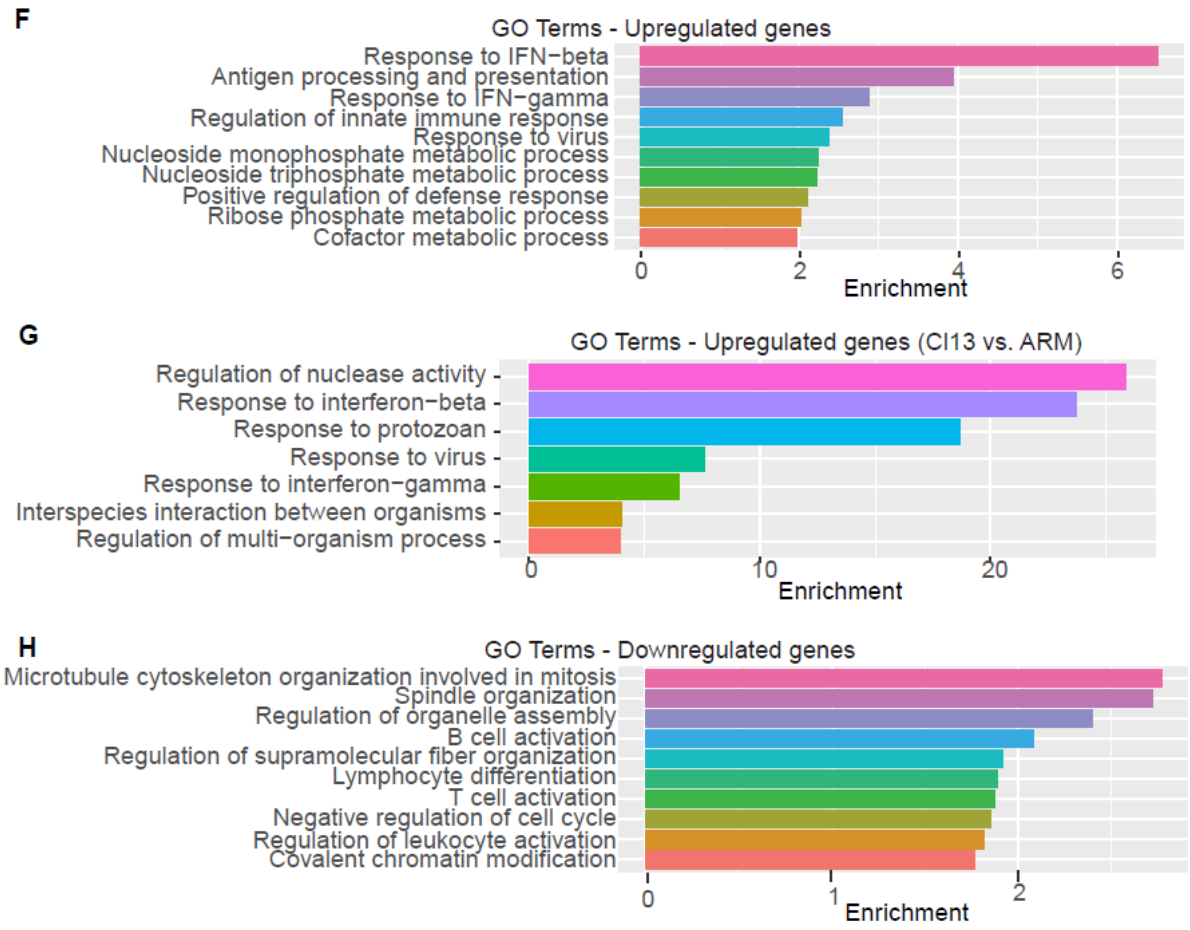

Figure 3-1. Acute and chronic LCMV infection induce large-scale changes in transcriptomes in DC progenitors, Continued (F-H) DEGs were subjected to overrepresentation analysis using WebGestalt. Gene Ontology (GO) Biological Processes overrepresented by DEGs that were upregulated in progenitors during both ARM and Cl13 infection (F), DEGs that were upregulated in progenitors during Cl13 compared to ARM infection (G), DEGs that were downregulated in progenitors during both ARM and Cl13 infection (H) are shown.

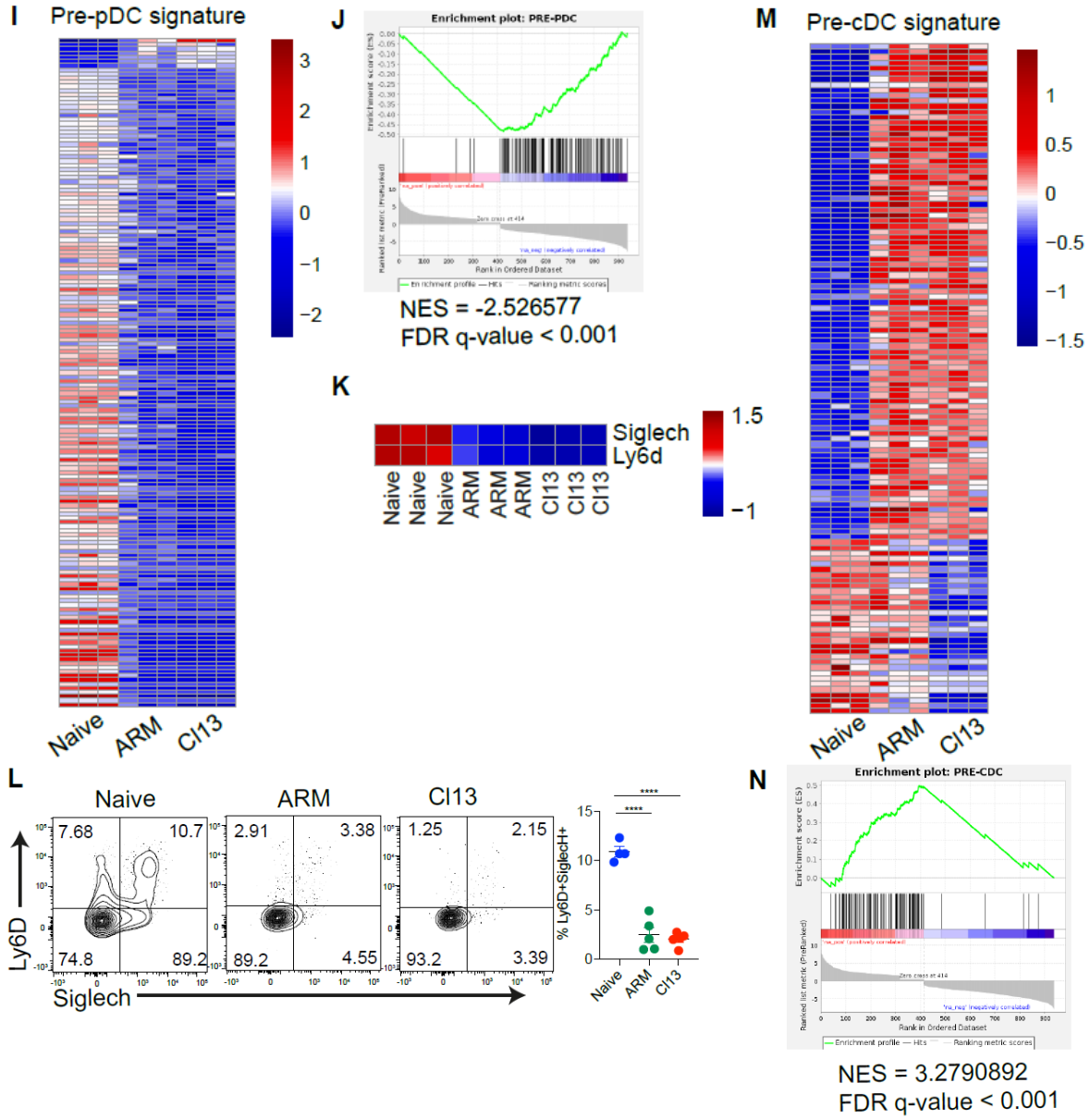

Figure 3-1. Acute and chronic LCMV infection induce large-scale changes in transcriptomes in DC progenitors, Continued (I) Heatmap of DEGs altered in progenitors during both ARM and Cl13 infection that were defined as pre-pDC signature in Dress, et al., 2019. (J) GSEA and normalized enrichment score (NES) of infection-specific DEGs for pre-pDC signature ($q < 0.001$). (K) Heatmap for Siglech and Ly6d expression from RNA-seq. (L) Representative FACS plot for Ly6d and Siglech expression and frequency of Ly6d+Siglech+ precursors within progenitors. Graphs depict mean ± SEM and symbols represent individual mice. Data are representative of from 2 independent experiments. ****<0.0001 (One-way ANOVA). (M) Heatmap of DEGs altered in progenitors during both ARM and Cl13 infection that were defined as pre-cDC signature in Dress, et al., 2019. (N) GSEA and normalized enrichment score (NES) of infection-specific DEGs for pre-cDC signature ($q < 0.001$).

3.3.2 Acute and chronic LCMV infection induce large-scale changes in chromatin landscapes in DC progenitors

PCA and hierarchical clustering of ATAC-seq profiles of DC progenitors from naïve, LCMV ARM- or Cl13-infected mice at day 8 p.i. revealed that progenitors from naïve mice had distinct chromatin landscapes, whereas their counterparts from ARM- and Cl13-infected mice were more closely related to each other (Fig. 3-2A and B). Approximately 79% of differentially open chromatin regions upon ARM infection were also differentially upon Cl13 infection, as detected by Diffbind with FDR <0.05 (Fig. 3-2C). In addition, there was no significant difference in chromatin landscape when progenitors from ARM and Cl13 infection were compared, supporting the high degree of similarity in chromatin remodeling in response to both infections. Compared to non-differential regions, differential regions upon infection were depleted of exons and promoters but enriched for intergenic areas and introns and suggested that distal regulatory elements were primarily involved in shaping the alterations in chromatin landscapes upon infection (Fig. 3-2D). Over 90% of differentially open regions became more accessible upon both ARM and Cl13 infection, indicating that progenitors underwent large-scale gain, rather than loss, of chromatin accessibility in response to infection (Fig. 3-2E). Differential regulatory regions with increased accessibility upon infection were enriched for several pathways related to immune responses (Fig. 3-2F) and were associated with immune-related genes (e.g. Cxcr4) (Fig. 3-2G). Staining for Cxcr4 showed that increased accessibility in regions near the Cxcr4 locus translated to increased Cxcr4 protein expression in progenitors upon infection (Fig. 3-2H). In contrast, differential regulatory regions with decreased accessibility upon infection included regions associated with genes that were downregulated (e.g. Siglech) (Fig. 3-2I and 3-1L). In addition to immune-related pathways, differential regulatory regions that gained accessibility upon infection

were also enriched for apoptosis and a few other signaling pathways (Fig. 3-2J). Indeed, larger proportion of progenitors underwent apoptosis upon infection, as shown by staining for active caspase 3, possibly contributing to reduction in their numbers (Fig. 3-2K). Taken together, both acute and chronic LCMV infection involve a broad remodeling of chromatin landscapes in DC progenitors.

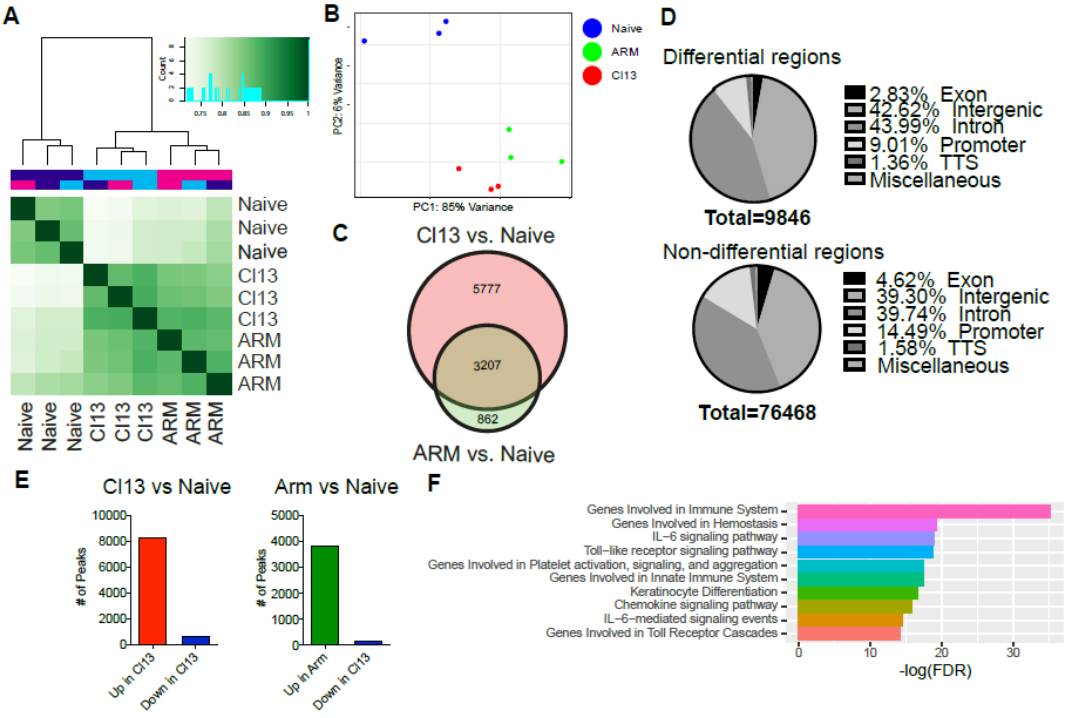

Figure 3-2. Acute and chronic LCMV infection induce large-scale changes in chromatin landscapes in DC progenitors. WT mice were infected with LCMV ARM or Cl13 or left uninfected and sacrificed at day 8 p.i. BM DC progenitors (Lin−c-kit$^{int/lo}$Flt3+) were isolated by flow cytometry for 3 independent ATAC-seq analyses. Lin includes markers for Thy1.2, CD19, NK1.1, CD3, CD4, CD8, B220, CD11b, Gr-1, CD11c and Ter119. (A) Correlation heatmap of ATAC-seq profiles. (B) Principal component analysis of peaks identified by ATAC-seq. Replicates are represented as separate data points and color-coded by presence/type of infection. (C) Venn diagram showing overlap between differentially accessible chromatin regions from Cl13 vs. naïve and Arm vs. naïve comparisons. ATAC-seq peaks were called by MACS2 and used to compute differential peaks with FDR < 0.05 by Diffbind. (D) Distribution of differential (top) and nondifferential (bottom) regions between progenitors from LCMV-infected vs. uninfected mice. TTS, transcription termination site. (E) Number of differential peaks that opened (left, red; right, green) or closed (blue) during infection. (F) MSigDB pathways enriched in regions that become more accessible in progenitors during both acute and chronic LCMV infection. The enrichment was achieved by using GREAT to compare these regions with whole genome background.

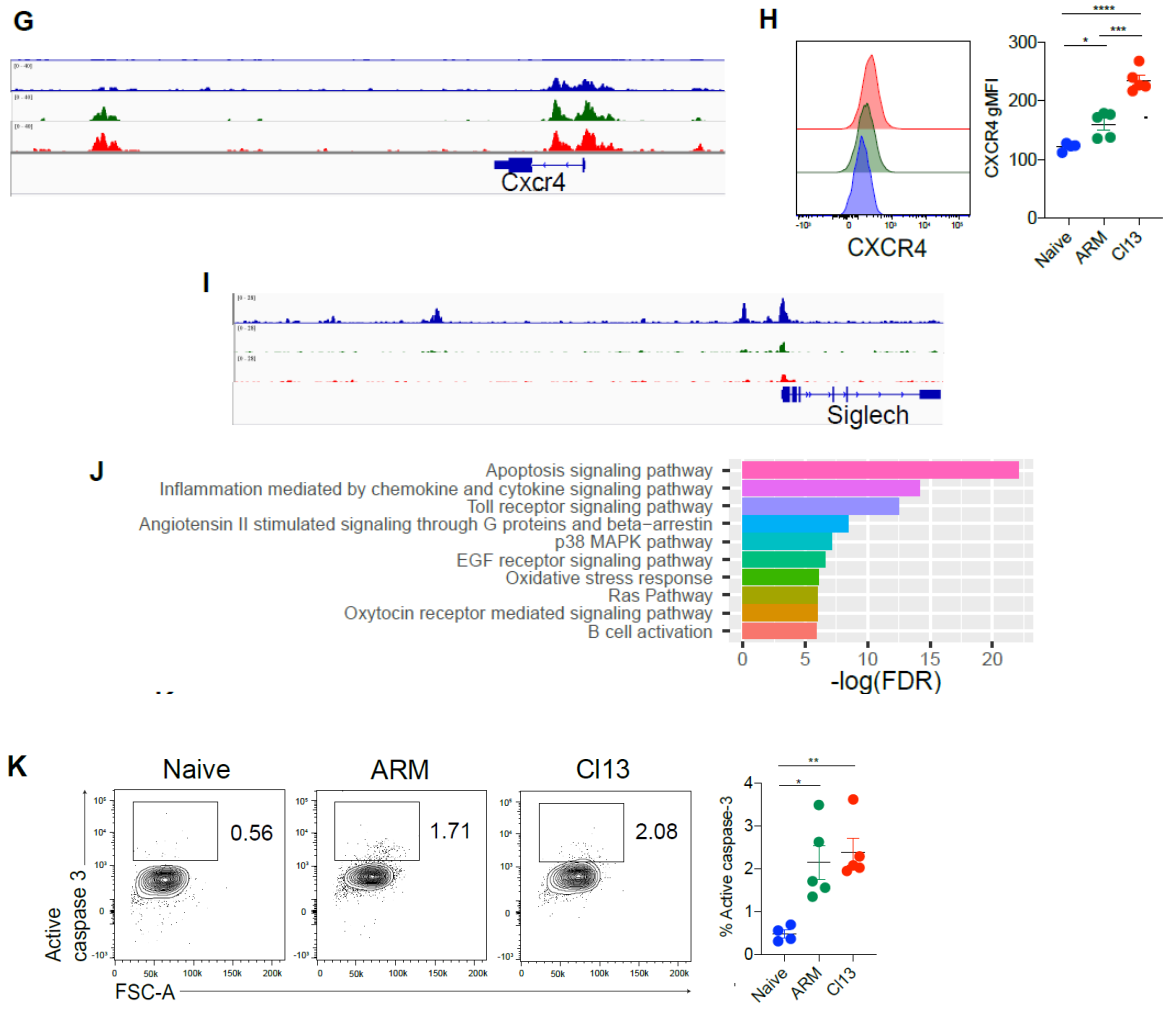

Figure 3-2. Acute and chronic LCMV infection induce large-scale changes in chromatin landscapes in DC progenitors, Continued (G) Representative examples of ATAC-seq signal profiles in progenitors around Cxcr4. Visualization of the loci was performed using the Integrative Genomics Viewer (IGV). (H) Geometric mean fluorescence intensity (gMFI) of Cxcr4 expression in progenitors analyzed by flow cytometry. (I) Representative examples of ATAC-seq signal profiles in progenitors around Siglech. Visualization of the loci was performed using the Integrative Genomics Viewer (IGV). (J) Panther pathways enriched in regions that become more accessible in progenitors during both acute and chronic LCMV infection. The enrichment was achieved by using GREAT to compare these regions with whole genome background. (K) Frequency of progenitors with active Caspase-3 analyzed by flow cytometry. Graphs depict mean ± SEM and symbols represent individual mice. Data are representative of from 2 independent experiments. * < 0.05, ** < 0.01 (One way ANOVA).

3.3.3 Genomic analysis in DC progenitors predicts TFs with altered activity during LCMV infection

A large number of TFs have been found to play important roles in development and/or activation of specific immune cell lineages over the years[187]. Consistently, multiple TFs have been demonstrated to constitute the transcriptional basis for the development and function of the individual types of DCs through regulation of their target genes (reviewed in [47]). Among the DEGs in progenitors common to ARM and Cl13 infection (>2-fold change, FDR < 0.05), there were 96 TFs upregulated and 21 TFs downregulated compared to their counterparts from uninfected mice (Fig. 3-3A and B). Consistent with the compromised pDC development from progenitors upon LCMV infection, TFs that have been shown to be critical for pDC development such as Tcf4, SpiB, Bcl11a, and Runx2 were significantly downregulated in progenitors upon both ARM and Cl13 infection[106,109,111,112,188] (Fig. 3-3A). In contrast, while expression of Nfil3, a TF essential for the development of cDC1s[129], was significantly downregulated in progenitors upon LCMV infection, expression of Batf2, a TF which can compensate for Batf3[148]and thereby may also compensate for the loss of Nfil3 to promote cDC1 development[129], was significantly upregulated, consistent with enhanced cDC1 development from progenitors during LCMV infection (Fig. 3B). Moreover, expression of Id1, which has been shown to be responsible for the switch from DC differentiation to myeloid-derived suppressor cell expansion during tumor progression[189], was significantly upregulated, suggesting a similar role of this TF to compromise overall DC differentiation potential of the progenitors in the context of viral infection (Fig. 3-3B).

While studies of differentially expressed TFs and their targets can provide some explanations for the selectivity of the pathways for development and functional responses of DCs, however, a growing body of evidence supports that, in addition to expression, distinct chromatin

features of different subsets of genes play active roles in these responses[150]. Moreover, the expression level of a TF does not always correlate with its activity and a TF that does not vary in its own expression level can possibly exhibit differential activities and influential roles in different contexts[154]. Therefore, in order to have a better understanding of biologically important TFs based on chromatin features of their target genes and prediction of their activities, we used a software package called Taiji, which integrates ATAC-seq and RNA-seq data and implements personalized PageRank analysis to assess the global importance of TFs in each biological condition[155]. This computational strategy has already successfully predicted TFs with previously unappreciated roles to have crucial regulatory functions in the differentiation of circulating and resident memory CD8+ T cells[156,157]. After implementing Taiji, we selected TFs predicted to exhibit altered activities in progenitors from both ARM- and Cl13-infected mice compared to their counterparts from uninfected mice (more than 2-fold change in rank) and that passed minimum expression level threshold (TPM >1) (Table 3-1). Since the phenotype of the BM progenitors in ARM vs. Cl13 infected mice is almost indistinguishable at day 8 p.i.[185] and we aim to find the driver of these common phenotypes, we selected TFs with altered activity in both ARM- and Cl13-infected mice to increase robustness of our analysis. Notably, 11 out of 35 (31%) TFs previously shown to be associated with DC development and/or function showed up in our analysis[106,189-201]. Our analysis predicted several TFs with altered expression in progenitors during both ARM and Cl13 infection, such as Id1, Stat1, Cebpb, and Tcf4, to exhibit differential activities as expected (Table 3-1, Fig. 3-3A and B). These results illustrate the power of Taiji to predict TFs with potential roles in regulation of DC development and/or function. Interestingly, the TF predicted to have the largest difference in rank between progenitors from infected vs. uninfected mice was Glucocorticoid Modulatory Element Binding protein 1 (Gmeb1), which had homogeneous expression in every

condition studied (Fig. 3C) and reflects the strength of Taiji analysis to highlight novel TF candidates with regulatory roles.

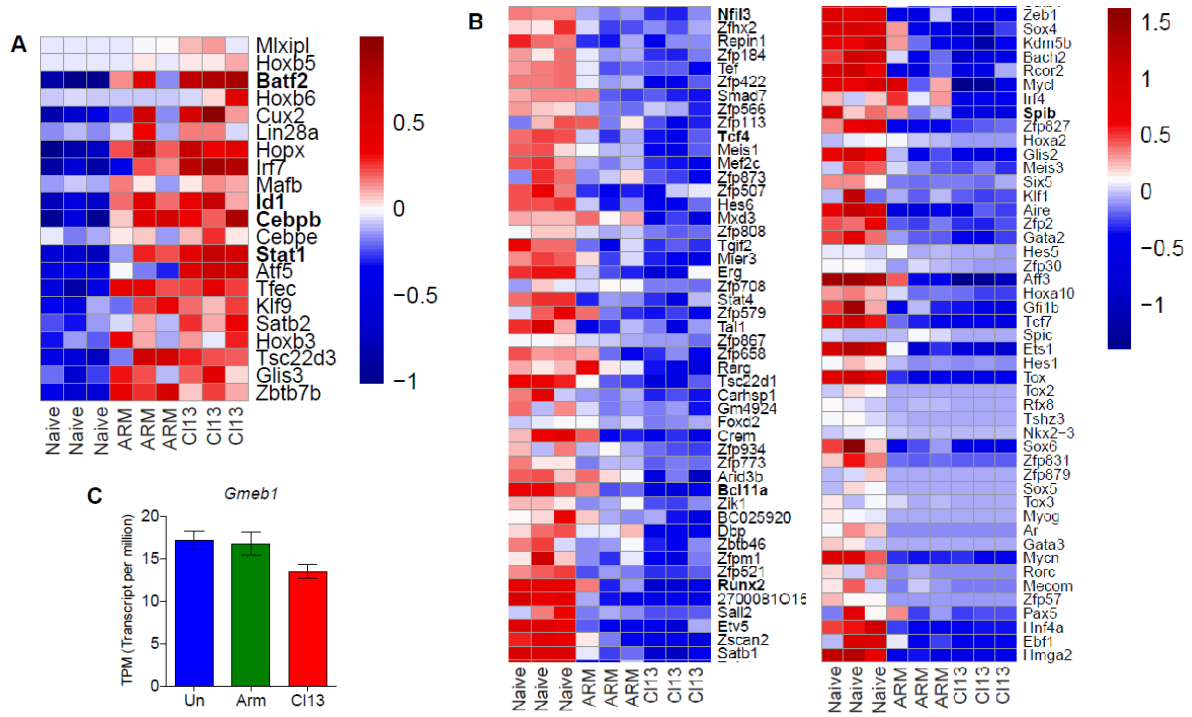

Figure 3-3. Transcription factors (TFs) are differentially regulated in progenitors during both ARM and Cl13 infection. WT mice were infected with LCMV ARM or Cl13 or left uninfected and sacrificed at day 8 p.i. BM DC progenitors (Lin−c-kit$^{int/lo}$Flt3+) were isolated by flow cytometry for 3 independent RNA-seq analyses. Lin includes markers for Thy1.2, CD19, NK1.1, CD3, CD4, CD8, B220, CD11b, Gr-1, CD11c and Ter119. (A-B) RSEM counts were used to identify differentially expressed TFs by DESeq2 (FDR < 0.05, > 2-fold-change). Heatmaps of TFs that are significantly upregulated (A) or downregulated (B) in progenitors during both ARM and Cl13 infection compared to their counterparts from uninfected are shown. (C) Expression levels of Gmeb1 in progenitors. Bars depict mean ± SEM of Transcripts Per Million (TPM) from 3 independent replicates.

Table 3-1. Table of key TFs with higher or lower activity in BM DC progenitors from LCMV ARM- and Cl13-infected (day 8 p.i.) compared to uninfected mice. Key TFs were filtered using three criteria. 1) Average rank of all conditions is greater than 0.0001. 2) The fold change between progenitors from LCMV-infected and uninfected mice is over 2 or below 0.5 in both Arm vs. uninfected and Cl13 vs. uninfected comparisons. 3) The expression level of TF passes minimum expression threshold (TPM>1). Gmeb1 and Zfp524, the top 2 TFs predicted to exhibit the most differential activity in progenitors during infection among the 24 TFs without any known roles in DC biology, were chosen for further studies. * denotes previous link with DC development or function in the cited references.

TF regulators with higher activity in Arm and Cl13 compared to uninfected	Average(rank Arm/rank uninfected, rank Cl13/rank uninfected)	TF regulators with lower activity in Arm and Cl13 compared to uninfected	Average(rank Arm/rank uninfected, rank Cl13/rank uninfected)
Gmeb1	16.6152868	Tcf4* *Cisse, et al. 2008*	0.131921165
Irf9	7.130281881	Zfp524	0.183286976
Atf7	4.288442225	Mbd1	0.194483894
Nfatc3* *Bao, et al. 2016*	3.989128613	Cic	0.213898691
Cebpg	3.83534193	Mecp2	0.268683774
Elk3	3.212677989	Irf2* *Ichikawa, et al. 2004* *Honda, et al. 2004*	0.277786726
Cebpb* *Bornstein, et al. 2014*	3.100666533	Hes1	0.333192785
Mtf1	3.046185919	E2f4* *Enos, et al. 2008*	0.343270146
Irf7* *Owens, et al. 2012* *Lazear, et al. 2013* *Bao, et al. 2016*	3.024421259	Glis2	0.347702709
Myb* *Papathanasiou, et al. 2017*	3.001929117	Jund* *Hara, et al. 2013*	0.353176705
Stat1* *Jackson, et al. 2004* *Longman, et al. 2007*	2.965794512	Hnf4a	0.378750552
Zbtb6	2.873073962	Zkscan1	0.42062241
Nr2f6	2.734521409	Hoxa3	0.4256718
Id1* *Papaspyridonos, et al. 2015*	2.717082432	Nr3c1	0.443796765
Hbp1	2.670195844	Tfdp1	0.446273311
Hmbox1	2.602539449	Bach2* *Itoh-Nakadai, et al. 2017*	0.45289583
Mlxip	2.547257227		
Mybl1	2.445517652		
Zfp691	2.208894358		

3.3.4 Gmeb1 suppresses pDC development in a glucocorticoid-dependent manner, but suppresses cDC maturation and promotes cDC1 development independently of glucocorticoid *in vitro*

The role of Gmeb1 in DC development and function is unknown. Based on the Taiji prediction of enhanced activity of Gmeb1 in progenitors during infections, we hypothesized that abrogated expression of Gmeb1 would attenuate infection-specific DC phenotypes. To evaluate the role of Gmeb1 in progenitor-derived DCs, we transduced uninfected BM-Flt3L culture with retroviral particles encoding shRNA against Gmeb1 or non-targeting control shRNA at day 2 and 3 post culture (p.c.). At day 8 p.c., transduced cells were distinguished by reporter expression and Gmeb1 expression was reduced with ~50% knockdown efficiency (Fig. 3-4A and B). Upon Gmeb1 knockdown, we observed significantly enhanced differentiation into pDCs as well as reduced differentiation into $CD24^{high}$ cDCs, while differentiation into $CD11b^{high}$ cDCs was not significantly changed in 2 out of 3 experiments (Fig. 3-4C). In addition, Gmeb1 knockdown increased expression of maturation marker CD86 in $CD24^{high}$ and $CD11b^{high}$ cDCs (Fig. 3-4D). Gmeb1 knockdown also induced a very modest but statistically significant increase in CD86 expression in pDCs (Fig. 3-4D). Consistent with the Taiji prediction of enhanced Gmeb1 activity in progenitors during infection, Gmeb1 knockdown in BM-Flt3L cultures from Cl13-infected mice at day 8 p.i. also significantly enhanced pDC development and CD86 expression on cDCs but decreased $CD24^{high}$ cDC development (Fig. 3-4E and F). Again, differentiation into $CD11b^{high}$ cDCs was not significantly changed upon Gmeb1 knockdown (Fig. 3-4E). In addition, a small increase in CD86 expression in pDCs upon Gmeb1 knockdown was not reproduced in culture from Cl13-infected mice (Fig. 3-4F). These data support a previously unrecognized role for Gmeb1 in the suppression of pDC development and cDC maturation as well as promotion of cDC1

development. Moreover, these data are consistent with the predicted higher Gmeb1 activity in LCMV infection, where pDCs exhibit compromised development while cDCs exhibit enhanced development and compromised maturation.

Gmeb1 has been shown to increase sensitivity to bind to glucocorticoid modulatory elements and increase sensitivity to low glucocorticoid concentrations[202,203]. On the other hand, Gmeb1 can mediate transactivation of its target genes as a homodimer or a heterodimer with Gmeb2[202]. Therefore, we asked if Gmeb1-mediated modulation of DC progenitors is dependent on glucocorticoid or its intrinsic transactivation activity. We confirmed the presence of ~300pg/ml corticosterone in media used for culture and supernatants taken every day over the course of Flt3L culture used for our knockdown study (Fig. 3-4G). After we transduced uninfected BM-Flt3L culture with retroviral particles encoding shRNA against Gmeb1 or non-targeting control shRNA at day 2 and 3 p.c., we treated the culture with mifepristone, glucocorticoid receptor (GR) antagonist, or vehicle control until day 8 p.c. As shown in Fig. 3-4H, while pDC development was significantly enhanced upon Gmeb1 knockdown in the presence of vehicle, there was no significant difference in pDC development between control shRNA-transduced cells and Gmeb1 shRNA-transduced cells upon blockade of GR signaling. In contrast, we observed compromised $CD24^{high}$ cDC development and enhanced CD86 expression on $CD24^{high}$ cDCs upon Gmeb1 knockdown regardless of the presence of mifepristone (Fig. 3-4H). CD86 expression on $CD11b^{high}$ cDCs was still enhanced upon Gmeb1 knockdown in only 1 out of 2 experiments, so dependence of cDC2 maturation on Gmeb1 awaits further investigation. Collectively, these data demonstrated that Gmeb1-mediated suppression of pDC development is at least partially dependent on glucocorticoid, while Gmeb1-mediated enhancement of cDC1 development and suppression of cDC1 maturation was independent of glucocorticoid.

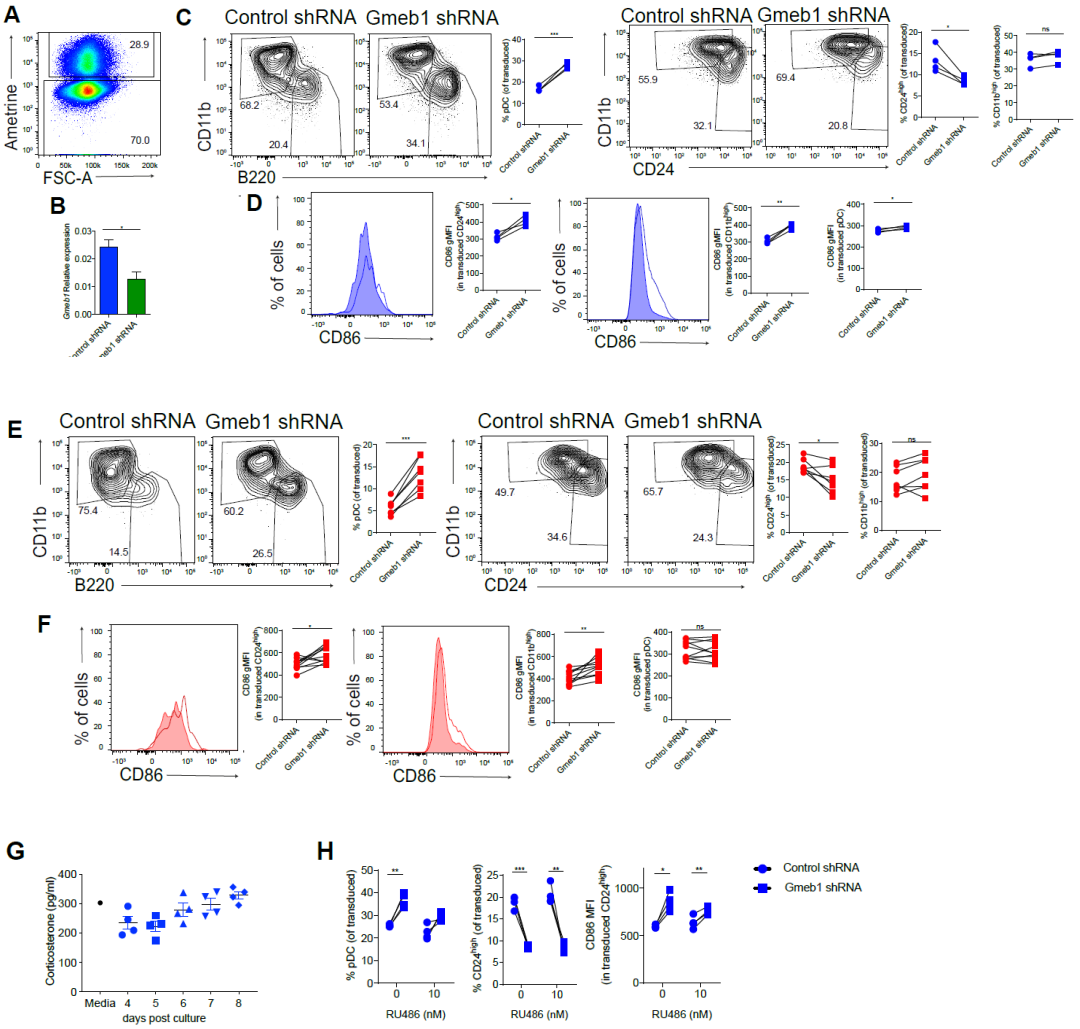

Figure 3-4. Gmeb1 suppresses pDC development but promotes cDC1 development and suppresses cDC maturation. BM Flt3L culture from uninfected (A-D, H) or day 8 LCMV Cl13-infected (E, F) mice were transduced at day 2 and 3 post-culture (p.c.) with retroviral particles (RV) encoding Gmeb1-targeting or control shRNA and analyzed at day 8 p.c. (A) Representative FACS plot showing transduced cells. (B) Gmeb1 knockdown evaluated by qPCR in FACS-purified pDCs. Frequency (C and E) and geometric mean fluorescence intensity (gMFI) of CD86 (D and F) of pDCs, CD24^{high} cDCs, and CD11b^{high} cDCs within transduced cells were analyzed by flow cytometry. (D and F) Representative histograms of CD86 expression on CD24^{high} cDCs and CD11b^{high} cDCs from culture that received control shRNA (filled) or Gmeb1 shRNA (open). (G) Concentration of corticosterone measured in media and BM Flt3L culture from day 4 to 8 p.c. by ELISA. (H) Culture was treated with mifepristone (RU486) or vehicle from day 3 onwards and analyzed for frequency of pDCs and CD24^{high} cDCs within transduced cells and CD86 gMFI within transduced CD24^{high} cDCs by flow cytometry. (A, C-H) Graphs depict mean ± SEM and symbols represent individual mice. (B) Bars represent mean ± SEM from technical triplicates. (A-C, E, G-H) Data are representative of 2-4 independent experiments. (D and F) Data are pooled from 3 independent experiments. *<0.05, **<0.01 ***<0.001. (Unpaired t-test (B) or paired t-test (C-F, H)).

3.3.5 Glucocorticoid suppresses pDC development *in vivo* during LCMV chronic infection

Given that negative regulation of pDC development by Gmeb1 is dependent on glucocorticoid, we hypothesized that glucocorticoid suppresses pDC development and the heightened activity of Gmeb1 in progenitors during LCMV infection aggravates this effect. Glucocorticoid has been shown to suppress pDC differentiation in *in vitro* BM Flt3L culture[204]. To determine if glucocorticoid suppresses pDC development to a different extent during LCMV infection, we treated BM Flt3L culture from uninfected vs. LCMV Cl13-infected mice with different doses of corticosterone for 8 days. pDC development within DCs was severely compromised with increasing doses of corticosterone in cultures from both uninfected and LCMV Cl13-infected mice, supporting that glucocorticoid compromises pDC development (Fig. 3-5A). Notably, pDC development was compromised in the presence of corticosterone to a larger extent in culture from Cl13-infected mice than culture from uninfected mice, suggesting that progenitors from Cl13-infected mice are more sensitive to glucocorticoid than their counterparts from uninfected mice, consistent with the predicted enhancement in Gmeb1 activity (Fig. 3-5A).

Previous studies have shown that pDCs are highly sensitive to glucocorticoid-induced apoptosis[205]. Since the reduction in pDCs in response glucocorticoid was observed after 8 days of culture with glucocorticoid (Fig. 3-5A), it is possible that it was caused by glucocorticoid-induced apoptosis of mature pDCs rather than glucocorticoid-mediated regulation of development from progenitors. In order to limit the effect of glucocorticoid to progenitors in the developmental window of pDCs, we treated Flt3L culture from uninfected mice with high dose of corticosterone for only 1 day starting from day 3.5, the time-point at which Flt3L culture is enriched for DC progenitors and most irrelevant cells are dead[116], and replaced the culture with fresh medium that does not contain corticosterone. Strikingly, in response to short spike of corticosterone, pDC

development was selectively compromised at day 8 p.c., while development of cDC subsets was not significantly altered or even slightly enhanced (Fig. 3-5B). Importantly, when Flt3L culture was given 1-day spike of corticosterone from day 6 to 7 p.c., when most progenitors have developed into DC subsets, pDC development was not altered, further supporting the glucocorticoid-mediated suppression of pDC developmental capacity of progenitors (Fig. 3-5C).

Next, we assessed the effect of glucocorticoid on pDC development *in vivo* during LCMV Cl13 infection. To evaluate this, we infected adrenalectomized (ADX) mice, in which adrenal glands are surgically removed and a major source of systemic glucocorticoid is absent, and sham-operated mice with LCMV Cl13. Since ADX mice do not survive beyond day 5 post p.i. (Fig. 3-5D), we decided to investigate pDC development in ADX vs. sham-operated mice at day 4 p.i. Surprisingly, there was no significant difference in number of pDCs in spleen (Fig. 3-5E) or BM (Fig. 3-5F) between uninfected ADX vs. sham-operated mice. In sharp contrast, number of pDCs in spleen (Fig. 3-5E) and BM (Fig. 3-5F) was significantly increased in ADX mice compared to sham-operated mice upon Cl13 infection. Number of cDC1s or cDC2s in spleen were not significantly altered in the absence of glucocorticoid even after LCMV infection (Fig. 3-5G). ADX and sham-operated mice did not present any significant difference in the level of systemic IFN-I at day 1 p.i. (Fig. 3-5H) or expression of PD-1, a marker induced by TCR stimulation that serves as a surrogate marker for the amount of antigen, on CD8+ T cells specific to $GP_{33-41,}$ an immunodominant peptide derived from LCMV (Fig. 3-5I). Consistent with the role of IFN-I and TLR7 signaling in pDC proliferation[185], there was no significant increase in spleen pDC proliferation in Cl13-infected ADX compared to sham-operated mice as measured by Ki67 expression (Fig. 3-5J). BM pDCs from ADX mice even demonstrated reduced proliferation compared to sham-operated mice (Fig. 3-5K). TLR activation in pDCs has been shown to override

glucocorticoid-mediated pDC apoptosis[206,207]. Consistent with persistent TLR stimulation in pDCs during Cl13 infection, there was no significant difference in pDC apoptosis between Cl13-infected ADX and sham-operated mice, as measured by the frequency of cells with active Caspase-3 (Fig. 3-5L and M). Taken together, enhanced number of pDCs in spleen and BM in ADX mice compared to sham-operated mice upon Cl13 infection was not due to increased proliferation or decreased apoptosis, suggesting that developmental output of pDCs from progenitors is enhanced in the absence of glucocorticoid.

In line with this, while there was no significant difference in number of CLPs or CDPs between uninfected or LCMV Cl13-infected ADX and sham-operated mice upon Cl13 infection (Fig. 3-5M), number of CD115- CDP-like pDC progenitors with higher potential to commit to pDCs than to other DC subsets (Onai, et al., 2013) was significantly increased in ADX mice compared to sham-operated mice upon LCMV infection (Fig. 3-5N). Collectively, these data demonstrate that glucocorticoid suppresses pDC development *in vivo* during LCMV infection.

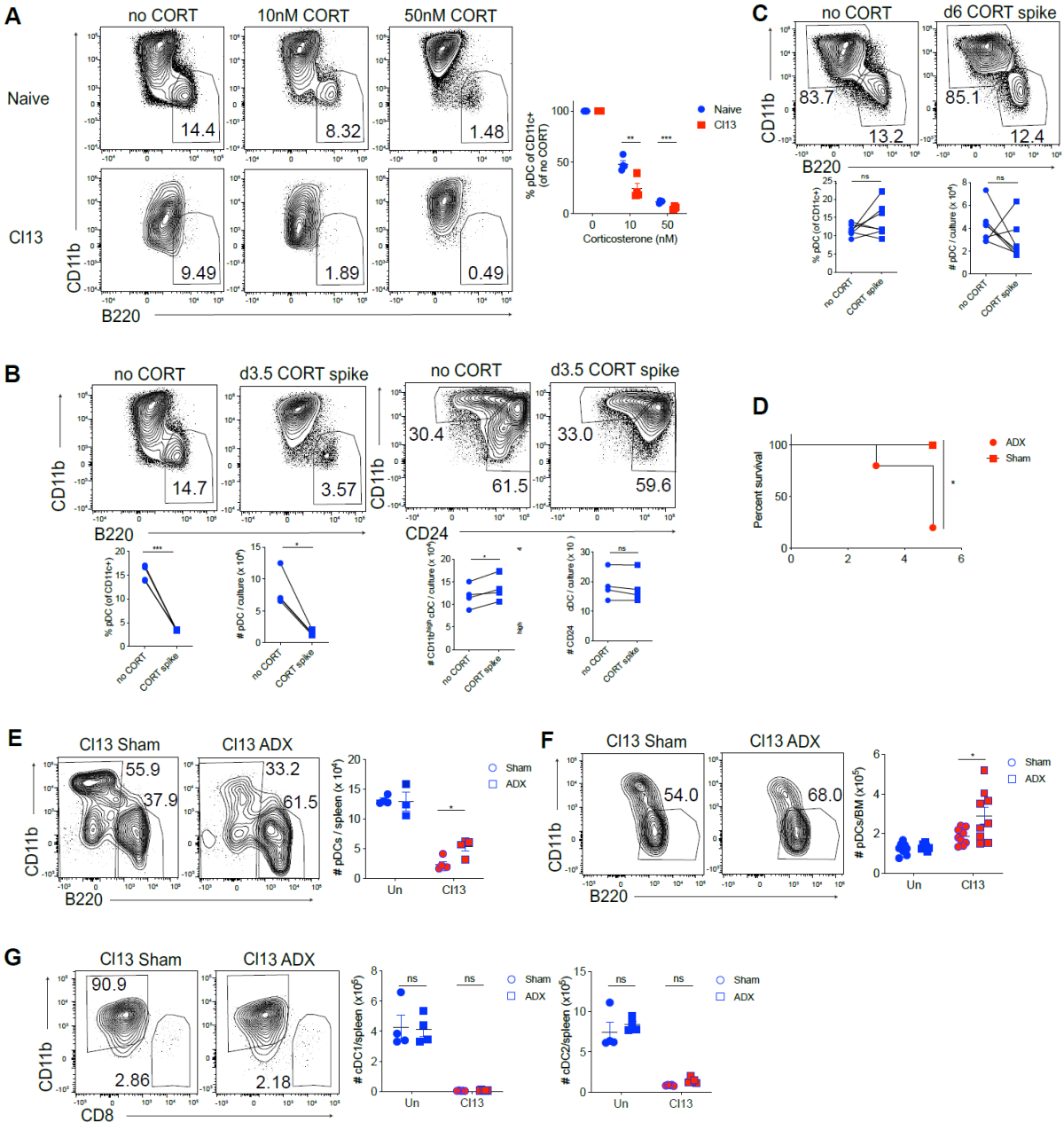

Figure 3-5. Glucocorticoid suppresses pDC development *in vivo* during LCMV infection. (A) BM Flt3L culture from uninfected or day 8 LCMV Cl13-infected mice was treated with vehicle or corticosterone at indicated concentrations for 8 days and frequency of pDCs within dendritic cells (CD11c+) was compared that in culture treated with vehicle. (B-C) BM Flt3L culture from uninfected mice was given a spike of 1uM corticosterone for 1 day from day 3.5 p.c. (B) or day 6 p.c. (C) and was replaced with fresh medium. Number and frequency of pDCs within CD11c+ were analyzed at day 8 p.c. (D-F) Sham-operated (Sham) or adrenalectomized (ADX) B6 mice were uninfected or infected with LCMV Cl13. (D) Survival rates of Cl13-infected sham and ADX mice (n=5 / group) determined over a 5-day experimental period. (E-F) Number of splenic pDCs (E), BM pDCs (F), and splenic cDC1s and CDC2s were evaluated by flow cytometry.

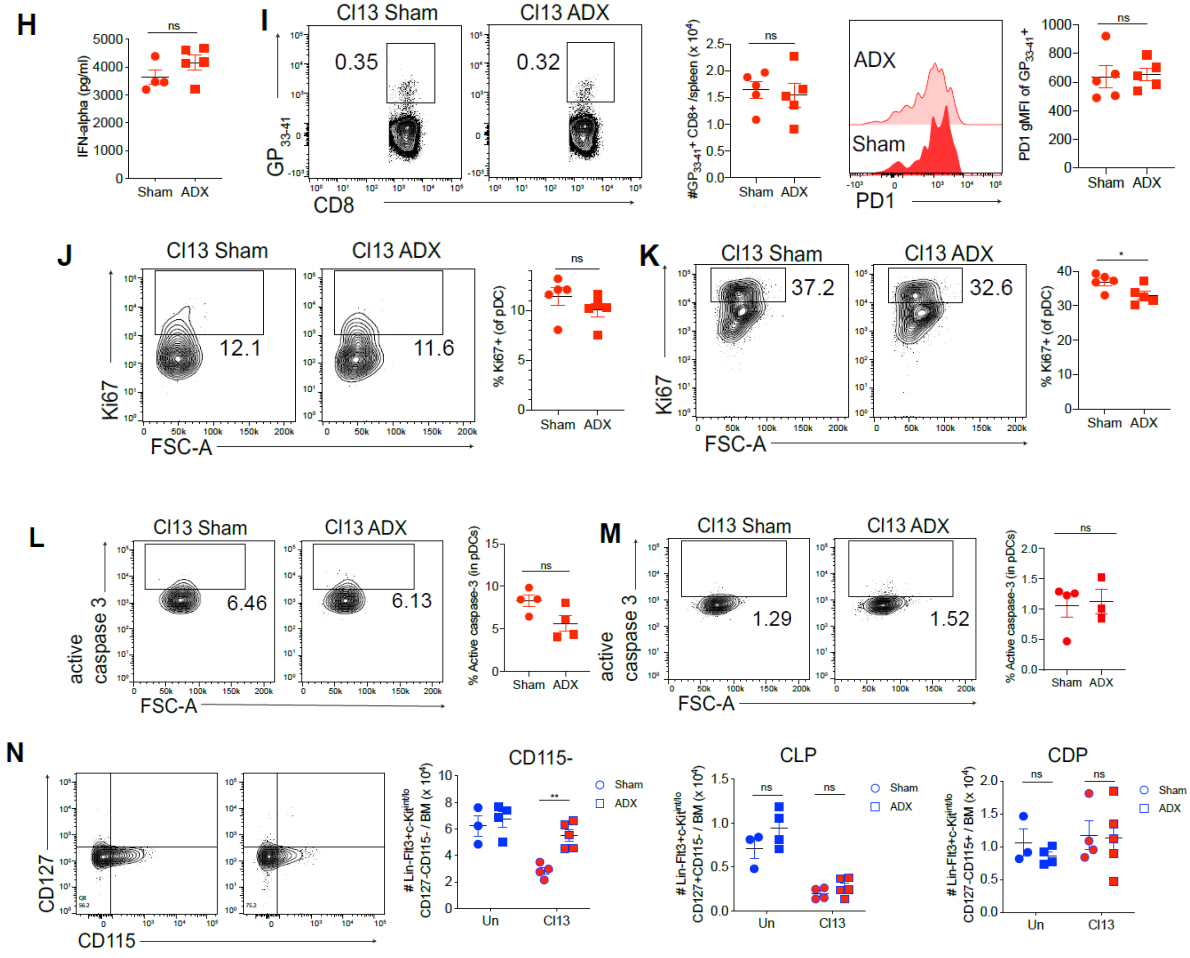

Figure 3-5. Glucocorticoid suppresses pDC development *in vivo* during LCMV infection, Continued (H) The amount of IFN-α in the serum at day 1 p.i. was quantified by ELISA. (G) The number of to GP_{33-41}-specific CD8+ T cells in the spleen and PD-1 gMFI in these cells were evaluated by flow cytometry. Splenic (I, K) and BM pDCs (J, L) were analyzed for Ki67 expression (I, J) and Caspase 3 activity (K, L) and BM was analyzed for number of CD115- CDP-like pDC progenitors (Lin-Flt3+c-Kit$^{int/lo}$CD127-CD115-), CLPs (Lin-Flt3+c-Kit$^{int/lo}$CD127+CD115-), and CDPs (Lin-Flt3+c-Kit$^{int/lo}$CD127-CD115+) by flow cytometry . Lin includes markers for Thy1.2, CD19, NK1.1, CD3, CD4, CD8, B220, CD11b, Gr-1, CD11c and Ter119. Graphs depict mean ± SEM and symbols represent individual mice. (A-B, E, G-K, N) Data are representative of 2-4 independent experiments. (C) Data are pooled from 2 independent experiments. (D, L, M) Data are from 1 experiment. (F) Data are pooled from 2 independent experiments. *<0.05, **<0.01 ***<0.001 ns, not significant (Unpaired t-test (A, H-M), paired t-test (B-C), Mantel-cox test (D), or 2-way ANOVA (E-G, N)).

3.3.6 Gmeb1 suppresses pDC development and cDC1 maturation as well as promotes cDC1 development *in vivo* during LCMV chronic infection

Given that progenitor development into pDCs and maturation of progenitor-derived cDC1s were compromised while cDC1 development was enhanced upon Gmeb1 knockdown *in vitro* (Fig. 3-4), we decided to evaluate the role of Gmeb1 in DC progenitors *in vivo* during chronic LCMV infection. For this, uninfected BM-Flt3L culture was transduced with retroviral particles encoding shRNA against Gmeb1 or non-targeting control shRNA at day 2 and 3 p.c. At day 3.5p.c., some transduced cells were distinguished by reporter (Ametrine) expression (data not shown) but it was still possible that some cells transduced during the 2nd transduction at day 3 p.c. does not express the reporter yet. Therefore, pool of Ametrine+ and Ametrine- pro-DCs were purified from retrovirally-transduced culture and transferred into congenically marked recipient mice (CD45.1+) infected with LCMV Cl13 for 8 days (Fig. 3-6A and B). 6 days after transfer, Ametrine+ cells could be clearly distinguished within CD45.2+ donor-derived cells (Fig. 3-6C).

When frequency of each DC subset was compared between cells derived from transduced pro-DCs that received Gmeb1 shRNA to their counterparts that received control shRNA, there was increased frequency of pDCs derived from pro-DCs in which Gmeb1 was knocked down (Fig. 3-6D). Also, pro-DCs consistently generated decreased frequency of cDC1s upon Gmeb1 knockdown *in vivo* in Cl13-infected recipients in 3 out of 3 experiments, while frequency of pro-DC-derived cDC2s demonstrated inconsistent pattern between pro-DCs that received control shRNA vs. Gmeb1 shRNA (Fig. 3-6D). These observations are in agreement with Gmeb1 knockdown in *in vitro* Flt3L culture and further support that Gmeb1 suppressed pDC development while promoting cDC1 development during Cl13 infection *in vivo*. Moreover, cDC1s derived from pro-DCs that received Gmeb1 shRNA demonstrated higher CD86 expression, in line with our

observation *in vitro* that Gmeb1 suppresses CDC maturation (Fig. 3-6E). Together, these data extend our observation from *in vitro* knockdown experiments and demonstrate that Gmeb1 suppresses pDC development and cDC1 maturation as well as promotes cDC1 development *in vivo* during chronic LCMV infection.

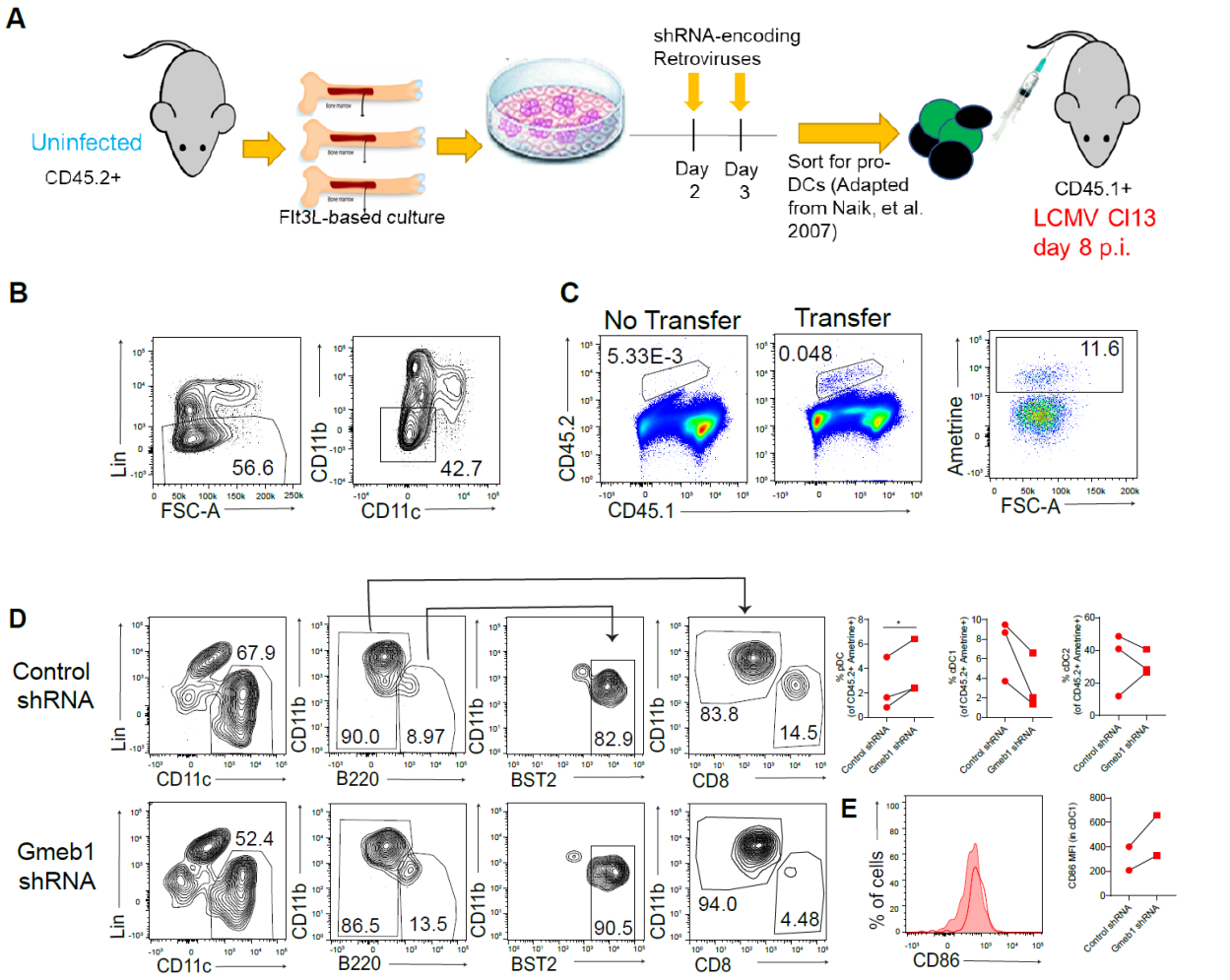

Figure 3-6. Gmeb1 suppresses pDC development and cDC1 maturation as well as promotes cDC1 development *in vivo* during LCMV chronic infection. Uninfected BM-Flt3L culture from donor mice (CD45.2+) was transduced with RVs encoding shRNA against Gmeb1 or non-targeting control shRNA at day 2 and 3 p.c. At day 3.5p.c., pool of Ametrine+ and Ametrine- pro-DCs (~600000 cells) were purified from culture and intravenously transferred into congenically marked recipient mice (CD45.1+) infected with LCMV Cl13 for 8 days. 6 days after transfer, splenocytes of recipient mice were analyzed by flow cytometry. (A) Schematic of the experiment. (B) Gating strategy for purifying pro-DCs (Lin-CD11b$^{-/lo}$CD11c-) from Flt3L culture at day 3.5 p.c. Lin includes markers for Thy1.2, CD19, NK1.1, CD3, CD4, CD8, B220, CD11b, Gr-1, Ter119, CD127, and MHCII. (C) Gating strategy for donor-derived cells in the spleen of recipient mouse at day 6 post transfer (left) and Ametrine expression within donor-derived cells (right). (D) Gating strategy for pDCs (Lin-CD11c+B220+BST2+), CDC1s (Lin-CD11c+B220-CD8+CD11b-), and CDC2s (Lin-CD11c+B220-CD8-CD11b+) within transduced (Ametrine+) donor-derived cells. (E) Representative histograms of CD86 expression on splenic cDC1s derived from donor pro-DCs that received control shRNA (red filled) or Gmeb1 shRNA (red open). Graphs depict CD86 gMFI on transduced donor-derived splenic cDC1s. Data are pooled from 3 independent experiments and symbols represent one experiment in which 2-3 recipients are pooled. * < 0.05 (paired t-test)

3.3.7 Zfp524 promotes cytokine production by pDCs but suppresses cytokine production by cDCs

Zfp524 displays an annotated DNA binding motif and has been identified as differentially regulated in several system level analyses[208-212], but its role in DC development and function is unknown. Based on the Taiji prediction of compromised activity of Zfp524 in progenitors during infections, we hypothesized that reducing expression of Zfp524 and thereby reducing its activity in progenitors from uninfected mice would recapitulate some infection-specific DC phenotypes. To evaluate the role of Zfp524 in progenitor-derived DCs, we transduced uninfected BM-Flt3L culture with retroviral particles encoding shRNA against Zfp524 or non-targeting control shRNA at day 2 and 3 p.c. At day 8 p.c., we observed a knockdown efficiency of 50-70% (Fig. 3-7A) There was no significant difference in DC differentiation or maturation upon Zfp524 knockdown (Fig. 3-7B). We did, however, detect reduced and enhanced cytokine production in pDC and cDCs upon Zfp524 knockdown, as shown for two Zfp524-specific shRNA constructs in Fig 3-7C and 3-7D. These results support a novel role for Zfp524 in promoting pDC cytokine production while attenuating cDC cytokine production. Notably, at day 8-10 after Cl13 infection, cDCs exhibit enhanced TNFα secretion (Fig. 3-7E), while pDCs show decreased TNFα and IFN-I secretion upon TLR stimulation (Macal, et al., 2018). Our data with Zfp524 knockdown are consistent with the predicted lower Zfp524 activity in progenitors during LCMV infection, where pDCs exhibit compromised cytokine production while cDCs exhibit enhanced cytokine production. These results support the power of our experimental design and Taiji to identify TFs with important roles in DC biology.

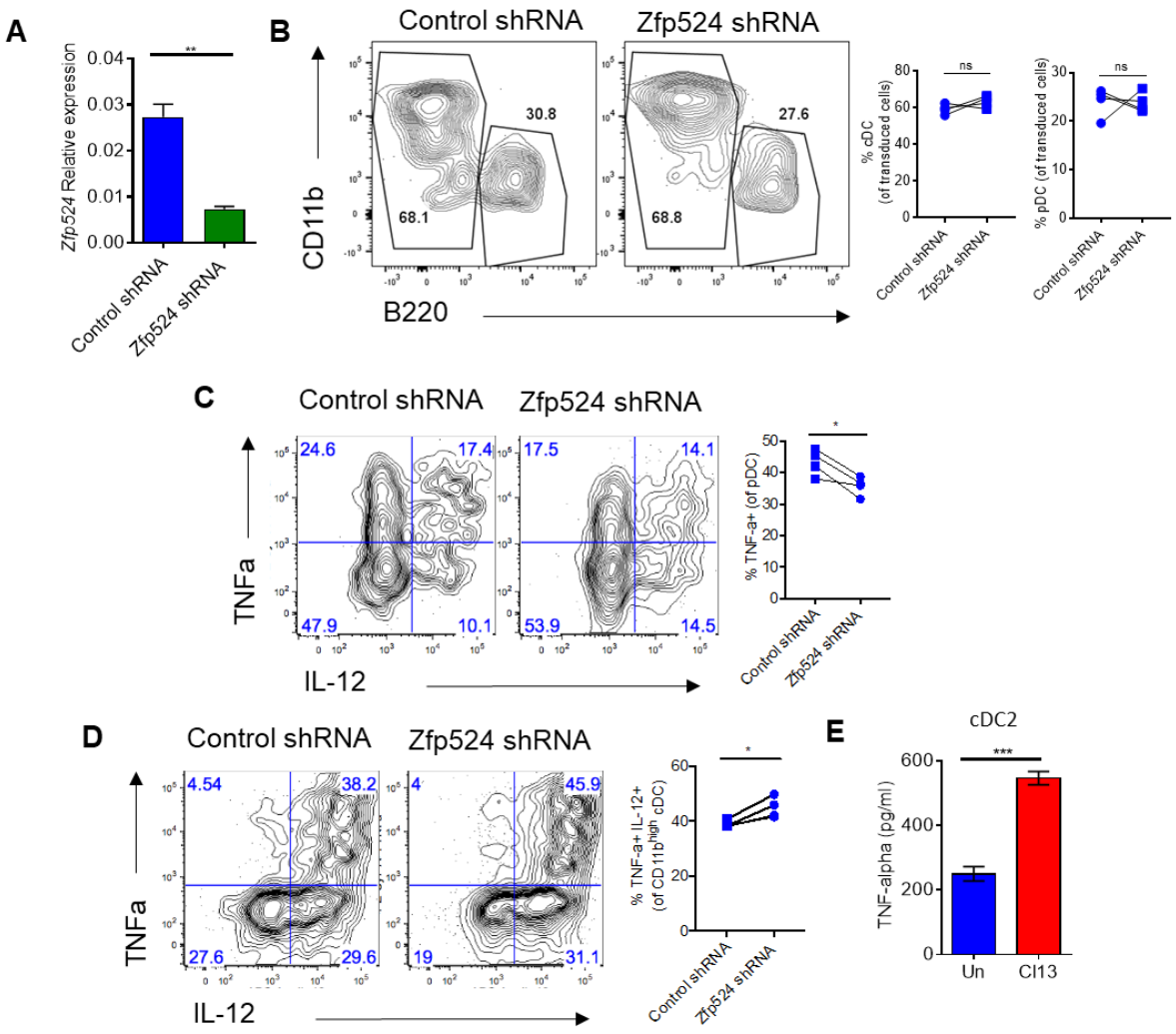

Figure. 3-7. Zfp524 oppositely modulates cytokine production in pDCs and cDCs. (A-D) BM Flt3L culture from B6 mice was transduced at day 2 and 3 p.c. with RV encoding Zfp524-targeting shRNA or non-targeting shRNA and analyzed at day 8 p.c (A) Zfp524 knockdown was evaluated by qPCR in FACS-purified pDCs from culture. (B) Frequency of pDCs and cDCs (CD11c+B220-) within transduced cells was analyzed by flow cytometry. Upon stimulation with CpG-B for 7 hours, TNF-a and IL-12 production by transduced pDCs (C) and CD11b^{high} cDCs (D) was analyzed by flow cytometry. (E) WT mice were uninfected (Un) or LCMV Cl13-infected (Cl13) for 10 days FACS-purified splenic cDC2s were stimulated with CpG-B for 15 hours and TNF-α was quantified in the supernatant by ELISA. (A) Bars depict mean ± SEM from technical replicates. (B-D) Graphs depict mean ± SEM. Symbols represent individual mice. (E) Bars depict mean ± SEM from different wells of stimulation of pooled cells. Data are from 2-4 independent experiments with 3-4 mice. *p<0.05, ***p<0.001, ns, not significant (unpaired t-test (A, E) or paired t-test (B-D)).

3.4 Discussion

Different subsets of DCs specialize in diverse aspects of immune responses, bridging innate and adaptive immunity[213] (Merad, et al., 2013). Although DCs play crucial roles in mounting effective antiviral defenses[54-58], they are subverted or adapted during chronic viral infections[3,59-62,185]. Intriguingly, not only DCs but their progenitors also adapt during chronic viral infection, resulting in altered repopulation of different DC subsets and sustained changes in maturation and function of short-lived DC progeny[62,65,185]. Importantly, all progenitor adaptations sustained during chronic infection are also detectable early after acute infection[185], suggesting that mechanisms common to acute and chronic infection initiate progenitor adaptations. Here we used acute and chronic LCMV infection in its natural rodent host during early phase of infection (day 8 p.i.) and focused on their commonality at this time point to study the mechanisms underlying the adaptation of DC progenitors. Our study revealed highly similar transcriptome and chromatin landscapes of progenitors from ARM- and Cl13-infected mice, concomitant with activation and repression of multiple biological pathways common to both infections. Furthermore, analysis of commonly accessible regions during ARM and Cl13 infections identified a TF with higher activity during infections, Gmeb1, and a TF with lower activity during infections, Zfp524, as novel regulators of DC progenitors. Surprisingly, Gmeb1 suppressed pDC development in a manner dependent on glucocorticoid, which suppressed pDC development during *in vivo* LCMV infection, while promoting development but suppressing maturation of cDC1s in a glucocorticoid-independent manner. On the other hand, Zfp524 oppositely modulated cytokine production by cDCs and pDCs.

Despite the high similarity in progenitor transcriptome between ARM and Cl13 infection at the time point studied, there were a significant number of differentially expressed genes and pathways that involve these genes. It will be important to discern in the future studies if these

genes and pathways are involved in the persistence of adaptation mechanisms exclusive to chronic infection during the later phase. In contrast, both ARM and Cl13 infection induced a significant gain in chromatin accessibility in progenitors and no single differentially accessible chromatin region could be found between two infections despite resolution of acute infection at the time point studied. This is reminiscent of innate immune memory found in myeloid cells where the intracellular signals in response to primary immune activation are translated into long-term enhancement in chromatin accessibility through epigenetic reprogramming, which provides a 'primed' or 'trained' state that enables the more efficient induction of genes upon re-infection[214]. It will be important to investigate how long such changes in chromatin accessibility are maintained after resolution of infection and study how DC progenitors and DCs respond to re-infection to elucidate this possibility.

Our data also revealed a balance between gain and loss of gene expression in contrast to a prominent increase in chromatin accessibility in progenitors upon infection. Differentially accessible chromatin regions during infection were depleted of promoter regions, whose chromatin accessibility correlates better with gene expression than accessibility in gene bodies[215], suggesting that chromatin accessibility alone cannot fully explain patterns of gene expression in our study. An important factor to consider in transcriptional regulation of gene expression is TF. TF activity is a combinatorial function of many factors that includes not only TF expression level but also availability of other cooperative TFs and specific combinations of cofactors as well as their post-translational modification[216]. With the notion that TFs preferentially bind within open chromatin[217], the analysis package used in this study, Taiji, was designed to more accurately predict TF activity based on both chromatin accessibility and expression of target genes[155]. Indeed, we validated Gmeb1, a driver TF with no variation in its own expression but predicted by Taiji to have higher

activity in progenitors during infection, to have important roles in development and maturation of progenitor-derived DCs. Conventional approaches focused on differential gene expression would not have identified Gmeb1 as an important TF regulator. Deciphering the roles of other candidate TFs identified by Taiji to have differential activity in progenitors during infection is an exciting area for future work.

We showed that Gmeb1 suppressed pDC development *in vivo* during LCMV infection. Interestingly, while glucocorticoid did not suppress pDC development in uninfected mice, it suppressed pDC development during LCMV infection *in vivo*. This discrepancy could be due to heightened activity of Gmeb1 in progenitors, which increases sensitivity to glucocorticoid[202] during infection. Even though a significant increase in systemic glucocorticoid production is only briefly observed during chronic LCMV infection around day 7 p.i., but not during acute infection[159], significantly increased expression of a glucocorticoid-induced TF, Gilz (Tsc22d3)[218], in progenitors from both acute and chronic infection (Fig 3-3A) is indicative of increased GR activation and supports enhanced activity of Gmeb1 in progenitors during both infections. Glucocorticoid-mediated suppression of pDC development during early phase of infection may be part of adaptation to prevent excessive immunopathology by restraining output of pDCs capable of producing copious amounts of IFN-I and other proinflammatory cytokines. Glucocorticoid can be induced by IFN-I[219,220] and could be mediating suppression of pDC development by IFN-I signaling[185]. This is in line with suppressive effects of glucocorticoids that have been reported during the inflammatory state[162].

On the other hand, we showed that Gmeb1 enhanced cDC1 development while suppressing cDC maturation in a glucocorticoid-independent manner. Consistently, while Gmeb1 enhanced cDC1 development, glucocorticoid did not alter cDC1 development during LCMV infection *in*

vivo. This was unexpected based on previously known effects of glucocorticoid on cDC differentiation[221-223]. It is likely that, at the time point of this study when adrenalectomized mice were examined, the physiological concentration of glucocorticoid and the extent of GR signaling induced by LCMV infection were not as high as the counterparts used in other studies, where glucocorticoid was experimentally induced to increase several-fold. Uncoupling of Gmeb1-mediated enhancement of cDC1 development from glucocorticoid signaling suggests that it occurs through a separate pathway from pDC development. One possible mechanism could be Batf3-independent pathway in mice for cDC1 development operating during infection through Batf2 induced by cytokines as in the infection with intracellular pathogens[148]. Alternatively, Gmeb1 activity could crosstalk mTOR signaling, which has been shown to be particularly important for development of cDC1s over other DC subsets[105]. Chromatin immunoprecipitation with antibodies against Gmeb1 and GR will be able to parse out glucocorticoid-dependent and -independent targets of Gmeb1 that are differentially regulated in progenitors during infection. While mechanism of Gmeb1 action needs to be elucidated, it is tempting to speculate that Gmeb1 activity is enhanced in progenitors to preferentially generate cDC1s to support CD8+ T cell immunity in the face of ongoing antigen, albeit with reduced maturation such that consequent immune responses are attenuated enough to prevent excessive immunopathology.

By applying genomics tools to DC progenitors in the unique context of LCMV infection where progenitors and progenitor-derived DCs are functionally altered, we have uncovered novel TF regulators of DC biology that have not been linked to DC biology before. While immunotherapies with individual DC subsets have been previously performed, it has only been effective in a few contexts[224], possibly due to the need for the sustained supply of multiple (and probably empowered) DC subsets that could simultaneously act to restore immune responses in

immunosuppressive settings as in the case of chronic infections or tumors. Targeting and manipulating DC progenitors that have longer lifespans than DCs themselves and generate multiple DC subsets could therefore be an attractive solution. Our study significantly deepens our understanding of DC biology and provides potential new targets for DC-based immunotherapies and vaccines in infectious and non-infectious diseases.

3.5 Materials and Methods

3.5.1 Experimental Model and Subject Details

Mice

C57BL/6 mice, CD45.1+ mice, sham-operated and ADX mice were obtained from Taconic laboratories. (6-8 weeks old) were purchased from The Jackson Laboratory. ADX mice were maintained on drinking water containing 1% NaCl per manufacturer's instruction. All mice were housed under specific-pathogen-free conditions at the University of California, San Diego. Mice were bred and maintained in a closed breeding facility and mouse handling and experiments conformed to the requirements of the National Institute of Health and the Institutional Animal Care and Use Guidelines of UC San Diego. Unless stated otherwise, experiments were initiated in mice (female and male) at 7-12 weeks of age.

Virus strains

Mice were infected with 2×10^6 plaque-forming units (pfu) of LCMV Arm (ARM) or LCMV clone 13 (Cl13) intravenously (i.v.) via tail vein. Viruses were propagated on BHK cells and quantified by plaque assay performed on Vero cells[183]. Briefly, Vero cell monolayers were infected with 500 µL of serially diluted viral stock and incubated for 60 minutes at 37°C in 5% CO_2 with gentle shaking every 15 minutes. Agarose overlay was added to infected cells and placed

in incubator for 6 days at 37°C in 5% CO_2. Cells were fixed with formaldehyde and stained with crystal violet for 5 minutes at room temperature and plaques were counted.

Cell lines

HEK293T cells were cultured in DMEM containing 10% FBS, penicillin-streptomycin, and supplements of L-glutamine. $1.5x10^6$ cells were passaged every 3 days. Cells were washed in PBS pH 7.4 then lifted from culture flasks with 0.05% Trypsin-EDTA. Trypsin was deactivated by addition of serum containing media.

Primary cell culture

BMDCs were differentiated at the concentration of $2x10^6$ cells/ml for 8 days in 5ml of RPMI-1640 supplemented with 10% (vol/vol) fetal bovine serum, L-glutamine, penicillin-streptomycin, and HEPES pH 7.2 supplemented with 100ng/mL Flt3L (provided by CellDex Therapeutics) and 50μM β-mercaptoethanol. Half of the medium was replaced after 5 days with fresh cytokines added.

3.5.2 Method details

Mouse Cell Purification

Spleens were incubated with 1mg/mL collagenase D for 20 min at 37˚C and passed through a 100μm strainer to achieve a single cell suspension. BM DC progenitors were enriched by using EasySep™ Mouse Streptavidin RapidSpheres™ Isolation Kit (Stemcell Technologies,), biotin-conjugated anti-Thy1.2 (53-2.1), anti-B220 (RA3-6B2), anti-CD11b (M1/70), anti-CD4 (RM4-5), anti-CD19 (6D5) and anti-CD8 (536.7). Fractions unbound to streptavidin beads were stained with PI and FACS-purified using a BD ARIA II (BD) or ARIA Fusion (BD) for progenitors ($PI^-CD11c^-c\text{-}Kit^{intermediate/dim}Flt3^+$) after B (CD19, B220), T (Thy1.2, CD3, CD4, and CD8), NK

(Nk1.1), red blood cell (Ter119), granulocyte (Gr-1), and monocyte (CD11b) exclusion. Pro-DCs derived from culture of BM cells with Flt3L were enriched by using EasySep™ Mouse Streptavidin RapidSpheres™ Isolation Kit (Stemcell Technologies,), biotin-conjugated anti-Gr-1 (RB6-8C5), anti-CD19 (6D5) and anti-CD127 (A7R34). Fractions unbound to streptavidin beads were stained with PI and FACS-purified using a BD ARIA II (BD) for progenitors ($PI^-CD11c^-CD11b^{-/low}$) after B (CD19, B220), T (Thy1.2, CD3, CD4, CD8, CD127), NK (Nk1.1), red blood cell (Ter119), granulocyte (Gr-1), monocyte (CD11b), and MHCII exclusion. Purity of the cells was > 95% (data not shown).

Flow Cytometry

The following antibodies were used to stain single cell suspensions prepared from murine BM or spleens: Thy 1.2 (53-2.1), CD19 (eBio1D3), NK 1.1 (PK136), Gr-1 (RB6-8C5), CD11c (N418), CD11b (M1/70), B220 (RA36B2), BST2 (eBio927), CD45.2 (104), CD4 (RM4-5), CD8 (53-6.7), Ter119 (TER-119), CD3 (145-2C11), CD45.1 (A20), MHC class II (I-A/I-E) (M5/114.15.2), Ki67 (SolA15), c-kit (2B8), CD115 (AFS98), Flt3 (A2F10), Streptavidin, CD127 (eBioRDR5), CD86 (GL1), Ly6d (49-H4), Siglech (440c), Ly6G (1A8), CD138 (281-2), TNFα (MP6-XT22), IL-12p70 (C17.8), and PD-1 (29F.1A12). PI or Ghost dye (Tonbo Biosciences, San Diego, CA) was used to exclude dead cells. LCMV-specific tetramers D^b:$GP_{33–41}$ were provided by the NIH tetramer core facility. Cells were pre-incubated with CD16/CD32 Fc block (BD Pharmingen) prior to surface staining. Staining for Ki67 (SolA15) was performed as directed using the Foxp3 / Transcription Factor Staining kit. Active caspase-3 staining protocol was performed following manufacturer's instructions (PE active caspase-3 apoptosis kit, BD Pharmingen). Surface and intracellular cytokine staining was performed as previously described unless stated

otherwise[99]. Cells were acquired with a LSRII flow cytometer (BD Biosciences) or ZE5 analyzer (Biorad) and data were analyzed using FlowJo software 9.9.6 or 10 (Treestar, Inc.).

Cytokine Measurements

For cytokine measurement in culture supernatants, spleen BM cells from individual mice in the same group were pooled prior to FACS purification. FACS-purified pDCs (3×10^4 cells/well) were incubated in 120ul complete media (RPMI-1640 supplemented with 10% (vol/vol) fetal bovine serum, L-glutamine, penicillin-streptomycin, HEPES pH 7.2, and 50μM β-mercaptoethanol) in the presence or absence of 1uM CpG-B 1668 (Integrated DNA Technologies) for 15 hours at 37˚C. Supernatants were collected and stored at −80°C until further analysis. IFNα in culture supernatant and serum were measured by Lumikine mIFNα ELISA (InvivoGen), following manufacturer instructions. TNFα was measured by Mouse TNF alpha ELISA Ready-SET-Go!® (eBioscience) following manufacturer instructions. To measure intracellular cytokines by flow cytometry, cells were incubated in 200ul complete media in the presence or absence of 1uM CpG-B 1668 (Integrated DNA Technologies) for 7 hours at 37˚C. Brefeldin A (Sigma) was added 5 hours prior to staining.

Quantitative Real-time RT-PCR (qRT-PCR) Analysis

For qRT-PCR analysis, spleen or BM cells from individual mice in the same group were pooled prior to FACS purification. Total RNA was extracted using RNeasy kits (Qiagen), digested with DNase I (RNase-free DNase set; Qiagen) and reverse-transcribed into cDNA using Superscript III RT (Invitrogen). The expression of various genes was quantified using Fast SYBR Green Master Mix (Thermo Fisher Scientific) and CFX384 Touch Real-Time PCR Detection System (Bio-Rad). The following primers for the test genes and probe sets were used: Gmeb1 primer F: 5’- GAGAACCCGGAAGACACTAAAAC-3’; Gmeb1 primer R: 5’-

GGCTACAACTGCTGCGCTAT-3'; Zfp524 primer F: 5'- CAGACCCGTTGCCTTCAACTT-3'; Zfp524 primer R: 5'- GAGTCCGATTGGAGGTGGTG-3'. The relative transcript levels were normalized against murine *Gapdh* as described previously[225] .

Sub-cloning of shRNAmirs into retroviral vectors

shRNAmir inserts for Gmeb1 and non-targeting control were amplified from purified pLMN shRNAmir clones (Transomics RRUM-154954 and LMN NTC1, respectively, purchased from La Jolla Institute for Immunology functional genomics core) using primers specific for common regions in the flanking miR-30 sequences, and that included restriction enzyme sequences (XhoI and EcoRI) compatible with directional cloning (restriction enzymes sequences are underlined: XhoI-5'mir30, CAGAAGGCTCGAGAAGGTATATTGCTGTTGACAGTGAGCG; EcoRI-3'mir30, CTAAAGTAGCCCCTTGAATTCCGAGGCAGTAGGCA)[226]. All shRNAmir were amplified with the Pfx50 DNA Polymerase (Fisher Scientific). Amplification of each shRNAmir was confirmed by agarose gel electrophoresis. PCR products were digested with EcoRI and XhoI to generate sticky ends and were gel purified after restriction enzyme digestion using Qiaquick columns. Inserts prepared with each method were ligated separately into 100 ng of pLMPd-Amt in a 2.5:1 molar ratio (Rapid Ligation Kit, Thermo Scientific), and 10% of each ligation was transformed into 50 µl of XL10-Gold chemically competent cells (Agilent Technologies). Colonies from transformation were picked, cultured in 5ml LB media containing 100ug/ml ampicillin, purified by using spin miniprep kit (Qiagen) and were sent for standard DNA sequencing (Eton Bioscience Inc.). PLMN shRNAmir clones for Zfp524 shRNA and non-targeting control (Transomics ULTRA-3368224 and LMN NTC1, respectively) were purchased from La Jolla Institute for Immunology functional genomics core).

Generation of retroviral particles (RVs) and retroviral transduction

HEK293T cells were transfected targeting or control shRNAs, LT1 transfection reagent (Mirus Bio, Madison, WI), and the PCL-Eco packaging plasmid. Supernatants were harvested 48 hours later and kept at 4 ˚C until media were replaced with fresh media and second supernatants were harvested 24 hours after media change (72 hours post-transfection). Fresh RV supernatant was used for retroviral transduction. At day 2 post-Flt3L culture, BM cells were transduced with RV encoding target or control shRNA and 10ug/ml polybrene reagent (Fisher Scientific) and spin-infected at room temperature at 1000g for 90 min. Cells were incubated at 37˚C overnight. On day 3 post-Flt3L culture, cells were again transduced with RV encoding target or control shRNA and were incubated at 37˚C for 3 hours. Cells were then washed in PBS twice and placed in fresh DC medium + Flt3L.

RNA sequencing

Total RNA was prepared from 1×10^5 cells. Total RNA was subsequently processed by UCSD IGM Genomics center to generate an mRNA-seq library using a TruSeq RNA Library Prep Kit v2 (Illumina). The libraries were using Hiseq 4000 for 50 cycles (single read). FastQ files were aligned to a mouse genome (mm10; Genome Reference Consortium GRCm38) by using Spliced Transcripts Alignment to a Reference (STAR) aligner[227]. Transcript data from STAR were subsequently analyzed using RSEM[228] for quantification of gene expression. Downstream analyses and heatmaps were performed with R 3.5.3[229] and Bioconductor 3.8[230,231]. Pathway analyses were done with WebGestalt[232]. Genes that were commonly upregulated or downregulated in progenitors from ARM- and Cl13-infected mice compared to their counterparts from uninfected mice were compiled into a pre-ranked list in the order of average between Arm vs. uninfected and Cl13 vs. uninfected fold changes computed from DESeq2[233]. This list was subjected to gene set

enrichment analysis for pre-cDC and pre-pDC signatures defined in [121] through GSEA software[234,235].

ATAC sequencing

ATAC-seq was be performed according to a published protocol[186] with minor modification. Briefly, cells were sorted (2.5×10^4 cells), resuspended in lysis buffer and then spun down 600 × g for 30 min at 4 °C. Nuclei pellet was resuspended into transposition reaction mixture containing Tn5 transposase from Nextera DNA Sample Prep Kit (Illumina) and incubated for 30 min with gentle shaking. Following purification, we first amplified the full libraries for 5 cycles and the additional number of cycles needed for the remaining reaction was determined as published in original protocol[186]. The libraries were purified using a Qiagen PCR cleanup kit in 20 μL. Libraries were amplified for a total of 10–12 cycles. The library was pooled and size-selected to range between 100bp and 600bp by using PippinHT (Sage Sciences). Finally, the libraries were sequenced using Hiseq 4000 for 50 cycles (single read). Peaks were called for each individual replicate by using MACS2 with a relaxed threshold (p-value 0.01). Downstream analyses and heatmaps were performed with R 3.5.3[229] and Bioconductor 3.8[230,231]. Pathway analyses were done with Genomic Regions Enrichment of Annotations Tool (GREAT)[236].

Pro-DC Transfer Assay

Uninfected BM cells were from donor mice (CD45.2+) were depleted of CD11b+ cells using EasySep™ Mouse Streptavidin RapidSpheres™ Isolation Kit (Stemcell Technologies) and biotin-conjugated anti-CD11b (M1/70) and cultured with Flt3L. At day 2 p.c., Flt3L culture was enriched again using EasySep™ Mouse Streptavidin RapidSpheres™ Isolation Kit (Stemcell Technologies), anti-Gr-1 (RB6-8C5), anti-CD19 (6D5) and anti-CD127 (A7R34). Fractions unbound to streptavidin beads were transduced with RV encoding target or control shRNA and

10ug/ml polybrene reagent (Fisher Scientific) and spin-infected at room temperature at 1000g for 90 min. Cells were incubated 37˚C overnight. On day 3 post Flt3L culture, cells were again transduced with RV encoding target or control shRNA and were incubated 37˚C for 3 hours. Cells were then washed in PBS twice and placed in fresh DC medium + Flt3L. At day 3.5p.c., pool of Ametrine+ and Ametrine- pro-DCs[116] (~6 x 10^5 cells) were purified from culture and intravenously transferred into congenically marked recipient mice (CD45.1+) infected with LCMV Cl13 for 8 days. pro-DCs were gated as Lin-CD11b$^{-/lo}$CD11c- from Flt3L culture at day 3.5 p.c. Lin includes markers for Thy1.2, CD19, NK1.1, CD3, CD4, CD8, B220, CD11b, Gr-1, Ter119, CD127, and MHCII.6 days after transfer, splenocytes of recipient mice were analyzed by flow cytometry.

Quantification and statistical analysis

All statistical parameters are described in figure legends. Student's t tests (two-tailed, unpaired, or where indicated paired), one-way Anova, two-way Anova, and multiple comparisons were performed by using GraphPad Prism 8.0 (GraphPad). Significance was defined as $p \leq 0.05$. In all figures, error bars indicate S.E.M.

3.6 Acknowledgements

Chapter 3, in part, is currently being prepared for submission for publication of the material by Jo, Y. Yeara Jo was the primary investigator and author of this material. I would like to thank Dr. Kai Zhang and Dr. Wei Wang for their bioinformatics expertise and Dr. Simone Dallari and Nuha Marooki for their assistance with preparing for samples. I would also like to acknowledge UCSD IGM genomics center for making my RNA-seq libraries and performing sequencing on my samples.

Concluding Remarks

Chronic viral infections are significant global health burdens and it is crucial to understand the biology of the immune system that responds to these infections. Chronic viral infection can be considered an equilibrium between pathogen and host whereby host adapts to pathogen, thereby preventing excessive immunopathology and preserving its survival at the expense of delayed pathogen clearance. Nevertheless, characterization of the mechanisms underlying such adaptation in adaptive immune cells has unlocked powerful immunotherapies that can be beneficial in not only infectious diseases but also non-infectious diseases like cancer. However, the mechanisms sustaining numerical and functional adaptations of short-lived innate cells to chronic inflammatory settings have remained unknown.

Using acute and chronic models of murine viral infection, we found that DC adaptation involves concerted changes in gene expression and signaling events at central (bone marrow progenitors) and local (differentiated DCs in lymphoid organs) compartments. Intriguingly, all progenitor and DC adaptations that we observed during chronic LCMV infection were also detected early after acute LCMV infection. In this sense, innate immune cell adaptation is distinct from adaptive immune cell adaptation in which cells from acute and chronic infection have divergent phenotypes from very early on. This may be reflective of the crucial roles of innate immune cells as the first responders to immune challenge and supports a unique view particularly relevant for innate immune cells that their adaptations initiate as general responses to microbial exposure. This suggests the importance of understanding how innate immune cells initiate their adaptation mechanism.

Here we used genomic analyses to elucidate how innate immune cell adaptation initiate at the level of progenitors and identified several transcription factor regulators with potential roles in

regulating DC development, maturation, and function during acute and chronic viral infection. Modulating these TFs in progenitors will not only help us gain insight into basic biology of DCs but also provide some targets that could be combined with existing treatments targeting adaptive immune cells. Such combination will provide more effective control of chronic infections and their associated opportunistic pathogens and/or tumors through potentiation of adaptive immune responses by empowered innate immune cells and/or synergistic effects between reinvigorated adaptive and innate immune cells.

References

1 Stelekati, E. & Wherry, E. J. Chronic bystander infections and immunity to unrelated antigens. *Cell Host Microbe* **12**, 458-469, doi:10.1016/j.chom.2012.10.001 (2012).

2 Virgin, H. W., Wherry, E. J. & Ahmed, R. Redefining chronic viral infection. *Cell* **138**, 30-50, doi:10.1016/j.cell.2009.06.036 (2009).

3 Zuniga, E. I., Macal, M., Lewis, G. M. & Harker, J. A. Innate and Adaptive Immune Regulation During Chronic Viral Infections. *Annual review of virology* **2**, 573-597, doi:10.1146/annurev-virology-100114-055226 (2015).

4 Attanasio, J. & Wherry, E. J. Costimulatory and Coinhibitory Receptor Pathways in Infectious Disease. *Immunity* **44**, 1052-1068, doi:10.1016/j.immuni.2016.04.022 (2016).

5 Moir, S. & Fauci, A. S. B-cell exhaustion in HIV infection: the role of immune activation. *Curr Opin HIV AIDS* **9**, 472-477, doi:10.1097/COH.0000000000000092 (2014).

6 Wherry, E. J. T cell exhaustion. *Nat Immunol* **12**, 492-499 (2011).

7 McLane, L. M., Abdel-Hakeem, M. S. & Wherry, E. J. CD8 T Cell Exhaustion During Chronic Viral Infection and Cancer. *Annu Rev Immunol* **37**, 457-495, doi:10.1146/annurev-immunol-041015-055318 (2019).

8 Kang, S. S. & McGavern, D. B. Lymphocytic choriomeningitis infection of the central nervous system. *Front Biosci* **13**, 4529-4543 (2008).

9 Muckenfuss, R. S. Clinical Observations and Laboratory Investigations on the 1933 Epidemic of Encephalitis in St. Louis. *Bull N Y Acad Med* **10**, 444-453 (1934).

10 Armstrong, C. & Lillie, R. D. Experimental Lymphocytic Choriomeningitis of Monkeys and Mice Produced by a Virus Encountered in Studies of the 1933 St. Louis Encephalitis Epidemic. *Public Health Reports (1896-1970)* **49**, 1019-1027, doi:10.2307/4581290 (1934).

11 Emonet, S., Lemasson, J. J., Gonzalez, J. P., de Lamballerie, X. & Charrel, R. N. Phylogeny and evolution of old world arenaviruses. *Virology* **350**, 251-257, doi:10.1016/j.virol.2006.01.026 (2006).

12 Salvato, M. S. & Shimomaye, E. M. The completed sequence of lymphocytic choriomeningitis virus reveals a unique RNA structure and a gene for a zinc finger protein. *Virology* **173**, 1-10, doi:10.1016/0042-6822(89)90216-x (1989).

13 Singh, M. K., Fuller-Pace, F. V., Buchmeier, M. J. & Southern, P. J. Analysis of the genomic L RNA segment from lymphocytic choriomeningitis virus. *Virology* **161**, 448-456, doi:10.1016/0042-6822(87)90138-3 (1987).

14 Southern, P. J. *et al.* Molecular characterization of the genomic S RNA segment from lymphocytic choriomeningitis virus. *Virology* **157**, 145-155, doi:10.1016/0042-6822(87)90323-0 (1987).

15 Oldstone, M. B. An Odyssey to Viral Pathogenesis. *Annu Rev Pathol* **11**, 1-19, doi:10.1146/annurev-pathol-012615-044107 (2016).

16 Matloubian, M., Somasundaram, T., Kolhekar, S. R., Selvakumar, R. & Ahmed, R. Genetic basis of viral persistence: single amino acid change in the viral glycoprotein affects ability of lymphocytic choriomeningitis virus to persist in adult mice. *J Exp Med* **172**, 1043-1048, doi:10.1084/jem.172.4.1043 (1990).

17 Matloubian, M., Kolhekar, S. R., Somasundaram, T. & Ahmed, R. Molecular determinants of macrophage tropism and viral persistence: importance of single amino acid changes in the polymerase and glycoprotein of lymphocytic choriomeningitis virus. *J Virol* **67**, 7340-7349 (1993).

18 Bergthaler, A. *et al.* Viral replicative capacity is the primary determinant of lymphocytic choriomeningitis virus persistence and immunosuppression. *Proc Natl Acad Sci U S A* **107**, 21641-21646, doi:10.1073/pnas.1011998107 (2010).

19 Sullivan, B. M. *et al.* Point mutation in the glycoprotein of lymphocytic choriomeningitis virus is necessary for receptor binding, dendritic cell infection, and long-term persistence. *Proc Natl Acad Sci U S A* **108**, 2969-2974, doi:10.1073/pnas.1019304108 (2011).

20 Wherry, E. J., Blattman, J. N., Murali-Krishna, K., van der Most, R. & Ahmed, R. Viral persistence alters CD8 T-cell immunodominance and tissue distribution and results in distinct stages of functional impairment. *J Virol* **77**, 4911-4927, doi:10.1128/jvi.77.8.4911-4927.2003 (2003).

21 Zajac, A. J. *et al.* Viral immune evasion due to persistence of activated T cells without effector function. *J Exp Med* **188**, 2205-2213, doi:10.1084/jem.188.12.2205 (1998).

22 Gallimore, A. *et al.* Induction and exhaustion of lymphocytic choriomeningitis virus-specific cytotoxic T lymphocytes visualized using soluble tetrameric major histocompatibility complex class I-peptide complexes. *J Exp Med* **187**, 1383-1393, doi:10.1084/jem.187.9.1383 (1998).

23 Lewis, K. L. & Reizis, B. Dendritic cells: arbiters of immunity and immunological tolerance. *Cold Spring Harb Perspect Biol* **4**, a007401, doi:10.1101/cshperspect.a007401 (2012).

24 Merad, M., Sathe, P., Helft, J., Miller, J. & Mortha, A. The dendritic cell lineage: ontogeny and function of dendritic cells and their subsets in the steady state and the inflamed setting. *Annual review of immunology* **31**, 563-604, doi:10.1146/annurev-immunol-020711-074950 (2013).

25 Reizis, B. Plasmacytoid Dendritic Cells: Development, Regulation, and Function. *Immunity* **50**, 37-50, doi:10.1016/j.immuni.2018.12.027 (2019).

26 Ivashkiv, L. B. & Donlin, L. T. Regulation of type I interferon responses. *Nat Rev Immunol* **14**, 36-49, doi:10.1038/nri3581 (2014).

27 Swiecki, M. & Colonna, M. The multifaceted biology of plasmacytoid dendritic cells. *Nature reviews. Immunology* **15**, 471-485, doi:10.1038/nri3865 (2015).

28 Guillerme, J. B. *et al.* Measles virus vaccine-infected tumor cells induce tumor antigen cross-presentation by human plasmacytoid dendritic cells. *Clin Cancer Res* **19**, 1147-1158, doi:10.1158/1078-0432.CCR-12-2733 (2013).

29 Lui, G. *et al.* Plasmacytoid dendritic cells capture and cross-present viral antigens from influenza-virus exposed cells. *PLoS One* **4**, e7111, doi:10.1371/journal.pone.0007111 (2009).

30 Tel, J. *et al.* Human plasmacytoid dendritic cells phagocytose, process, and present exogenous particulate antigen. *J Immunol* **184**, 4276-4283, doi:10.4049/jimmunol.0903286 (2010).

31 Tel, J. *et al.* Human plasmacytoid dendritic cells efficiently cross-present exogenous Ags to CD8+ T cells despite lower Ag uptake than myeloid dendritic cell subsets. *Blood* **121**, 459-467, doi:10.1182/blood-2012-06-435644 (2013).

32 Villadangos, J. A. & Young, L. Antigen-presentation properties of plasmacytoid dendritic cells. *Immunity* **29**, 352-361, doi:10.1016/j.immuni.2008.09.002 (2008).

33 Decalf, J. *et al.* Plasmacytoid dendritic cells initiate a complex chemokine and cytokine network and are a viable drug target in chronic HCV patients. *J Exp Med* **204**, 2423-2437, doi:10.1084/jem.20070814 (2007).

34 Guillerey, C. *et al.* Pivotal role of plasmacytoid dendritic cells in inflammation and NK-cell responses after TLR9 triggering in mice. *Blood* **120**, 90-99, doi:10.1182/blood-2012-02-410936 (2012).

35 Piqueras, B., Connolly, J., Freitas, H., Palucka, A. K. & Banchereau, J. Upon viral exposure, myeloid and plasmacytoid dendritic cells produce 3 waves of distinct chemokines to recruit immune effectors. *Blood* **107**, 2613-2618, doi:10.1182/blood-2005-07-2965 (2006).

36 Aspord, C., Leccia, M. T., Charles, J. & Plumas, J. Plasmacytoid dendritic cells support melanoma progression by promoting Th2 and regulatory immunity through OX40L and ICOSL. *Cancer Immunol Res* **1**, 402-415, doi:10.1158/2326-6066.CIR-13-0114-T (2013).

37 Ito, T. *et al.* Plasmacytoid dendritic cells prime IL-10-producing T regulatory cells by inducible costimulator ligand. *J Exp Med* **204**, 105-115, doi:10.1084/jem.20061660 (2007).

38 Jahrsdörfer, B. *et al.* Granzyme B produced by human plasmacytoid dendritic cells suppresses T-cell expansion. *Blood* **115**, 1156-1165, doi:10.1182/blood-2009-07-235382 (2010).

39 Pallotta, M. T. *et al.* Indoleamine 2,3-dioxygenase is a signaling protein in long-term tolerance by dendritic cells. *Nat Immunol* **12**, 870-878, doi:10.1038/ni.2077 (2011).

40 Sharma, M. D. *et al.* Plasmacytoid dendritic cells from mouse tumor-draining lymph nodes directly activate mature Tregs via indoleamine 2,3-dioxygenase. *J Clin Invest* **117**, 2570-2582, doi:10.1172/JCI31911 (2007).

41 Tokita, D. *et al.* High PD-L1/CD86 ratio on plasmacytoid dendritic cells correlates with elevated T-regulatory cells in liver transplant tolerance. *Transplantation* **85**, 369-377, doi:10.1097/TP.0b013e3181612ded (2008).

42 Mildner, A. & Jung, S. Development and function of dendritic cell subsets. *Immunity* **40**, 642-656, doi:10.1016/j.immuni.2014.04.016 (2014).

43 den Haan, J. M., Lehar, S. M. & Bevan, M. J. CD8(+) but not CD8(-) dendritic cells cross-prime cytotoxic T cells in vivo. *J Exp Med* **192**, 1685-1696, doi:10.1084/jem.192.12.1685 (2000).

44 Dudziak, D. *et al.* Differential antigen processing by dendritic cell subsets in vivo. *Science* **315**, 107-111, doi:10.1126/science.1136080 (2007).

45 Hochrein, H. *et al.* Differential production of IL-12, IFN-alpha, and IFN-gamma by mouse dendritic cell subsets. *J Immunol* **166**, 5448-5455, doi:10.4049/jimmunol.166.9.5448 (2001).

46 Böttcher, J. P. & Reis E Sousa, C. The Role of Type 1 Conventional Dendritic Cells in Cancer Immunity. *Trends Cancer* **4**, 784-792, doi:10.1016/j.trecan.2018.09.001 (2018).

47 Murphy, T. L. *et al.* Transcriptional Control of Dendritic Cell Development. *Annu Rev Immunol* **34**, 93-119, doi:10.1146/annurev-immunol-032713-120204 (2016).

48 Backer, R., van Leeuwen, F., Kraal, G. & den Haan, J. M. CD8- dendritic cells preferentially cross-present Saccharomyces cerevisiae antigens. *Eur J Immunol* **38**, 370-380, doi:10.1002/eji.200737647 (2008).

49 Chiang, M. C. *et al.* Differential uptake and cross-presentation of soluble and necrotic cell antigen by human DC subsets. *Eur J Immunol* **46**, 329-339, doi:10.1002/eji.201546023 (2016).

50 Lewis, K. L. *et al.* Notch2 receptor signaling controls functional differentiation of dendritic cells in the spleen and intestine. *Immunity* **35**, 780-791, doi:10.1016/j.immuni.2011.08.013 (2011).

51 Satpathy, A. T. *et al.* Notch2-dependent classical dendritic cells orchestrate intestinal immunity to attaching-and-effacing bacterial pathogens. *Nat Immunol* **14**, 937-948, doi:10.1038/ni.2679 (2013).

52 Persson, E. K. *et al.* IRF4 transcription-factor-dependent CD103(+)CD11b(+) dendritic cells drive mucosal T helper 17 cell differentiation. *Immunity* **38**, 958-969, doi:10.1016/j.immuni.2013.03.009 (2013).

53 Proietto, A. I. *et al.* Differential production of inflammatory chemokines by murine dendritic cell subsets. *Immunobiology* **209**, 163-172, doi:10.1016/j.imbio.2004.03.002 (2004).

54 Cervantes-Barragan, L. *et al.* Plasmacytoid dendritic cells control T-cell response to chronic viral infection. *Proc Natl Acad Sci U S A* **109**, 3012-3017, doi:10.1073/pnas.1117359109 (2012).

55 Swiecki, M., Gilfillan, S., Vermi, W., Wang, Y. & Colonna, M. Plasmacytoid dendritic cell ablation impacts early interferon responses and antiviral NK and CD8(+) T cell accrual. *Immunity* **33**, 955-966, doi:10.1016/j.immuni.2010.11.020 (2010).

56 Kassim, S. H., Rajasagi, N. K., Zhao, X., Chervenak, R. & Jennings, S. R. In vivo ablation of CD11c-positive dendritic cells increases susceptibility to herpes simplex virus type 1 infection and diminishes NK and T-cell responses. *J Virol* **80**, 3985-3993, doi:10.1128/JVI.80.8.3985-3993.2006 (2006).

57 McGill, J., Van Rooijen, N. & Legge, K. L. Protective influenza-specific CD8 T cell responses require interactions with dendritic cells in the lungs. *J Exp Med* **205**, 1635-1646, doi:10.1084/jem.20080314 (2008).

58 Martin-Gayo, E. & Yu, X. G. Dendritic Cell Immune Responses in HIV-1 Controllers. *Current HIV/AIDS reports* **14**, 1-7, doi:10.1007/s11904-017-0345-0 (2017).

59 Huang, J. *et al.* Dendritic cell dysfunction during primary HIV-1 infection. *The Journal of infectious diseases* **204**, 1557-1562, doi:10.1093/infdis/jir616 (2011).

60 Liu, B., Woltman, A. M., Janssen, H. L. & Boonstra, A. Modulation of dendritic cell function by persistent viruses. *Journal of leukocyte biology* **85**, 205-214, doi:10.1189/jlb.0408241 (2009).

61 Losikoff, P. T., Self, A. A. & Gregory, S. H. Dendritic cells, regulatory T cells and the pathogenesis of chronic hepatitis C. *Virulence* **3**, 610-620, doi:10.4161/viru.21823 (2012).

62 Ng, C. T., Sullivan, B. M. & Oldstone, M. B. The role of dendritic cells in viral persistence. *Current opinion in virology* **1**, 160-166, doi:10.1016/j.coviro.2011.05.006 (2011).

63 Auffermann-Gretzinger, S., Keeffe, E. B. & Levy, S. Impaired dendritic cell maturation in patients with chronic, but not resolved, hepatitis C virus infection. *Blood* **97**, 3171-3176 (2001).

64 Granelli-Piperno, A., Golebiowska, A., Trumpfheller, C., Siegal, F. P. & Steinman, R. M. HIV-1-infected monocyte-derived dendritic cells do not undergo maturation but can elicit IL-10 production and T cell regulation. *Proc Natl Acad Sci U S A* **101**, 7669-7674, doi:10.1073/pnas.0402431101 (2004).

65 Sevilla, N., McGavern, D. B., Teng, C., Kunz, S. & Oldstone, M. B. Viral targeting of hematopoietic progenitors and inhibition of DC maturation as a dual strategy for immune subversion. *The Journal of clinical investigation* **113**, 737-745, doi:10.1172/JCI20243 (2004).

66 Arima, S. *et al.* Impaired function of antigen-presenting dendritic cells in patients with chronic hepatitis B: localization of HBV DNA and HBV RNA in blood DC by in situ hybridization. *International journal of molecular medicine* **11**, 169-174 (2003).

67 van der Molen, R. G. *et al.* Functional impairment of myeloid and plasmacytoid dendritic cells of patients with chronic hepatitis B. *Hepatology* **40**, 738-746, doi:10.1002/hep.20366 (2004).

68 Snell, L. M. *et al.* CD8(+) T Cell Priming in Established Chronic Viral Infection Preferentially Directs Differentiation of Memory-like Cells for Sustained Immunity. *Immunity* **49**, 678-694 e675, doi:10.1016/j.immuni.2018.08.002 (2018).

69 Borrow, P. Innate immunity in acute HIV-1 infection. *Curr Opin HIV AIDS* **6**, 353-363, doi:10.1097/COH.0b013e3283495996 (2011).

70 Feldman, S. *et al.* Decreased interferon-alpha production in HIV-infected patients correlates with numerical and functional deficiencies in circulating type 2 dendritic cell precursors. *Clin Immunol* **101**, 201-210, doi:10.1006/clim.2001.5111 (2001).

71 Lee, L. N., Burke, S., Montoya, M. & Borrow, P. Multiple mechanisms contribute to impairment of type 1 interferon production during chronic lymphocytic choriomeningitis virus infection of mice. *J Immunol* **182**, 7178-7189, doi:10.4049/jimmunol.0802526 (2009).

72 Zuniga, E. I., Liou, L. Y., Mack, L., Mendoza, M. & Oldstone, M. B. Persistent virus infection inhibits type I interferon production by plasmacytoid dendritic cells to facilitate opportunistic infections. *Cell host & microbe* **4**, 374-386, doi:10.1016/j.chom.2008.08.016 (2008).

73 Ng, C. T., Mendoza, J. L., Garcia, K. C. & Oldstone, M. B. Alpha and Beta Type 1 Interferon Signaling: Passage for Diverse Biologic Outcomes. *Cell* **164**, 349-352, doi:10.1016/j.cell.2015.12.027 (2016).

74 Snell, L. M. & Brooks, D. G. New insights into type I interferon and the immunopathogenesis of persistent viral infections. *Curr Opin Immunol* **34**, 91-98, doi:10.1016/j.coi.2015.03.002 (2015).

75 Stacey, A. R. *et al.* Induction of a striking systemic cytokine cascade prior to peak viremia in acute human immunodeficiency virus type 1 infection, in contrast to more modest and

delayed responses in acute hepatitis B and C virus infections. *J Virol* **83**, 3719-3733, doi:10.1128/JVI.01844-08 (2009).

76 Sandler, N. G. *et al.* Type I interferon responses in rhesus macaques prevent SIV infection and slow disease progression. *Nature* **511**, 601-605, doi:10.1038/nature13554 (2014).

77 Vanderford, T. H. *et al.* Treatment of SIV-infected sooty mangabeys with a type-I IFN agonist results in decreased virus replication without inducing hyperimmune activation. *Blood* **119**, 5750-5757, doi:10.1182/blood-2012-02-411496 (2012).

78 Wang, Y. *et al.* Timing and magnitude of type I interferon responses by distinct sensors impact CD8 T cell exhaustion and chronic viral infection. *Cell Host Microbe* **11**, 631-642, doi:10.1016/j.chom.2012.05.003 (2012).

79 Blasius, A. L., Krebs, P., Sullivan, B. M., Oldstone, M. B. & Popkin, D. L. Slc15a4, a gene required for pDC sensing of TLR ligands, is required to control persistent viral infection. *PLoS Pathog* **8**, e1002915, doi:10.1371/journal.ppat.1002915 (2012).

80 Fonteneau, J. F. *et al.* Human immunodeficiency virus type 1 activates plasmacytoid dendritic cells and concomitantly induces the bystander maturation of myeloid dendritic cells. *J Virol* **78**, 5223-5232, doi:10.1128/jvi.78.10.5223-5232.2004 (2004).

81 Fan, Z., Huang, X. L., Kalinski, P., Young, S. & Rinaldo, C. R. Dendritic cell function during chronic hepatitis C virus and human immunodeficiency virus type 1 infection. *Clin Vaccine Immunol* **14**, 1127-1137, doi:10.1128/CVI.00141-07 (2007).

82 Op den Brouw, M. L. *et al.* Hepatitis B virus surface antigen impairs myeloid dendritic cell function: a possible immune escape mechanism of hepatitis B virus. *Immunology* **126**, 280-289, doi:10.1111/j.1365-2567.2008.02896.x (2009).

83 Bueno, S. M. *et al.* Host immunity during RSV pathogenesis. *Int Immunopharmacol* **8**, 1320-1329, doi:10.1016/j.intimp.2008.03.012 (2008).

84 Ng, C. T. & Oldstone, M. B. Infected CD8α- dendritic cells are the predominant source of IL-10 during establishment of persistent viral infection. *Proc Natl Acad Sci U S A* **109**, 14116-14121, doi:10.1073/pnas.1211910109 (2012).

85 Wilson, E. B. *et al.* Emergence of distinct multiarmed immunoregulatory antigen-presenting cells during persistent viral infection. *Cell Host Microbe* **11**, 481-491, doi:10.1016/j.chom.2012.03.009 (2012).

86 Buisson, S. *et al.* Monocyte-derived dendritic cells from HIV type 1-infected individuals show reduced ability to stimulate T cells and have altered production of interleukin (IL)-12 and IL-10. *J Infect Dis* **199**, 1862-1871, doi:10.1086/599122 (2009).

87 Saito, K. *et al.* Hepatitis C virus inhibits cell surface expression of HLA-DR, prevents dendritic cell maturation, and induces interleukin-10 production. *J Virol* **82**, 3320-3328, doi:10.1128/JVI.02547-07 (2008).

88 Pacanowski, J. *et al.* Reduced blood CD123+ (lymphoid) and CD11c+ (myeloid) dendritic cell numbers in primary HIV-1 infection. *Blood* **98**, 3016-3021, doi:10.1182/blood.v98.10.3016 (2001).

89 Dillon, S. M. *et al.* Plasmacytoid and myeloid dendritic cells with a partial activation phenotype accumulate in lymphoid tissue during asymptomatic chronic HIV-1 infection. *J Acquir Immune Defic Syndr* **48**, 1-12, doi:10.1097/QAI.0b013e3181664b60 (2008).

90 Foussat, A. *et al.* Deregulation of the expression of the fractalkine/fractalkine receptor complex in HIV-1-infected patients. *Blood* **98**, 1678-1686, doi:10.1182/blood.v98.6.1678 (2001).

91 Nascimbeni, M. *et al.* Plasmacytoid dendritic cells accumulate in spleens from chronically HIV-infected patients but barely participate in interferon-alpha expression. *Blood* **113**, 6112-6119, doi:10.1182/blood-2008-07-170803 (2009).

92 Malleret, B. *et al.* Effect of SIVmac infection on plasmacytoid and CD1c+ myeloid dendritic cells in cynomolgus macaques. *Immunology* **124**, 223-233, doi:10.1111/j.1365-2567.2007.02758.x (2008).

93 Duan, X. Z. *et al.* Decreased frequency and function of circulating plasmocytoid dendritic cells (pDC) in hepatitis B virus infected humans. *J Clin Immunol* **24**, 637-646, doi:10.1007/s10875-004-6249-y (2004).

94 Kanto, T. *et al.* Reduced numbers and impaired ability of myeloid and plasmacytoid dendritic cells to polarize T helper cells in chronic hepatitis C virus infection. *J Infect Dis* **190**, 1919-1926, doi:10.1086/425425 (2004).

95 Biancotto, A. *et al.* Abnormal activation and cytokine spectra in lymph nodes of people chronically infected with HIV-1. *Blood* **109**, 4272-4279, doi:10.1182/blood-2006-11-055764 (2007).

96 Brown, K. N., Wijewardana, V., Liu, X. & Barratt-Boyes, S. M. Rapid influx and death of plasmacytoid dendritic cells in lymph nodes mediate depletion in acute simian immunodeficiency virus infection. *PLoS Pathog* **5**, e1000413, doi:10.1371/journal.ppat.1000413 (2009).

97 Swiecki, M. *et al.* Type I interferon negatively controls plasmacytoid dendritic cell numbers in vivo. *J Exp Med* **208**, 2367-2374, doi:10.1084/jem.20110654 (2011).

98 McKenna, H. J. *et al.* Mice lacking flt3 ligand have deficient hematopoiesis affecting hematopoietic progenitor cells, dendritic cells, and natural killer cells. *Blood* **95**, 3489-3497 (2000).

99 Zuniga, E. I., McGavern, D. B., Pruneda-Paz, J. L., Teng, C. & Oldstone, M. B. Bone marrow plasmacytoid dendritic cells can differentiate into myeloid dendritic cells upon virus infection. *Nat Immunol* **5**, 1227-1234, doi:10.1038/ni1136 (2004).

100 Nakano, H. *et al.* Blood-derived inflammatory dendritic cells in lymph nodes stimulate acute T helper type 1 immune responses. *Nat Immunol* **10**, 394-402, doi:10.1038/ni.1707 (2009).

101 Naik, S. H. *et al.* Diverse and heritable lineage imprinting of early haematopoietic progenitors. *Nature* **496**, 229-232, doi:10.1038/nature12013 (2013).

102 Waskow, C. *et al.* The receptor tyrosine kinase Flt3 is required for dendritic cell development in peripheral lymphoid tissues. *Nat Immunol* **9**, 676-683, doi:10.1038/ni.1615 (2008).

103 Carotta, S. *et al.* The transcription factor PU.1 controls dendritic cell development and Flt3 cytokine receptor expression in a dose-dependent manner. *Immunity* **32**, 628-641, doi:10.1016/j.immuni.2010.05.005 (2010).

104 Laouar, Y., Welte, T., Fu, X. Y. & Flavell, R. A. STAT3 is required for Flt3L-dependent dendritic cell differentiation. *Immunity* **19**, 903-912 (2003).

105 Sathaliyawala, T. *et al.* Mammalian target of rapamycin controls dendritic cell development downstream of Flt3 ligand signaling. *Immunity* **33**, 597-606, doi:10.1016/j.immuni.2010.09.012 (2010).

106 Cisse, B. *et al.* Transcription factor E2-2 is an essential and specific regulator of plasmacytoid dendritic cell development. *Cell* **135**, 37-48, doi:10.1016/j.cell.2008.09.016 (2008).

107 Nagasawa, M., Schmidlin, H., Hazekamp, M. G., Schotte, R. & Blom, B. Development of human plasmacytoid dendritic cells depends on the combined action of the basic helix-loop-helix factor E2-2 and the Ets factor Spi-B. *European journal of immunology* **38**, 2389-2400, doi:10.1002/eji.200838470 (2008).

108 Li, H. S. *et al.* The signal transducers STAT5 and STAT3 control expression of Id2 and E2-2 during dendritic cell development. *Blood* **120**, 4363-4373, doi:10.1182/blood-2012-07-441311 (2012).

109 Ippolito, G. C. *et al.* Dendritic cell fate is determined by BCL11A. *Proc Natl Acad Sci U S A* **111**, E998-1006, doi:10.1073/pnas.1319228111 (2014).

110 Nagasawa, M., Schmidlin, H., Hazekamp, M. G., Schotte, R. & Blom, B. Development of human plasmacytoid dendritic cells depends on the combined action of the basic helix-loop-helix factor E2-2 and the Ets factor Spi-B. *Eur J Immunol* **38**, 2389-2400, doi:10.1002/eji.200838470 (2008).

111 Sasaki, I. *et al.* Spi-B is critical for plasmacytoid dendritic cell function and development. *Blood* **120**, 4733-4743, doi:10.1182/blood-2012-06-436527 (2012).

112 Wu, X. *et al.* Bcl11a controls Flt3 expression in early hematopoietic progenitors and is required for pDC development in vivo. *PLoS One* **8**, e64800, doi:10.1371/journal.pone.0064800 (2013).

113 Ghosh, H. S. *et al.* ETO family protein Mtg16 regulates the balance of dendritic cell subsets by repressing Id2. *J Exp Med* **211**, 1623-1635, doi:10.1084/jem.20132121 (2014).

114 Scott, C. L. *et al.* The transcription factor Zeb2 regulates development of conventional and plasmacytoid DCs by repressing Id2. *J Exp Med* **213**, 897-911, doi:10.1084/jem.20151715 (2016).

115 Sathe, P., Vremec, D., Wu, L., Corcoran, L. & Shortman, K. Convergent differentiation: myeloid and lymphoid pathways to murine plasmacytoid dendritic cells. *Blood* **121**, 11-19, doi:10.1182/blood-2012-02-413336 (2013).

116 Naik, S. H. *et al.* Development of plasmacytoid and conventional dendritic cell subtypes from single precursor cells derived in vitro and in vivo. *Nature immunology* **8**, 1217-1226, doi:10.1038/ni1522 (2007).

117 Onai, N. *et al.* Identification of clonogenic common Flt3+M-CSFR+ plasmacytoid and conventional dendritic cell progenitors in mouse bone marrow. *Nat Immunol* **8**, 1207-1216, doi:10.1038/ni1518 (2007).

118 Onai, N. *et al.* A clonogenic progenitor with prominent plasmacytoid dendritic cell developmental potential. *Immunity* **38**, 943-957, doi:10.1016/j.immuni.2013.04.006 (2013).

119 Schlitzer, A. *et al.* Tissue-specific differentiation of a circulating CCR9- pDC-like common dendritic cell precursor. *Blood* **119**, 6063-6071, doi:10.1182/blood-2012-03-418400 (2012).

120 Herman, J. S., Sagar & Grün, D. FateID infers cell fate bias in multipotent progenitors from single-cell RNA-seq data. *Nat Methods* **15**, 379-386, doi:10.1038/nmeth.4662 (2018).

121 Dress, R. J. *et al.* Plasmacytoid dendritic cells develop from Ly6D. *Nat Immunol* **20**, 852-864, doi:10.1038/s41590-019-0420-3 (2019).

122 Rodrigues, P. F. *et al.* Distinct progenitor lineages contribute to the heterogeneity of plasmacytoid dendritic cells. *Nat Immunol* **19**, 711-722, doi:10.1038/s41590-018-0136-9 (2018).

123 Liu, K. *et al.* In vivo analysis of dendritic cell development and homeostasis. *Science* **324**, 392-397, doi:10.1126/science.1170540 (2009).

124 Naik, S. H. *et al.* Intrasplenic steady-state dendritic cell precursors that are distinct from monocytes. *Nat Immunol* **7**, 663-671, doi:10.1038/ni1340 (2006).

125 Satpathy, A. T. *et al.* Zbtb46 expression distinguishes classical dendritic cells and their committed progenitors from other immune lineages. *J Exp Med* **209**, 1135-1152, doi:10.1084/jem.20120030 (2012).

126 Schlitzer, A. *et al.* Identification of cDC1- and cDC2-committed DC progenitors reveals early lineage priming at the common DC progenitor stage in the bone marrow. *Nat Immunol* **16**, 718-728, doi:10.1038/ni.3200 (2015).

127 Hacker, C. *et al.* Transcriptional profiling identifies Id2 function in dendritic cell development. *Nat Immunol* **4**, 380-386, doi:10.1038/ni903 (2003).

128 Hildner, K. *et al.* Batf3 deficiency reveals a critical role for CD8alpha+ dendritic cells in cytotoxic T cell immunity. *Science* **322**, 1097-1100, doi:10.1126/science.1164206 (2008).

129 Kashiwada, M., Pham, N. L., Pewe, L. L., Harty, J. T. & Rothman, P. B. NFIL3/E4BP4 is a key transcription factor for CD8α^{+} dendritic cell development. *Blood* **117**, 6193-6197, doi:10.1182/blood-2010-07-295873 (2011).

130 Schiavoni, G. *et al.* ICSBP is essential for the development of mouse type I interferon-producing cells and for the generation and activation of CD8alpha(+) dendritic cells. *J Exp Med* **196**, 1415-1425, doi:10.1084/jem.20021263 (2002).

131 Durai, V. *et al.* Cryptic activation of an Irf8 enhancer governs cDC1 fate specification. *Nat Immunol* **20**, 1161-1173, doi:10.1038/s41590-019-0450-x (2019).

132 Grajales-Reyes, G. E. *et al.* Batf3 maintains autoactivation of Irf8 for commitment of a CD8α(+) conventional DC clonogenic progenitor. *Nat Immunol* **16**, 708-717, doi:10.1038/ni.3197 (2015).

133 Bagadia, P. *et al.* An Nfil3-Zeb2-Id2 pathway imposes Irf8 enhancer switching during cDC1 development. *Nat Immunol* **20**, 1174-1185, doi:10.1038/s41590-019-0449-3 (2019).

134 Lau, C. M. *et al.* Transcription factor Etv6 regulates functional differentiation of cross-presenting classical dendritic cells. *J Exp Med* **215**, 2265-2278, doi:10.1084/jem.20172323 (2018).

135 Suzuki, S. *et al.* Critical roles of interferon regulatory factor 4 in CD11bhighCD8alpha-dendritic cell development. *Proc Natl Acad Sci U S A* **101**, 8981-8986, doi:10.1073/pnas.0402139101 (2004).

136 Caton, M. L., Smith-Raska, M. R. & Reizis, B. Notch-RBP-J signaling controls the homeostasis of CD8- dendritic cells in the spleen. *J Exp Med* **204**, 1653-1664, doi:10.1084/jem.20062648 (2007).

137 Tussiwand, R. *et al.* Klf4 expression in conventional dendritic cells is required for T helper 2 cell responses. *Immunity* **42**, 916-928, doi:10.1016/j.immuni.2015.04.017 (2015).

138 Borrow, P., Hou, S., Gloster, S., Ashton, M. & Hyland, L. Virus infection-associated bone marrow B cell depletion and impairment of humoral immunity to heterologous infection mediated by TNF-alpha/LTalpha. *Eur J Immunol* **35**, 524-532, doi:10.1002/eji.200425597 (2005).

139 Bordoni, V. *et al.* Chronic HIV-infected patients show an impaired dendritic cells differentiation of bone marrow $CD34^{+}$ cells. *J Acquir Immune Defic Syndr* **64**, 342-344, doi:10.1097/QAI.0b013e3182a40ff7 (2013).

140 Li, G. *et al.* HIV-1 infection depletes human CD34+CD38- hematopoietic progenitor cells via pDC-dependent mechanisms. *PLoS Pathog* **13**, e1006505, doi:10.1371/journal.ppat.1006505 (2017).

141 Nagai, Y. *et al.* Toll-like receptors on hematopoietic progenitor cells stimulate innate immune system replenishment. *Immunity* **24**, 801-812, doi:10.1016/j.immuni.2006.04.008 (2006).

142 Singh, P. *et al.* Vaccinia virus infection modulates the hematopoietic cell compartments in the bone marrow. *Stem Cells* **26**, 1009-1016, doi:10.1634/stemcells.2007-0461 (2008).

143 Schmid, M. A., Takizawa, H., Baumjohann, D. R., Saito, Y. & Manz, M. G. Bone marrow dendritic cell progenitors sense pathogens via Toll-like receptors and subsequently migrate to inflamed lymph nodes. *Blood* **118**, 4829-4840, doi:10.1182/blood-2011-03-344960 (2011).

144 Wakkach, A. *et al.* Characterization of dendritic cells that induce tolerance and T regulatory 1 cell differentiation in vivo. *Immunity* **18**, 605-617 (2003).

145 Silver, J. S. & Hunter, C. A. gp130 at the nexus of inflammation, autoimmunity, and cancer. *J Leukoc Biol* **88**, 1145-1156, doi:10.1189/jlb.0410217 (2010).

146 Seré, K. M. *et al.* Dendritic cell lineage commitment is instructed by distinct cytokine signals. *Eur J Cell Biol* **91**, 515-523, doi:10.1016/j.ejcb.2011.09.007 (2012).

147 Hahm, B., Trifilo, M. J., Zuniga, E. I. & Oldstone, M. B. Viruses evade the immune system through type I interferon-mediated STAT2-dependent, but STAT1-independent, signaling. *Immunity* **22**, 247-257, doi:10.1016/j.immuni.2005.01.005 (2005).

148 Tussiwand, R. *et al.* Compensatory dendritic cell development mediated by BATF-IRF interactions. *Nature* **490**, 502-507, doi:10.1038/nature11531 (2012).

149 Wherry, E. J. *et al.* Molecular signature of CD8+ T cell exhaustion during chronic viral infection. *Immunity* **27**, 670-684, doi:10.1016/j.immuni.2007.09.006 (2007).

150 Smale, S. T., Tarakhovsky, A. & Natoli, G. Chromatin contributions to the regulation of innate immunity. *Annu Rev Immunol* **32**, 489-511, doi:10.1146/annurev-immunol-031210-101303 (2014).

151 Youngblood, B. *et al.* Chronic virus infection enforces demethylation of the locus that encodes PD-1 in antigen-specific CD8(+) T cells. *Immunity* **35**, 400-412, doi:10.1016/j.immuni.2011.06.015 (2011).

152 Scott-Browne, J. P. *et al.* Dynamic Changes in Chromatin Accessibility Occur in CD8. *Immunity* **45**, 1327-1340, doi:10.1016/j.immuni.2016.10.028 (2016).

153 Sen, D. R. *et al.* The epigenetic landscape of T cell exhaustion. *Science* **354**, 1165-1169, doi:10.1126/science.aae0491 (2016).

154 Schacht, T., Oswald, M., Eils, R., Eichmüller, S. B. & König, R. Estimating the activity of transcription factors by the effect on their target genes. *Bioinformatics* **30**, i401-407, doi:10.1093/bioinformatics/btu446 (2014).

155 Zhang, K., Wang, M., Zhao, Y. & Wang, W. Taiji: System-level identification of key transcription factors reveals transcriptional waves in mouse embryonic development. *Sci Adv* **5**, eaav3262, doi:10.1126/sciadv.aav3262 (2019).

156 Milner, J. J. *et al.* Runx3 programs CD8. *Nature* **552**, 253-257, doi:10.1038/nature24993 (2017).

157 Yu, B. *et al.* Epigenetic landscapes reveal transcription factors that regulate CD8(+) T cell differentiation. *Nature immunology* **18**, 573-582, doi:10.1038/ni.3706 (2017).

158 Kino, T. & Chrousos, G. P. Virus-mediated modulation of the host endocrine signaling systems: clinical implications. *Trends Endocrinol Metab* **18**, 159-166, doi:10.1016/j.tem.2007.03.003 (2007).

159 Silverman, M. N., Pearce, B. D., Biron, C. A. & Miller, A. H. Immune modulation of the hypothalamic-pituitary-adrenal (HPA) axis during viral infection. *Viral Immunol* **18**, 41-78, doi:10.1089/vim.2005.18.41 (2005).

160 Borghetti, P., Saleri, R., Mocchegiani, E., Corradi, A. & Martelli, P. Infection, immunity and the neuroendocrine response. *Vet Immunol Immunopathol* **130**, 141-162, doi:10.1016/j.vetimm.2009.01.013 (2009).

161 Ganeshan, K. & Chawla, A. Metabolic regulation of immune responses. *Annu Rev Immunol* **32**, 609-634, doi:10.1146/annurev-immunol-032713-120236 (2014).

162 Cain, D. W. & Cidlowski, J. A. Immune regulation by glucocorticoids. *Nat Rev Immunol* **17**, 233-247, doi:10.1038/nri.2017.1 (2017).

163 Heijnen, C. J. Receptor regulation in neuroendocrine-immune communication: current knowledge and future perspectives. *Brain Behav Immun* **21**, 1-8, doi:10.1016/j.bbi.2006.08.008 (2007).

164 Miller, A. H. *et al.* 1996 Curt P. Richter Award. Effects of viral infection on corticosterone secretion and glucocorticoid receptor binding in immune tissues. *Psychoneuroendocrinology* **22**, 455-474 (1997).

165 Asselin-Paturel, C., Brizard, G., Pin, J. J., Brière, F. & Trinchieri, G. Mouse strain differences in plasmacytoid dendritic cell frequency and function revealed by a novel monoclonal antibody. *J Immunol* **171**, 6466-6477, doi:10.4049/jimmunol.171.12.6466 (2003).

166 Blasius, A. L. *et al.* Bone marrow stromal cell antigen 2 is a specific marker of type I IFN-producing cells in the naive mouse, but a promiscuous cell surface antigen following IFN stimulation. *J Immunol* **177**, 3260-3265, doi:10.4049/jimmunol.177.5.3260 (2006).

167 Liu, K. *et al.* Origin of dendritic cells in peripheral lymphoid organs of mice. *Nat Immunol* **8**, 578-583, doi:10.1038/ni1462 (2007).

168 Zhan, Y. *et al.* Plasmacytoid dendritic cells are short-lived: reappraising the influence of migration, genetic factors and activation on estimation of lifespan. *Sci Rep* **6**, 25060, doi:10.1038/srep25060 (2016).

169 Schlitzer, A. *et al.* Identification of CCR9- murine plasmacytoid DC precursors with plasticity to differentiate into conventional DCs. *Blood* **117**, 6562-6570, doi:10.1182/blood-2010-12-326678 (2011).

170 Li, H. S. *et al.* Cell-intrinsic role for IFN-α-STAT1 signals in regulating murine Peyer patch plasmacytoid dendritic cells and conditioning an inflammatory response. *Blood* **118**, 3879-3889, doi:10.1182/blood-2011-04-349761 (2011).

171 Martínez-Sobrido, L., Zúñiga, E. I., Rosario, D., García-Sastre, A. & de la Torre, J. C. Inhibition of the type I interferon response by the nucleoprotein of the prototypic arenavirus lymphocytic choriomeningitis virus. *J Virol* **80**, 9192-9199, doi:10.1128/JVI.00555-06 (2006).

172 Macal, M. *et al.* Plasmacytoid dendritic cells are productively infected and activated through TLR-7 early after arenavirus infection. *Cell host & microbe* **11**, 617-630, doi:10.1016/j.chom.2012.04.017 (2012).

173 Iwasaki, A. & Medzhitov, R. Control of adaptive immunity by the innate immune system. *Nat Immunol* **16**, 343-353, doi:10.1038/ni.3123 (2015).

174 Bruel, T. *et al.* Plasmacytoid dendritic cell dynamics tune interferon-alfa production in SIV-infected cynomolgus macaques. *PLoS Pathog* **10**, e1003915, doi:10.1371/journal.ppat.1003915 (2014).

175 Wilson, E. B. *et al.* Blockade of chronic type I interferon signaling to control persistent LCMV infection. *Science* **340**, 202-207, doi:10.1126/science.1235208 (2013).

176 Li, H., Evans, T. I., Gillis, J., Connole, M. & Reeves, R. K. Bone marrow-imprinted gut-homing of plasmacytoid dendritic cells (pDCs) in acute simian immunodeficiency virus infection results in massive accumulation of hyperfunctional CD4+ pDCs in the mucosae. *J Infect Dis* **211**, 1717-1725, doi:10.1093/infdis/jiu671 (2015).

177 McNab, F., Mayer-Barber, K., Sher, A., Wack, A. & O'Garra, A. Type I interferons in infectious disease. *Nat Rev Immunol* **15**, 87-103, doi:10.1038/nri3787 (2015).

178 Jarrett, R. F. Viruses and lymphoma/leukaemia. *J Pathol* **208**, 176-186, doi:10.1002/path.1905 (2006).

179 Kohler, M., Rüttner, B., Cooper, S., Hengartner, H. & Zinkernagel, R. M. Enhanced tumor susceptibility of immunocompetent mice infected with lymphocytic choriomeningitis virus. *Cancer Immunol Immunother* **32**, 117-124 (1990).

180 Fuertes, M. B., Woo, S. R., Burnett, B., Fu, Y. X. & Gajewski, T. F. Type I interferon response and innate immune sensing of cancer. *Trends Immunol* **34**, 67-73, doi:10.1016/j.it.2012.10.004 (2013).

181 Callahan, M. K., Postow, M. A. & Wolchok, J. D. Targeting T Cell Co-receptors for Cancer Therapy. *Immunity* **44**, 1069-1078, doi:10.1016/j.immuni.2016.04.023 (2016).

182 Lund, J. M. *et al.* Recognition of single-stranded RNA viruses by Toll-like receptor 7. *Proc Natl Acad Sci U S A* **101**, 5598-5603, doi:10.1073/pnas.0400937101 (2004).

183 Ahmed, R., Salmi, A., Butler, L. D., Chiller, J. M. & Oldstone, M. B. Selection of genetic variants of lymphocytic choriomeningitis virus in spleens of persistently infected mice. Role in suppression of cytotoxic T lymphocyte response and viral persistence. *J Exp Med* **160**, 521-540, doi:10.1084/jem.160.2.521 (1984).

184 Jiang, Z. *et al.* CD14 is required for MyD88-independent LPS signaling. *Nat Immunol* **6**, 565-570, doi:10.1038/ni1207 (2005).

185 Macal, M. *et al.* Self-Renewal and Toll-like Receptor Signaling Sustain Exhausted Plasmacytoid Dendritic Cells during Chronic Viral Infection. *Immunity* **48**, 730-744 e735, doi:10.1016/j.immuni.2018.03.020 (2018).

186 Buenrostro, J. D., Giresi, P. G., Zaba, L. C., Chang, H. Y. & Greenleaf, W. J. Transposition of native chromatin for fast and sensitive epigenomic profiling of open chromatin, DNA-binding proteins and nucleosome position. *Nat Methods* **10**, 1213-1218, doi:10.1038/nmeth.2688 (2013).

187 Smale, S. T. Transcriptional regulation in the immune system: a status report. *Trends Immunol* **35**, 190-194, doi:10.1016/j.it.2014.03.003 (2014).

188 Sawai, C. M. *et al.* Transcription factor Runx2 controls the development and migration of plasmacytoid dendritic cells. *J Exp Med* **210**, 2151-2159, doi:10.1084/jem.20130443 (2013).

189 Papaspyridonos, M. *et al.* Id1 suppresses anti-tumour immune responses and promotes tumour progression by impairing myeloid cell maturation. *Nat Commun* **6**, 6840, doi:10.1038/ncomms7840 (2015).

190 Bao, M. *et al.* NFATC3 promotes IRF7 transcriptional activity in plasmacy--toid dendritic cells. *J Exp Med* **213**, 2383-2398, doi:10.1084/jem.20160438 (2016).

191 Bornstein, C. *et al.* A negative feedback loop of transcription factors specifies alternative dendritic cell chromatin States. *Mol Cell* **56**, 749-762, doi:10.1016/j.molcel.2014.10.014 (2014).

192 Hara, M. *et al.* Transcriptional regulation of the mouse CD11c promoter by AP-1 complex with JunD and Fra2 in dendritic cells. *Mol Immunol* **53**, 295-301, doi:10.1016/j.molimm.2012.08.004 (2013).

193 Honda, K., Mizutani, T. & Taniguchi, T. Negative regulation of IFN-alpha/beta signaling by IFN regulatory factor 2 for homeostatic development of dendritic cells. *Proc Natl Acad Sci U S A* **101**, 2416-2421, doi:10.1073/pnas.0307336101 (2004).

194 Ichikawa, E. *et al.* Defective development of splenic and epidermal CD4+ dendritic cells in mice deficient for IFN regulatory factor-2. *Proc Natl Acad Sci U S A* **101**, 3909-3914, doi:10.1073/pnas.0400610101 (2004).

195 Jackson, S. H., Yu, C. R., Mahdi, R. M., Ebong, S. & Egwuagu, C. E. Dendritic cell maturation requires STAT1 and is under feedback regulation by suppressors of cytokine signaling. *J Immunol* **172**, 2307-2315, doi:10.4049/jimmunol.172.4.2307 (2004).

196 Lazear, H. M. *et al.* IRF-3, IRF-5, and IRF-7 coordinately regulate the type I IFN response in myeloid dendritic cells downstream of MAVS signaling. *PLoS Pathog* **9**, e1003118, doi:10.1371/journal.ppat.1003118 (2013).

197 Longman, R. S. *et al.* Dendritic-cell maturation alters intracellular signaling networks, enabling differential effects of IFN-alpha/beta on antigen cross-presentation. *Blood* **109**, 1113-1122, doi:10.1182/blood-2006-05-023465 (2007).

198 Owens, B. M., Moore, J. W. & Kaye, P. M. IRF7 regulates TLR2-mediated activation of splenic CD11c(hi) dendritic cells. *PLoS One* **7**, e41050, doi:10.1371/journal.pone.0041050 (2012).

199 Papathanasiou, P., Petvises, S., Hey, Y. Y., Perkins, A. C. & O'Neill, H. C. Impact of the c-MybE308G mutation on mouse myelopoiesis and dendritic cell development. *PLoS One* **12**, e0176345, doi:10.1371/journal.pone.0176345 (2017).

200 Enos, M. E., Bancos, S. A., Bushnell, T. & Crispe, I. N. E2F4 modulates differentiation and gene expression in hematopoietic progenitor cells during commitment to the lymphoid lineage. *J Immunol* **180**, 3699-3707, doi:10.4049/jimmunol.180.6.3699 (2008).

201 Itoh-Nakadai, A. *et al.* A Bach2-Cebp Gene Regulatory Network for the Commitment of Multipotent Hematopoietic Progenitors. *Cell Rep* **18**, 2401-2414, doi:10.1016/j.celrep.2017.02.029 (2017).

202 Kaul, S., Blackford, J. A., Jr., Chen, J., Ogryzko, V. V. & Simons, S. S., Jr. Properties of the glucocorticoid modulatory element binding proteins GMEB-1 and -2: potential new modifiers of glucocorticoid receptor transactivation and members of the family of KDWK proteins. *Molecular endocrinology* **14**, 1010-1027, doi:10.1210/mend.14.7.0494 (2000).

203 Thériault, J. R., Charette, S. J., Lambert, H. & Landry, J. Cloning and characterization of hGMEB1, a novel glucocorticoid modulatory element binding protein. *FEBS Lett* **452**, 170-176, doi:10.1016/s0014-5793(99)00634-1 (1999).

204 Abe, M. & Thomson, A. W. Dexamethasone preferentially suppresses plasmacytoid dendritic cell differentiation and enhances their apoptotic death. *Clin Immunol* **118**, 300-306, doi:10.1016/j.clim.2005.09.019 (2006).

205 Lepelletier, Y. *et al.* Toll-like receptor control of glucocorticoid-induced apoptosis in human plasmacytoid predendritic cells (pDCs). *Blood* **116**, 3389-3397, doi:10.1182/blood-2010-05-282913 (2010).

206 Guiducci, C. *et al.* TLR recognition of self nucleic acids hampers glucocorticoid activity in lupus. *Nature* **465**, 937-941, doi:10.1038/nature09102 (2010).

207 Soulier, A. *et al.* Cell-intrinsic regulation of murine dendritic cell function and survival by prereceptor amplification of glucocorticoid. *Blood* **122**, 3288-3297, doi:10.1182/blood-2013-03-489138 (2013).

208 Agca, C. & Agca, Y. Molecular and ultrastuctural changes of rat pre-implantation embryos during two-cell developmental arrest. *Journal of assisted reproduction and genetics* **31**, 767-780, doi:10.1007/s10815-014-0213-4 (2014).

209 Creaney, J. *et al.* Strong spontaneous tumor neoantigen responses induced by a natural human carcinogen. *Oncoimmunology* **4**, e1011492, doi:10.1080/2162402X.2015.1011492 (2015).

210 Nault, R., Fader, K. A. & Zacharewski, T. RNA-Seq versus oligonucleotide array assessment of dose-dependent TCDD-elicited hepatic gene expression in mice. *BMC genomics* **16**, 373, doi:10.1186/s12864-015-1527-z (2015).

211 Papageorgiou, A., Rapley, J., Mesirov, J. P., Tamayo, P. & Avruch, J. A genome-wide siRNA screen in mammalian cells for regulators of S6 phosphorylation. *PloS one* **10**, e0116096, doi:10.1371/journal.pone.0116096 (2015).

212 Porreca, I. *et al.* Pesticide toxicogenomics across scales: in vitro transcriptome predicts mechanisms and outcomes of exposure in vivo. *Scientific reports* **6**, 38131, doi:10.1038/srep38131 (2016).

213 Merad, M., Sathe, P., Helft, J., Miller, J. & Mortha, A. The dendritic cell lineage: ontogeny and function of dendritic cells and their subsets in the steady state and the inflamed setting. *Annu Rev Immunol* **31**, 563-604, doi:10.1146/annurev-immunol-020711-074950 (2013).

214 Gourbal, B. *et al.* Innate immune memory: An evolutionary perspective. *Immunol Rev* **283**, 21-40, doi:10.1111/imr.12647 (2018).

215 Hendrickson, D. G., Soifer, I., Wranik, B. J., Botstein, D. & Scott McIsaac, R. in *Computational Cell Biology: Methods and Protocols* (eds Louise von Stechow & Alberto Santos Delgado) 317-333 (Springer New York, 2018).

216 Reiter, F., Wienerroither, S. & Stark, A. Combinatorial function of transcription factors and cofactors. *Curr Opin Genet Dev* **43**, 73-81, doi:10.1016/j.gde.2016.12.007 (2017).

217 Lambert, S. A. *et al.* The Human Transcription Factors. *Cell* **175**, 598-599, doi:10.1016/j.cell.2018.09.045 (2018).

218 Ayroldi, E. & Riccardi, C. Glucocorticoid-induced leucine zipper (GILZ): a new important mediator of glucocorticoid action. *FASEB J* **23**, 3649-3658, doi:10.1096/fj.09-134684 (2009).

219 Menzies, R. *et al.* The effect of interferon-alpha on the pituitary-adrenal axis. *Journal of interferon & cytokine research : the official journal of the International Society for Interferon and Cytokine Research* **16**, 619-629, doi:10.1089/jir.1996.16.619 (1996).

220 Anisman, H., Poulter, M. O., Gandhi, R., Merali, Z. & Hayley, S. Interferon-alpha effects are exaggerated when administered on a psychosocial stressor backdrop: cytokine, corticosterone and brain monoamine variations. *Journal of neuroimmunology* **186**, 45-53, doi:10.1016/j.jneuroim.2007.02.008 (2007).

221 Piemonti, L. *et al.* Glucocorticoids affect human dendritic cell differentiation and maturation. *Journal of immunology* **162**, 6473-6481 (1999).

222 Hunzeker, J. T. *et al.* A marked reduction in priming of cytotoxic CD8+ T cells mediated by stress-induced glucocorticoids involves multiple deficiencies in cross-presentation by dendritic cells. *J Immunol* **186**, 183-194, doi:10.4049/jimmunol.1001737 (2011).

223 Rea, D. *et al.* Glucocorticoids transform CD40-triggering of dendritic cells into an alternative activation pathway resulting in antigen-presenting cells that secrete IL-10. *Blood* **95**, 3162-3167 (2000).

224 Sabado, R. L., Balan, S. & Bhardwaj, N. Dendritic cell-based immunotherapy. *Cell research* **27**, 74-95, doi:10.1038/cr.2016.157 (2017).

225 Macal, M. *et al.* CD28 Deficiency Enhances Type I IFN Production by Murine Plasmacytoid Dendritic Cells. *J Immunol* **196**, 1900-1909, doi:10.4049/jimmunol.1501658 (2016).

226 Chen, R. *et al.* In vivo RNA interference screens identify regulators of antiviral CD4(+) and CD8(+) T cell differentiation. *Immunity* **41**, 325-338, doi:10.1016/j.immuni.2014.08.002 (2014).

227 Dobin, A. *et al.* STAR: ultrafast universal RNA-seq aligner. *Bioinformatics* **29**, 15-21, doi:10.1093/bioinformatics/bts635 (2013).

228 Li, B. & Dewey, C. N. RSEM: accurate transcript quantification from RNA-Seq data with or without a reference genome. *BMC Bioinformatics* **12**, 323, doi:10.1186/1471-2105-12-323 (2011).

229 R: A language and environment for statistical computing. (R Foundation for Statistical Computing, Vienna, Austria, 2018).

230 Gentleman, R. C. *et al.* Bioconductor: open software development for computational biology and bioinformatics. *Genome Biol* **5**, R80, doi:10.1186/gb-2004-5-10-r80 (2004).

231 Huber, W. *et al.* Orchestrating high-throughput genomic analysis with Bioconductor. *Nat Methods* **12**, 115-121, doi:10.1038/nmeth.3252 (2015).

232 Wang, J., Vasaikar, S., Shi, Z., Greer, M. & Zhang, B. WebGestalt 2017: a more comprehensive, powerful, flexible and interactive gene set enrichment analysis toolkit. *Nucleic Acids Res* **45**, W130-W137, doi:10.1093/nar/gkx356 (2017).

233 Love, M. I., Huber, W. & Anders, S. Moderated estimation of fold change and dispersion for RNA-seq data with DESeq2. *Genome Biol* **15**, 550, doi:10.1186/s13059-014-0550-8 (2014).

234 Mootha, V. K. *et al.* PGC-1alpha-responsive genes involved in oxidative phosphorylation are coordinately downregulated in human diabetes. *Nat Genet* **34**, 267-273, doi:10.1038/ng1180 (2003).

235 Subramanian, A. *et al.* Gene set enrichment analysis: a knowledge-based approach for interpreting genome-wide expression profiles. *Proc Natl Acad Sci U S A* **102**, 15545-15550, doi:10.1073/pnas.0506580102 (2005).

236 McLean, C. Y. *et al.* GREAT improves functional interpretation of cis-regulatory regions. *Nat Biotechnol* **28**, 495-501, doi:10.1038/nbt.1630 (2010).